MAPPING THE DNA BINDING SITE OF HIV-1 INTEGRASE USING FLUORESCENT OLIGONUCLEOTIDES AND FLUORESCENCE POLARIZATION

by

Natalya Voloshchuk

A dissertation submitted to the Graduate Faculty in Biochemistry in partial fulfillment of the requirements for the degree of Doctor of Philosophy, The City University of New York

2004

INFORMATION TO USERS

The quality of this reproduction is dependent upon the quality of the copy submitted. Broken or indistinct print, colored or poor quality illustrations and photographs, print bleed-through, substandard margins, and improper alignment can adversely affect reproduction.

In the unlikely event that the author did not send a complete manuscript and there are missing pages, these will be noted. Also, if unauthorized copyright material had to be removed, a note will indicate the deletion.

ProQuest Information and Learning Company
300 North Zeeb Road
P.O. Box 1346
Ann Arbor, MI 48106-1346

This manuscript has been read and accepted for the Graduate Faculty in Biochemistry in satisfaction of the dissertation requirement for the degree of Doctor of Philosophy.

4/16/04
Date

L. Davenport
Chair of Examining Committee

4/16/04
Date

L. Davenport
Executive Officer

Supervisory Committee

The City University of New York

The City University of New York

Abstract

MAPPING THE DNA BINDING SITE OF HIV-1 INTEGRASE USING FLUORESCENT OLIGONUCLEOTIDES AND FLUORESCENCE POLARIZATION

by

Natalya Voloshchuk

Advisor: Professor Lesley Davenport

The binding site of HIV-1 integrase (HIV-1 IN) for viral DNA has been characterized using double and single-stranded 21-base pair model oligonucleotide substrates of the U5 and U3 LTR termini, labeled with fluorescent guanosine pteridine analogs at various positions along the specific sequence. HIV-1 IN recognizes viral DNA ends specifically during the 3'-processing reaction prior to the non-specific chromosomal integration step. At 20°C, the 3'-processing activity of HIV-1 integrase is negligible and binding of the protein with the oligonucleotide sequences may be studied exclusively. Two pteridine probes, 3-MI and 6-MI, have been site-selectively inserted along the U5 sequence and all exhibit rotational sensitivity on binding to HIV-1 IN. Varying the position of the fluorescent probe along the viral DNA

sequence permits mapping of contact sites between HIV-1 IN and the model substrate using steady-state fluorescence emission anisotropy (EA). Apparent K_D values, obtained from direct EA titrations, reveal relatively high affinity interactions between the protein and double-stranded oligonucleotide substrates (~10^{-7} M) fluorescently labeled on either the plus or minus strand. For the U5 end a 2-fold preference for binding to positions 2 and 5 on the plus strand of the oligonucleotide over the negative strand was determined. Indeed, the K_D^{app} values determined from the negative strand 21-base pair model viral substrates showed less selectivity, similar to a control oligonucleotide with random sequence. Lower binding affinities are observed for single-stranded over duplex substrates. Here, determined affinities are relatively invariant to the fluorophore position along the length of the single-stranded oligonucleotide suggesting no specificity for binding. In agreement with other in vitro systems, the U3 end 21-mer oligonucleotide appears to be less active than the U5 end short oligonucleotide as reflected by lower binding affinity and reduced activity of HIV-1 integrase with the U3 end model oligonucleotide. There was no U5 or U3 end preference observed for HIV-1 IN interaction with longer oligonucleotides (41bp) over shorter oligonucleotides (21bp) for this system. The influence of the divalent cations, Mg^{2+}, Mn^{2+} and Zn^{2+} on the binding to the protein, revealed that Mn^{2+} is

required for binding, which correlates with the activity observed for this protein.

ACKNOWLEDGMENTS

I would like to thank Professor Leslie Davenport for her guidance, assistance and encouragement during my research and throughout the writing of this dissertation.

I would like to thank Dr. Mary E. Hawkins for her expert advice, assistance and support. I would like to thank Professors J.B. Alexander Ross, Zhen Huang, and Richard S. Magliozzo for serving on my Thesis Committee.

My special thanks is to Caleen Ramsook and Yasemin Kopkalli for their friendship and support throughout my graduate study.

I am most grateful to my husband, Yevgeniy Voloshchuk, for his understanding, support and encouragement throughout my studies. I also would like to thank my family and friends for their support.

TABLE OF CONTENTS

LIST OF TABLES

LIST OF FIGURES

LIST OF ABBREVIATIONS

HEPES	N-2-hydroxyethylpiperazine-N'2-ethanesulfonic acid
Tris-HCl	tris(hydroxymethyl)aminomethane-HCl
MOPS	3-(N-morpholino) propanesulfonic acid
IN	HIV-1 integrase
DNA	deoxyribose nucleic acid
LTR	long terminal repeat
3-MI	3-methyl-8- (2-deoxy- β-D-ribofuranosyl) isoxanthopterin
6-MI	6-methyl-8- (2-deoxy- β-D-ribofuranosyl) isoxanthopterin
CHAPS	3-[(3-cholamidopropyl)-dimethyl-ammonio]-1-propanesulfonic acid
EA	fluorescence emission anisotropy
2-ME	2-mercaptoethanol
PIC	preintegration complex
MA	matrix protein
NC	nucleocapsid
Vpr	viral protein R
RT	reverse transcriptase
bp	base pair

Chapter 1: INTRODUCTION AND AIMS

1.1 HIV-1 Integrase Structure and Function

Human immunodeficiency virus type 1 (HIV-1) belongs to the lentivirus genus of retroviruses (1,2). The virus carries two RNA copies of its genome within virus particles (2, Figure 1). Viral reverse transcriptase mediates the production of a DNA copy of the virus's RNA genome in the cytoplasm of the infected cell (2, 3, 4-7, Figure 2). The resultant viral DNA (about 9000 nucleotides) contains nine genes: *gag*, *pol*, and *env* - standard retroviral genes which are present along with six other genes, flanked by long terminal repeats (LTR) (1, Figure 1). Integration of the viral DNA into the host chromosome in the nucleus follows and ensures the use of the cell's genetic machinery for production of new viral particles (2,4-7). HIV-1 integrase (HIV-1 IN) mediates the incorporation of virally derived DNA into the human genome and, therefore, the protein is essential to the viral life cycle (4-8). HIV-1 integrase is encoded by the *pol* gene, translated as a part of a *gag-pol* polyprotein, and processed into its active form by a virus-encoded protease (9,10).

Viral reverse transcriptase and protease were the first targets in the development of antiviral drugs (2). Another promising target in

anti-HIV drug development is the interaction of HIV-1 with cell-surface receptors (2). Since HIV-1 integrase is essential for retroviral replication and there is no known analogue for this protein in humans, this protein is also an attractive target for the development of new anti-HIV-1 agents (4,6).

1.1.1 Catalytic Activities

HIV-1 integrase carries out the permanent incorporation of a linear DNA copy of the retroviral HIV-1 genome into host cell chromosomal DNA in two steps (Figure 3). In the 3'-processing reaction, the first step of integration, HIV-1 integrase removes a dinucleotide from each 3' end of the viral DNA leaving a two-nucleotide overhang (5,6). In the following joining or strand transfer reaction, the recessed 3' ends of the viral DNA are covalently joined to the 5' ends of the target DNA (5,6). These two reactions are mediated by full length HIV-1 integrase, which is the only protein needed to catalyze processing and joining *in vitro* (8). In infected cells large nucleoprotein complexes known as preintegration complexes (PICs) mediate integration (11). The exact composition of the PICs is not known but a number of cellular and viral proteins have been found associated with HIV-1 PICs (12). The integrase (IN), matrix (MA,

$p17^{Gag}$), nucleocapsid (NC, $p7^{Gag}$), Vpr, and reverse transcriptase (RT) are viral proteins found within PICs (12, Figure 2).

The 3'-processing reaction takes place in the cytoplasm of the infected cell after reverse transcription of the viral RNA (13). This specific endonuclease reaction results in cleavage of the phosphodiester linkage immediately 3' to the adenine of highly conserved CA bases near the 3'-ends of unintegrated retroviral DNA (14). HIV-1 integrase recognizes specific sequences of the viral DNA, which are present at both U5 and U3 termini of the viral long terminal repeats (LTR) and removes the terminal dinucleotides (GT) leaving recessed 3'-hydroxyl ends (13).

Prior to mediating the strand transfer reaction, integrase as a part of the preintegration complex is transported to the nucleus of the host cell by an active transport process which requires ATP and is independent of cell division (15-17,12). Nuclear localization signals within MA, Vpr, and integrase proteins are thought to be involved in targeting PIC to the nucleus of the infected cell (12,16,17,18).

The joining reaction takes place in the nucleus, where the preintegration complex binds to the host DNA (13). The oxygen of the exposed 3'-hydroxyl group acts as a nucleophile in the joining reaction that inserts the processed viral DNA ends into the two strands

of cellular DNA at sites that are separated by five base pairs (14,19). Joining can be considered nonspecific but not a random process with respect to the target DNA; chromatin assembly at the site of integration, DNA bending, DNA-binding proteins, and target DNA sequence and structure are several factors that can influence target site selection for integration (19,20). This concerted transesterification reaction produces an intermediate in which the viral genome is flanked by 5-nucleotide gaps and is linked to the host DNA by its 3' ends (21).

To complete the integration process, the gapped intermediate, which is the product of the joining reaction, is repaired by removal of the two unpaired nucleotides at the 5'-ends of the viral DNA and by filling in the gaps between the viral and the target DNA in the so-called 5'-joining reaction (21,22). During repair, host DNA is duplicated at the integration site resulting in HIV-1 provirus flanked by 5-base pairs repeats of host DNA (5,23,24). Cellular proteins are thought to carry out the post-integration DNA repair (18,22,24).

In vitro, HIV-1 integrase is also able to carry out the disintegration reaction (a reversal of the joining reaction) in which viral DNA is excised from the target DNA (8,14). However, there is no evidence that disintegration is relevant *in vivo* (8). The catalytic

core domain of the HIV-1 integrase alone can carry out the disintegration reaction *in vitro* in contrast to the 3'-processing and joining reactions that require the full-length HIV-1 integrase (14).

While integration of viral DNA into chromosomal DNA is mediated by multiple cellular and viral factors, HIV-1 integrase plays the major role in the process (18). Integration does not require an exogenous energy source, but depends on an appropriate metal cofactor, either Mg^{2+} or Mn^{2+} (25). HIV-1 integrase must be able to recognize viral DNA ends specifically but bind to target DNA in a sequence independent fashion for a complete catalytic cycle (5,26). Because the processing reaction yields a product that becomes the substrate of the subsequent joining reaction, it is also important that the protein holds on to the ends of the processed viral DNA as it moves from the cytoplasm into the nucleus, where the joining reaction takes place (26).

Based on the current understanding of its biological role, there is no necessity for HIV-1 integrase to function more than once; a single recombination event should be sufficient to integrate a provirus (27). *In vitro* kinetic studies of the 3'-processing activity of HIV-1 integrase show very low catalytic turnover number ($K_{cat} = 0.126\ h^{-1}$ in the presence of 10 mM Mn^{2+} (28), $K_{cat} = 0.24\ h^{-1}$ in presence of 7.5

mM Mg^{2+} (13), 2.76 h^{-1} in presence of 5 mM Mn^{2+} (29), and 4.14 h^{-1} in presence of 5 mM Mg^{2+} (29)) suggesting that HIV-1 integrase is a single-turn-over protein.

The 3'-processing and DNA-joining reactions can be reproduced *in vitro* with purified HIV-1 integrase and short (21-mers) double-stranded oligonucleotides that mimic the U5 and U3 termini of HIV-1 DNA (30). These reactions require only integrase and a divalent metal cofactor (manganese or magnesium) (26,30-33). Activity assays have established that integrase can distinguish between viral DNA ends and other oligonucleotides; however, it remains unclear how the discrimination is accomplished (31). *In vitro*, IN binds to substrate DNAs with affinities similar to those of non-substrate DNAs as has been shown by a number of approaches, including ultraviolet (UV) cross-linking studies (31,34), filter binding assays (31), Southwestern blots (31), and electrophoretic mobility shift assays (35). Table 1a summarizes apparent K_D values obtained using surface plasmon resosnance and UV cross-linking approaches (26,29). Experiments suggest that several nucleotides, both distal and proximal to the scissile bond, contribute to the specificity in catalysis (31,36). It appears that the divalent metal cofactors, $Mn^{2+}$and Mg^{2+},

also contribute to the interaction between IN and the substrate DNAs (26,29,31,37,38).

(a)

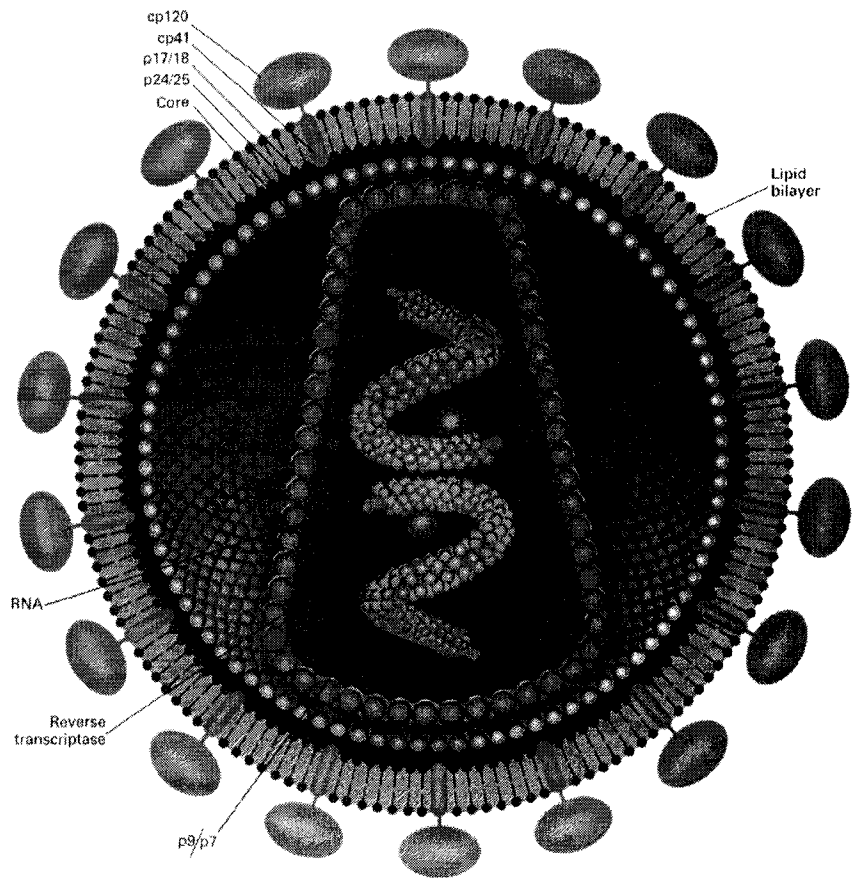

(b)

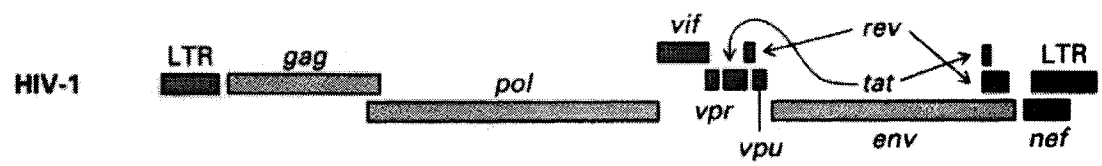

Figure 1. (a) Schematic structure of HIV particle. (b) Structure of HIV-1 genome. Reproduced from: H. Loodish, D. Baltimore, A. Berk, S.L. Zipursky, P. Matsudaira, J. Darnell. Molecular Cell Biology. 3rd ed. New York: W. H. Freeman and Company, 1997.

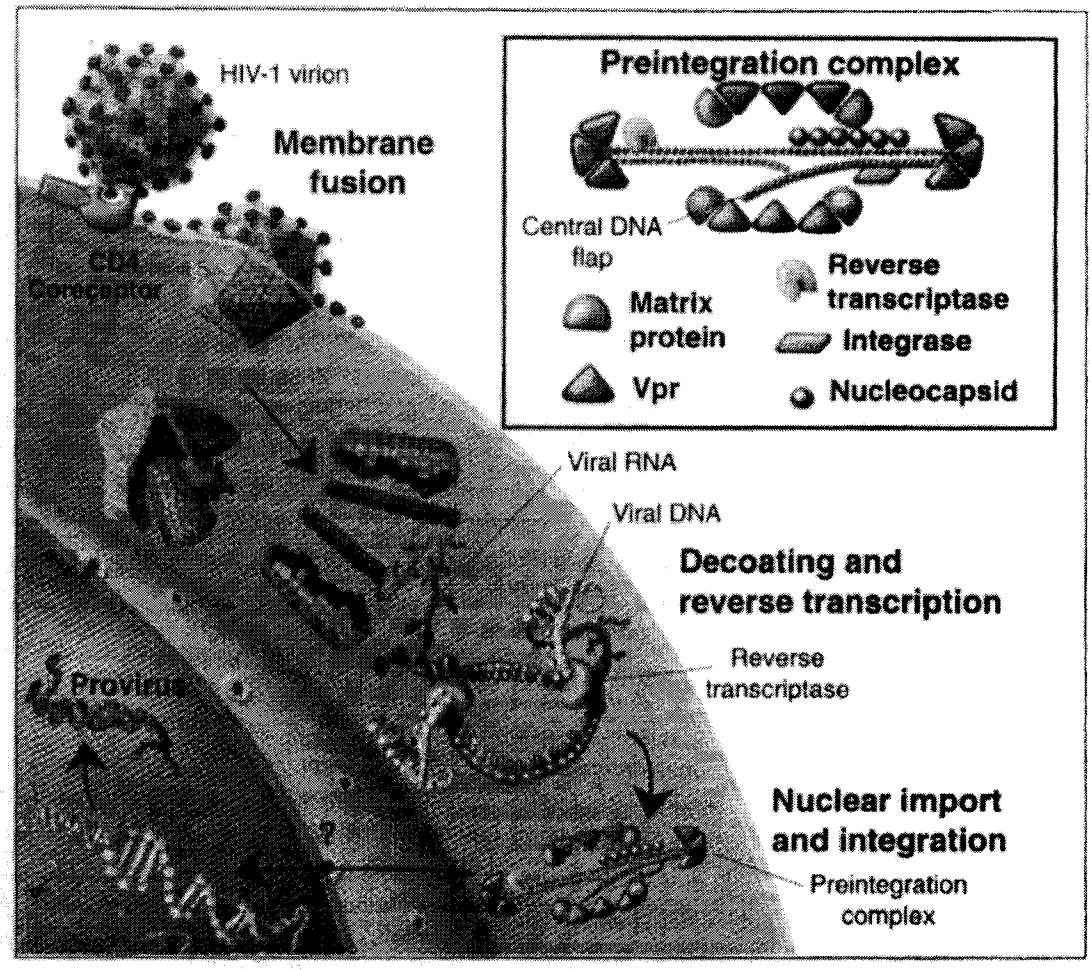

Figure 2. HIV in the host cell. HIV enters the cell and makes a DNA copy of its RNA genome. This copy is transported across the nuclear envelope as part of the preintegration complex. Within the nucleus, the virus integrates into the host chromosome and begins producing more viruses. Reproduced from: M. Chicurel. Probing HIV's elusive Activities within the host cell. 2000. Science 290, 1876 – 1879.

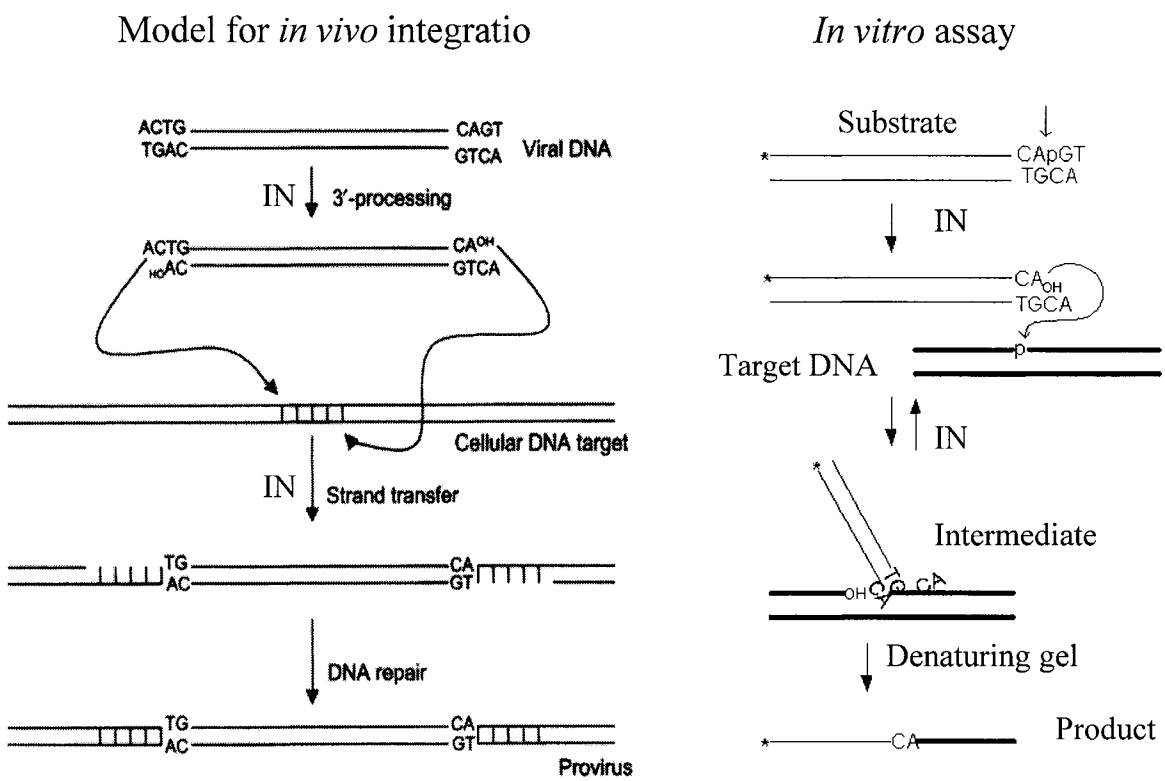

Figure 3. Overview of HIV-1 IN activities. *In vivo* integrase removes the terminal dinucleotide of the viral DNA in the cytoplasm, leaving the CA dinucleotide overhangs. In the nucleus integrase inserts the viral DNA into the two strands of the host DNA at the sites separated by five base pairs and produces a gapped intermediate. DNA repair and gap filling follows. *In vitro*, radioactively labeled short oligonucleotide substrate (15 to 21 bp long) is cut by integrase at the 3'processing site. The shortened strand can be separated by denaturing gel electrophoresis and detected using autoradiographs or phosphorimaging. Integrase joins the processed end to a target DNA forming a strand longer than substrate. Product of the joining reaction can be detected by denaturing gel electrophoresis. The product of the joining reaction, called Y intermediate, can be incubated with integrase to observe disintegration reaction, a reversal of the joining reaction that regenerates the processed and the target DNA.

Table 1a.
Literature apparent K_D values.

Oligonucleotide	UV cross-linking	surface plasmon resonance
DS U5 21 bp	10 mM Mn^{2+} 241 ± 45 nM	7.5 mM Mn^{2+} 9.2 ± 0.8 nM
	No metal 1144 ± 286 nM	
	5 mM Mg^{2+} 677 ± 189 nM	7.5 mM Mn^{2+} 15.8 ± 1.0 nM
SS U5 + strand	10 mM Mn^{2+} 148 ± 36 nM	
SS U5 – strand	10 mM Mn^{2+} 62 ±18 nM	
DS U3 20bp	10 mM Mn^{2+} 154 ± 26 nM	
SS U3 – strand	10 mM Mn^{2+} 165 ± 59 nM	
Random sequence 24 bp		7.5 mM Mn^{2+} 106 ± 2.1 nM
Pre-cleaved 21 bp viral DNA end		7.5 mM Mn^{2+} 25.2 ± 0.6 nM

1.1.2 Domain Structure of HIV-1 Integrase

Full length HIV-1 integrase contains 288 amino acid residues (~32kDa) (31,32,39). Through proteolysis and complementation studies, three functionally and structurally distinct domains of HIV-1 IN have been identified: an N-terminal domain, a catalytic core domain, and a C-terminal domain (31,32,39, Figure 4). All three domains are required for efficient 3'-processing and strand transfer activities of HIV-1 integrase; the core domain alone is sufficient for the disintegration activity (34,40,41). Studies of deletion mutants of HIV-1 IN show that central core domain and C-terminal domain bind to DNA substrates in gel-mobility shift assay and UV cross-linking analysis, while the N-terminal domain appears not to contribute to DNA-binding (41).

a. N-terminal domain

The N-terminal zinc-binding domain of HIV-1 IN (residues 1 to 50) contains an HHCC motif similar to the zinc-binding motif found in several DNA binding proteins and which is conserved in all retroviral integrases (8,31,42). The isolated N-terminal domain of HIV-1 integrase has been shown to bind zinc in a 1:1 molar ratio (39, 43). Binding of zinc is essential for folding of isolated N-terminal

domain and enhances multimerization of full-length integrase (39,44). The structure of the N-terminal domain has been determined by multidimensional heteronuclear nuclear magnetic resonance (NMR) (42). The N-terminal domain is composed of four α helices and has a helix-turn-helix fold which is characteristic of a number of DNA binding proteins (8,32,42, Figure 5). The N-terminal domain of HIV-1 integrase is a dimer (8,42). A structural element similar to a zinc finger might be expected to be involved in DNA binding (45). Indeed, some cross-linking studies show that the N-terminal domain is involved in DNA binding (46). Trans-complementation studies demonstrate the role of the N-terminus in specific recognition of viral DNA (47). Mutants containing substitutions in the HHCC region are shown to bind DNA suggesting that the N-terminus is not the only domain involved in DNA binding by HIV-1 integrase (45).

3'-processing and integration activities of the protein in the presence of Mg^{2+} (19) or Mn^{2+} (40,45) are diminished or abolished by mutations within the HHCC region of the N-terminus. Whereas disintegration activity of the protein appears to be unaffected by N-terminal mutations involving conserved pairs of histidine and cysteine residues (40,45). Since processing and integration activities, but not disintegration, are impaired by HHCC region mutations, this domain

may play a significant role in recognizing features of the viral DNA (40,45).

b. C-terminal domain

The C-terminal domain (residues 212 to 288) of HIV-1 IN is the least conserved of the three domains among retroviral integrases (8,10,19,31). Photo-cross-linking experiments have shown that residues 247-270 in the full-length HIV-1 IN contact bases A(6) and T(7) on the plus strand of the U5 viral DNA end (48,49). It is also known to bind DNA in a sequence independent manner suggesting involvement of the C-terminus in target (chromosomal) DNA binding (32,33,50). Since 220 to 270 region of the C-terminus contains mostly basic amino acids, it could be involved in non-specific DNA binding through contacts with the phosphate backbone of the DNA (50). Site-directed mutagenesis studies have shown that some mutations in the C-terminal reduce 3'-processing and DNA strand transfer activities of HIV-1 IN (51). Residues 220-270 have been shown to comprise a minimal region required for DNA binding (49,50). The structure of the C-terminal fragment, residues 220 to 270, was determined by multidimensional heteronuclear NMR (49,52,53, Figure 6). $IN^{220-270}$ is a dimer in solution (49,52,53). The dimer interface is formed by two

three-stranded antiparallel β-sheets (49,52). These β-sheets of the individual monomers are oriented approximately antiparallel to each other (52,53). Each monomer contains five β-strands that are organized into two antiparallel β-sheets (8,10, Figure 6). The structure resembles that of the Src homology 3 (SH3) domain found in several proteins involved in signal transduction (31,52,53) and one other protein involved in DNA binding, Sso7d (19). The C-terminal domain is also thought to be involved in HIV-1 integrase multimerization (54). Mutations L241A and L242A in the C-terminal of the full-length HIV-1 IN were shown to result in a loss of oligomerization (51).

c. Catalytic core domain

The catalytic domain (residues 50-212) is defined by carboxylate residues - the D, D (35) E motif (Asp-64, Asp-116, and Glu-152). It is well conserved among retroviral integrases (8,31). The catalytic core domain has an RNase H-type fold and belongs to the superfamily of polynucleotidyl transferases (32,33,55). The structure of the catalytic core domain was determined by X-ray crystallography (55). The core domain crystallizes as a dimer where each monomer contains a central five-stranded β sheet and six α helices (8,31,55,56,

Figure 7). The crystal structure of the HIV-1 integrase catalytic core in the presence of Mg^{2+} reveals that the divalent cation is coordinated by the two aspartic acid residues of the catalytic triad (19,57,58). Most substitutions of the triad residues result in inactivation of the protein except for D116N and D116E/E152D substitutions (19). The D116N mutant of HIV-1 IN is more active than the wild type *in vitro* (19). The D116E/E152D substitutions eliminate 3'-processing and strand transfer activities of HIV-1 integrase, but disintegration activity can be detected (19).

The three-dimensional structures of the HIV-1 integrase domains have been determined separately (6,32,55,49,56,57). The first multidomain structure, that includes the catalytic core and the C-terminal domains (residues 52-288), has been recently reported (56, Figure 8). Another multidomain structure determined by X-ray crystallography includes the N-terminal and the catalytic core domains (59, Figure 9). No crystal structure for the full-length integrase has yet been determined. Structural work on recombinantly expressed HIV-1 integrase has been hindered by the protein's low solubility and tendency for aggregation (60).

Spatial arrangement of the three domains within the monomer or assembly to higher-order species of HIV-1 integrase is not yet

defined. Therefore, how the whole protein interacts with the DNA substrates is not well understood (4).

1.1.3 Multimeric State of HIV-1 Integrase

Integrase is released as an isolated native protein by HIV protease cleavage of the *pol* polyprotein (10,19,42). The protein may be free of DNA at first, but at later times after infection, it forms a tight multimeric complex with DNA substrates (42). Since in the overall integration reaction IN should be able to carry out four DNA cleavage events: two viral DNA ends and two sites in the target host DNA, it is reasonable to conclude that HIV-1 integrase works as a multimer (24).

Although there are strong indications that retroviral integrases function as oligomers, the actual species have not been determined (8,26). Studies conducted to establish the multimeric state of purified recombinant full-length HIV-1 integrase suggest that the protein can exist in solution as a monomer, dimer, tetramer or higher order oligomers with the dimer being the most common oligomeric state (9,54,61-64, Table 1). It is not possible to exclude any species as catalytically inactive (27). *In vitro* studies show that at a protein concentration 0.2 mg/ml wild-type integrase exists in a monomer-

dimer equilibrium in the presence of the detergent CHAPS (54). The multimeric form of HIV-1 integrase that prevails in solution appears to depend on the protein concentration, the presence of CHAPS during purification procedure of the protein, ionic strength, presence of divalent cations (Mg^{2+} or Mn^{2+}, and Zn^{2+}), and the presence of DNA substrate (44,45,51,61-63).

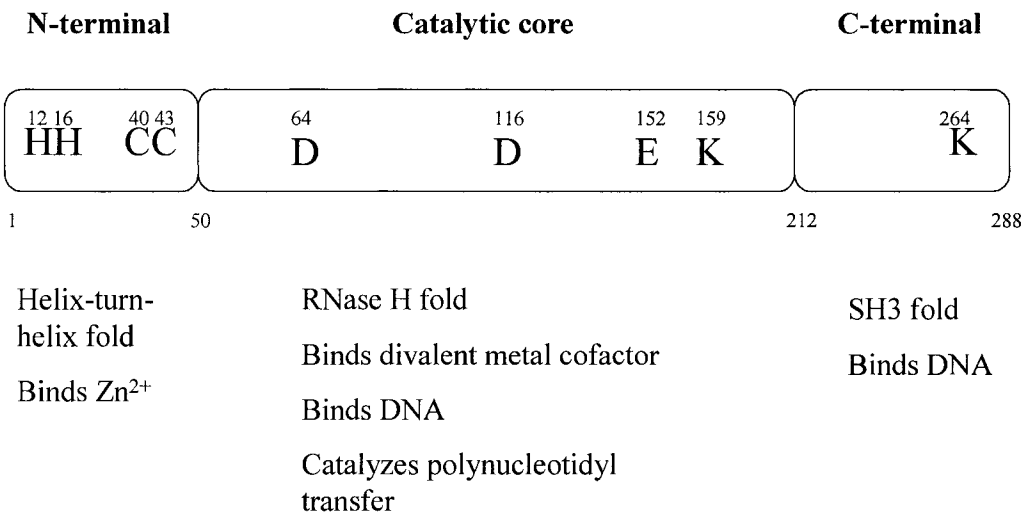

Figure 4. Schematic presentation of the domain structure of HIV-1 integrase. Three independently folding domains are shown. The conserved and catalytically important residues are indicated. The residue numbers that define domain boundaries are indicated below the figure. Also listed below the figure are features that describe the domains.
References: D. Esposito and R. Craigie. Advances in Virus Research, 1999, vol.52, 319-333. E. Asante-Appiah and A.M. Skalka, Advances in Virus Research, 1999, vol.52, 351-369. K. Sayasith, G. Sauve, J. Yelle, Expert Opin. Ther. Targets, 2001, vol.5, 443-464.

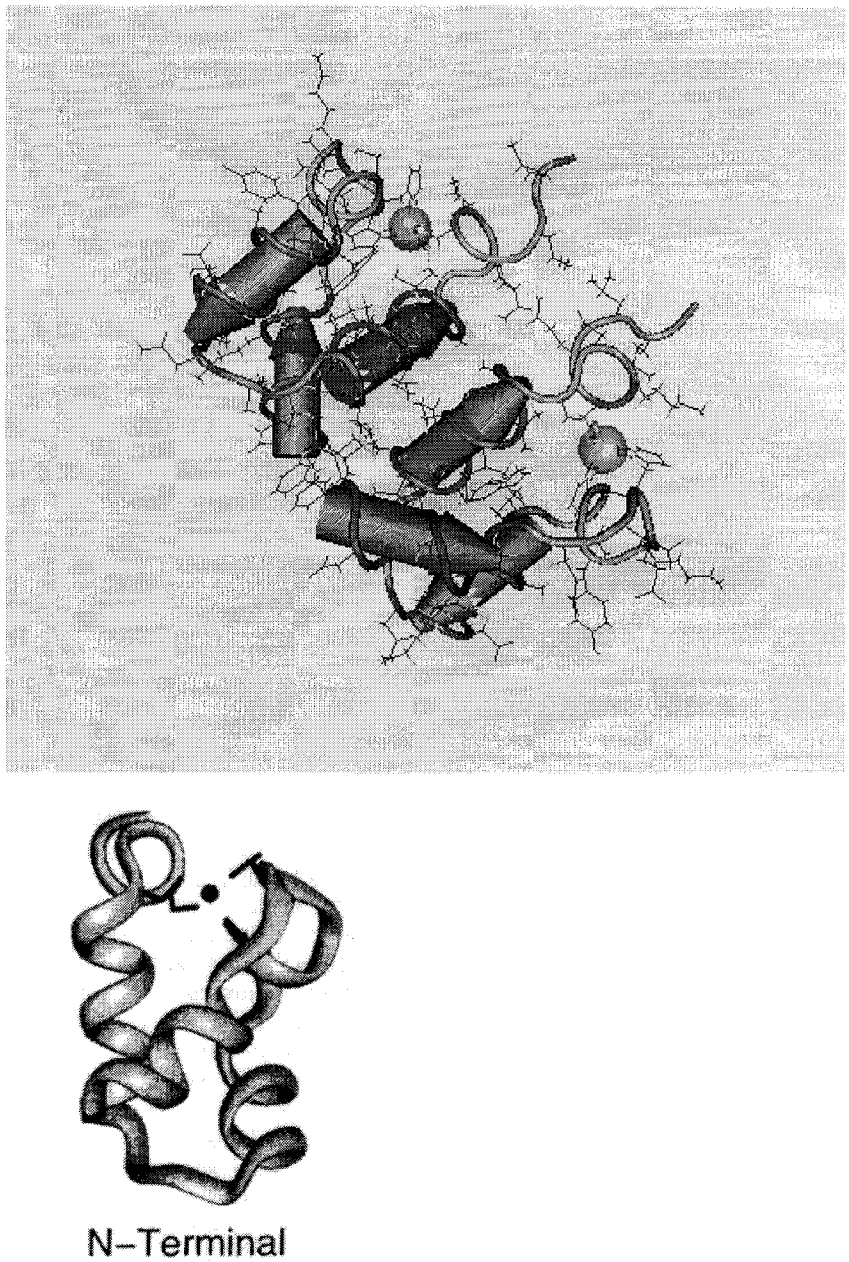

Figure 5. Structure of the N-terminal domain of the HIV-1 integrase (top) as determined by NMR (PDB file 1WJA), depicted as a dimer. Ribbon diagram of the N-terminal domain of the HIV-1 integrase (bottom) is based on PDB file 1WJA, coordinating a single zinc cation (black sphere) by using the HHCC motif. Residues His12, His16, Cys40, and Cys43 are depicted as black sticks (Reproduced from: P. Hindmarsh and J. Leis. Retroviral DNA integration. Microbiology and Molecular Biology Reviews. 1999, 63(4): 836-843).

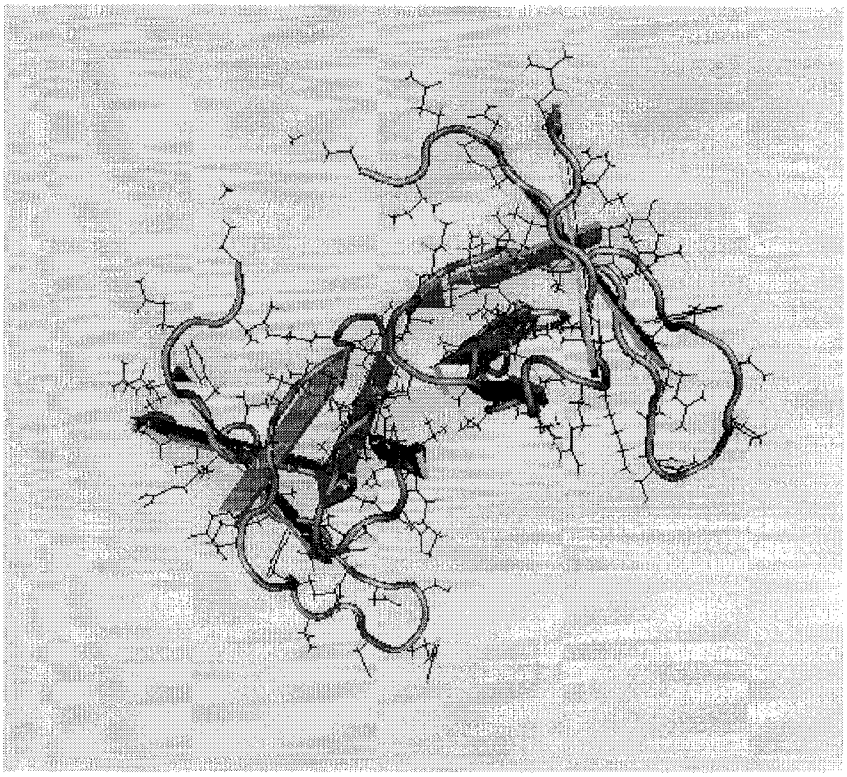

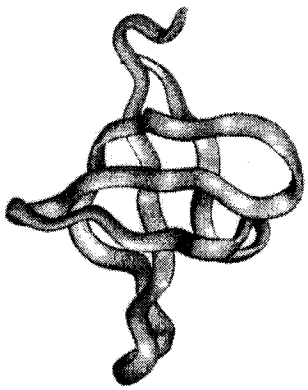

C–Terminal

Figure 6. Structure of the C-terminal domain of the HIV-1 integrase (PDB file 1IHV) determined by NMR is shown as a dimer (top). Ribbon diagram of the C-terminal DNA binding domain of the HIV-1 integrase, based on coordinates in PDB file 1IHV, shows the domain as a monomer (Reproduced from: P. Hindmarsh and J. Leis. Retroviral DNA integration. Microbiology and Molecular Biology Reviews. 1999, 63(4): 836-843).

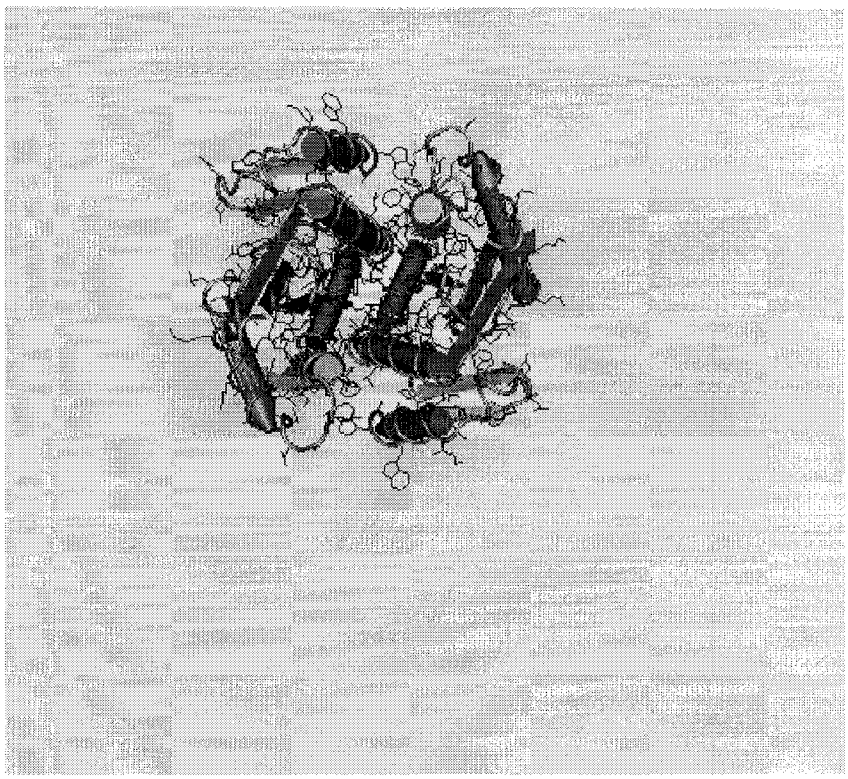

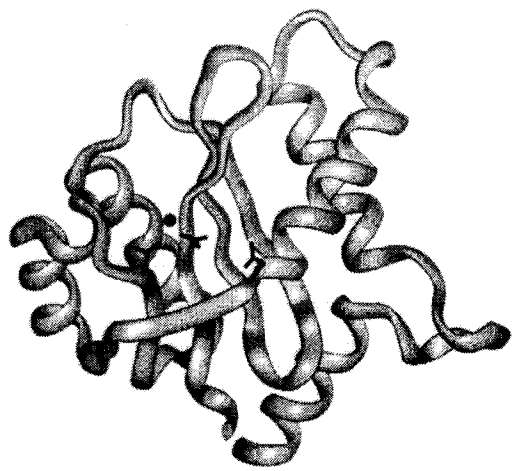

Catalytic Core

Figure 7. Structure of the catalytic core domain of the HIV-1 integrase (PDB file 1BI4) determined by X-ray crystallography, is shown as a dimer (top). Ribbon diagram of the monomer of the core catalytic domain of the HIV-1 integrase (bottom) is based on 1BI4 PDB file showing the active form of the HIV IN catalytic domain. Active site residues Asp116, Asp64, and Glu152 (D,D(35)E motif) shown as black sticks from left to right. Side chains of the two Asp residues bind a single magnesium cation shown as black sphere (Reproduced from: P. Hindmarsh and J. Leis. Retroviral DNA integration. Microbiology and Molecular Biology Reviews. 1999, 63(4): 836-843).

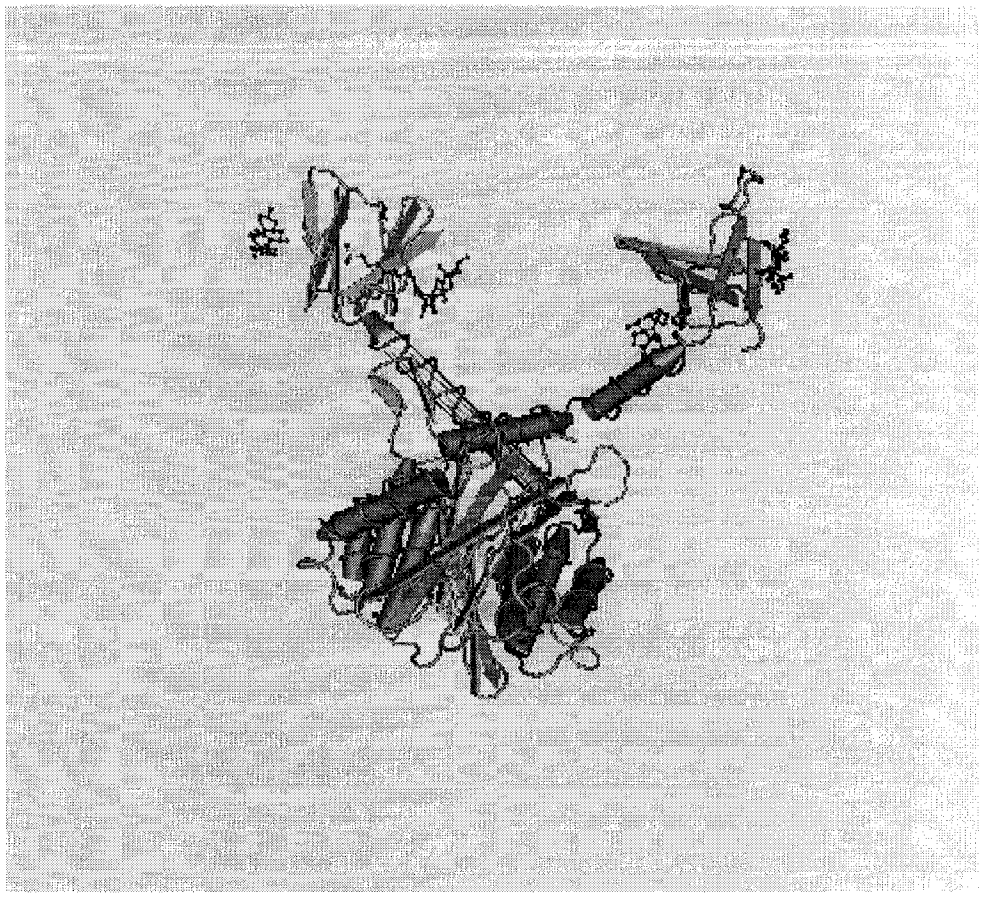

Figure 8. Structure of the HIV-1 integrase catalytic core and C-terminal domains determined by X-ray crystallography, PBD file 1EX4. The structure is a Y-shaped dimer. Within the dimer, the catalytic core domains form the only dimer interface, and the C-terminal domains are located 55 Å apart. Also shown are four CHAPS (detergent) molecules. To improve the solubility of the protein, five mutations were introduced into the primary sequence: C56S, W131D, F139D, F185K, and C280S. The mutations did not alter the structure of the catalytic core compared with other structures containing only one of the four mutations: F185K or F185H. The finding of an identical catalytic core domain structure alone (IN^{52-210}) or attached to the C-terminal domain (IN^{52-288}) argues that the dimeric core structure also will be found in full-length IN.

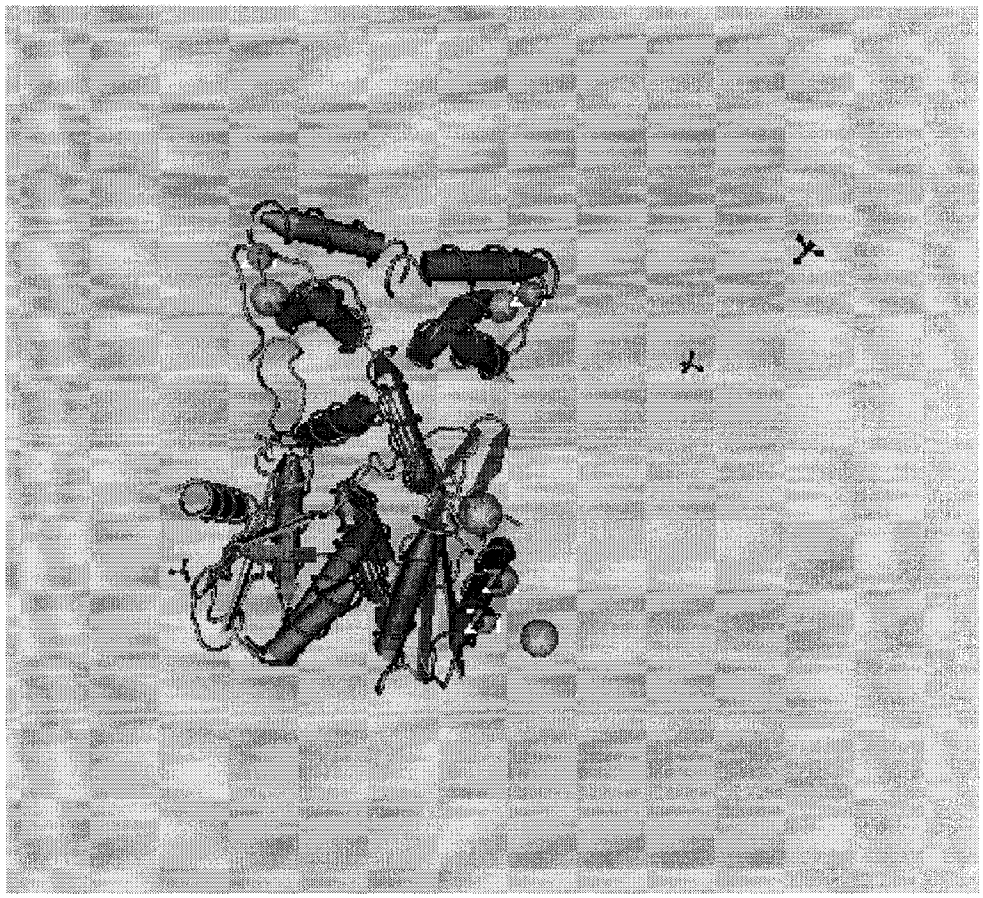

Figure 9. Structure of the HIV-1 integrase N-terminal and catalytic core domains determined by X-ray crystallography, PBD file 1K6Y. Three mutations were introduced into the IN^{1-212} primary sequence: W131D, F139D, F185K. Residues 47-55, which connect the N-terminal and catalytic domains, are disordered. Also shown are potassium and zinc cations (grey spheres) and phosphate ions (presented as ball and stick models).

Table 1.
Multimeric State of HIV-1 Integrase.

[IN]	[salt]	multimeric state	method
60 nM	0.1M NaCl	tetramers	UV-photo-cross-linking (35)
	0.1M NaCl, 3.0 mM $MnCl_2$	monomers,dimers, tetramers	
≤ 200 nM	1.0M NaCl	monomers	time resolved anisotropy (62,63)
	1.0M NaCl, 50μM $ZnCl_2$	monomers,dimers	
	1.0mM NaCl, 10mM $MnCl_2$	monomers	
900 nM	1.0M NaCl	monomers	exclusion chromatography (9)
1μM	25mM NaCl	monomers	UV-photo-cross-linking (38)
	25mM NaCl, 25mM $MnCl_2$	dimers,trimers, tetramers	
3μM	1.0M NaCl	monomers	gel filtration (29)
	0.4M NaCl	monomers,dimers	
	< 0.4M NaCl	tetramers, aggregates	
1-10μM	500mM KCl	dimers	exclusion chromatography (64)
	500mM KCl, 5mM $MnCl_2$	40%aggregate 60% dimers	
0.3 mg/ml	1.0M NaCl	dimers	gel filtration (45)
30 μM	1.0M NaCl	dimers, tetramers	gel filtration (51)
10μM	1.0M NaCl	dimer-monomer $K_D = 1.85 \times 10^{-5}$ M tetramer-dimer $K_D = 1.27 \times 10^{-5}$ M	analytical centrifugation (44)
	1.0M NaCl, 10μM Zn^{2+}	tetramer-dimer $K_D = 2.85 \times 10^{-6}$ M octamer-tetramer $K_D = 2.97 \times 10^{-6}$ M	
0.2 mg/ml	0.5M NaCl	monomer-dimer $K_D = 2.5 \times 10^{-5}$ M	analytical centrifugation (65)

1.1.4 Role of Divalent Cations

a. Magnesium and Manganese Cations

The divalent cation cofactors, Mn^{2+} and Mg^{2+}, appear to contribute to the interaction between HIV-1 integrase and the substrate DNAs. The involvement of the metal ions is apparently manifested in two steps: the metal cofactor facilitates the assembly of a stable IN-metal-DNA complex via conformational changes in the protein and subsequently promotes catalysis (26,29,66).

Divalent metal cofactors (Mn^{2+} and Mg^{2+}) induce conformational changes in the protein that appear to reorganize regions in the core and the C-terminal domains, thus activating the protein by recruiting the catalytic machinery to a favorable structure (31). Studies with the divalent metal ions have shown that when HIV-1 integrase is preincubated with its metal cofactor, the activity of the protein becomes significantly greater (at least five fold) (31). It has been shown that integrase can bind viral DNA in the absence of divalent metal cofactors, but the presence of the divalent cations facilitates the formation of the ternary protein-DNA-metal complex (29,31,34,61). The preference for Mn^{2+} over Mg^{2+} as a metal cofactor in *in vitro* catalysis has been explained by the ability of Mn^{2+} to

promote the formation of a more stable IN-metal-DNA complex (29). Using surface plasmon resonance for binding studies, it has been shown that metal cofactor contributes to substrate discrimination by modifying the binding constants (K_D) of both viral and potential target DNA (26).

Generally, purified recombinant HIV-1 IN requires Mn^{2+} for efficient activity *in vitro* (67-69). However, the concentration of Mg^{2+} is higher in cytoplasm of living cells (~ 10^{-3} M Mg^{2+} versus less than 10^{-7} M Mn^{2+}). Thus Mg^{2+} is more likely to be the physiological cofactor for HIV-1 IN activities (9,64,67-69). Nevertheless, under standard *in vitro* reaction conditions with purified IN, little or no strand transfer activity can be detected in the presence of Mg^{2+} (69). IN isolated from infected cells as part of a preintegration complex, however, can mediate efficient integration *in vitro* by using Mg^{2+} or Mn^{2+}(68). Mn^{2+} is known to influence specificities of many Mg^{2+}-dependent proteins, for example, polymerases and nucleases, which catalyze DNA-dependent reactions (68). One or several components of the preintegration complex may be required for the integrase activity *in vivo* and thus influence the protein's preference for divalent cation (69).

b. Zinc Cation

The N-terminal domain of HIV-1 IN contains the amino acid sequence motif His-Xaa_3-His-Xaa_{23}-Cys-Xaa_2-Cys (43). Similar sequences with histidine and cysteine residues, which are separated by various number of amino acids, have been proposed to form Zn^{2+} fingers where Zn^{2+} is coordinated by the histidine and cysteine residues (43). Zinc fingers have been identified in a variety of DNA-binding proteins and have been shown to mediate sequence specific DNA binding in a number of transcription factors, including a steroid hormone receptor and TFIIIA (43). The conserved amino acids of the HHCC motif (residues 12-43) of HIV-1 IN are required for efficient zinc binding (40). The zinc cation is tetrahedrally coordinated to His 12, His 16, Cys 40 and Cys 43 (42). HIV-1 IN binds Zn^{2+} with a stoichiometry of one Zn^{2+} per integrase monomer (39,42,43). An apparent $K_D \approx 6$ μM was determined at pH 7.5 in the presence of 1mM NaCl for zinc cation binding to HIV-1 integrase (39). Integrase purified in the presence of EDTA has been shown to contain 0.12 equivalents of Zn^{2+} per integrase monomer (44), whereas HIV-1 IN purified in presence of Zn^{2+} and without EDTA contains 0.67 equivalents of Zn^{2+} per integrase monomer (44). The presence of Zn^{2+} has been found to be important for the Mg^{2+}-dependent activity of

HIV-1 integrase but not as significant for the Mn^{2+}-dependent activity (70). The isolated N-terminal domain is unstructured in the absence of zinc cation, but folds into a structure with a high α-helical content in the presence of zinc cation (42).

While the presence of zinc cations appears to influence the folding of the isolated N-terminal domain of HIV-1 integrase, this is not reflected in the far UV CD spectra (to detect secondary structure) of full-length integrase, which is not detectably different in the presence or absence of bound zinc cation (39). This suggests that the N-terminal may therefore have significant secondary structure in the full-length protein even in the absence of zinc (39). In contrast, the near UV CD spectra (to detect tertiary structure) of the full-length integrase are quite different in the presence and absence of zinc, suggesting significant differences in the tertiary structure (39). In the context of full length integrase, zinc cation enhances both tetramerization and catalytic activity in *in vitro* assays, illustrating its functional importance in promoting an active multimeric state of the protein (39,44,70). The mechanism of HIV-1 IN stimulation by zinc has not yet been determined (39).

1.1.5 DNA Substrates

HIV-1 integrase acts on two types of substrates in the course of the integration process: viral DNA and chromosomal target DNA. During transcription of viral RNA into DNA by reverse transcriptase, long terminal repeats (LTRs) are formed at the ends of the linear DNA products (23). Thus, unintegrated linear viral DNA contains a several-hundred-base-pair long terminal repeat (LTR) sequence at each end (5). LTRs are involved in viral integration and in regulation of the viral genome (71). Each long terminal repeat (LTR) contains three regions that are organized as U3-R-U5 (5, Figure 10). The outermost four base pairs of the HIV-1 genome are related to each other as inverted repeats, and always have highly conserved CA dinucleotides located two nucleotides from the 3' ends of both DNA strands (5). Sequences at the viral DNA ends are involved in integration, serving as specific substrates for retroviral integrase (5). In contrast to the specificity of integration for viral DNA ends, no obvious sequence rules have been defined for the large number of sites in host chromosomal DNA that can serve as the target for integration (5).

Understanding how HIV-1 integrase recognizes its DNA substrates is important for modeling retroviral integration and for discovering new possible targets for antiretroviral therapy (67).

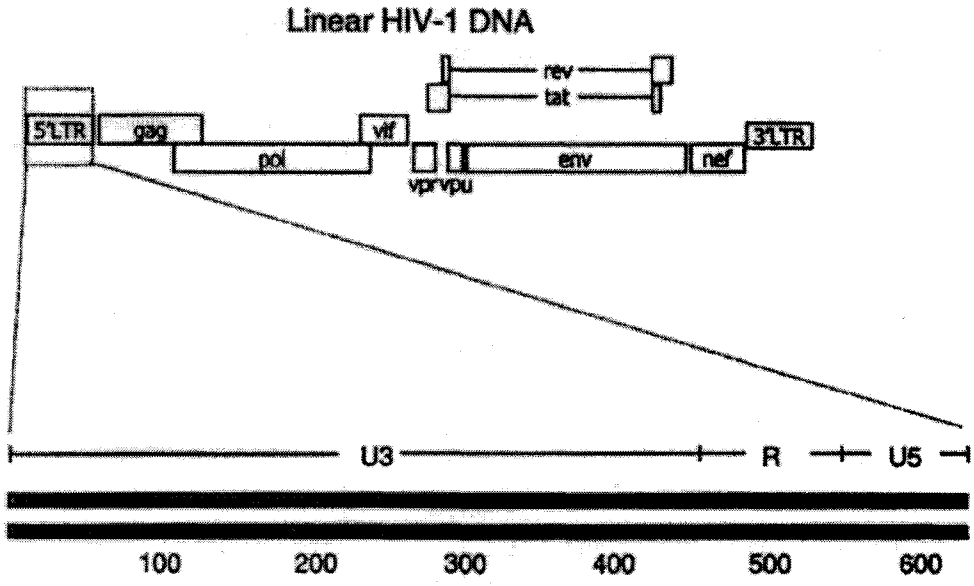

Figure 10. HIV-1 genome and structure of 5' long terminal repeat (LTR). Reproduced from: T.C. Pierson, Y. Zhou , T.L. Kieffer, C.T. Ruff, C. Buck, and R.F. Siliciano. Molecular characterization of preintegration latency in HIV-1 infection. J. Virol., vol. 76, 8518-8531.

1.2 Fluorescence Methods for Studying HIV-1 Integrase Binding

Fluorescence spectroscopy is one of the most widely used techniques in biochemistry and molecular biophysics (73). Sensitivity of the fluorescence signal to changes in the structural and dynamic properties of biomolecules and biomolecular complexes makes fluorescence methods valuable experimental tools (73).

1.2.1 Steady-state Fluorescence Emission Anisotropy

Fluorescence anisotropy measurements reveal the average angular dipole displacement of a fluorophore, which occurs between absorption and subsequent emission of a photon (74). Such angular displacement depends on the rate and extent of rotational diffusion during the lifetime of the excited state (74). Rotational motion of a fluorophore in solution depends on the viscosity of the solvent and size and shape of the diffusing species (74). Thus, changes in solution viscosity or altered shape and size of the fluorescent species can result in changes in their diffusive motions. Such altered rotational motions of the fluorophore will affect the angular displacement of the fluorophore. Measurement of the fluorescence emission anisotropy provides quantitative information on the angular displacement.

Fluorescence emission anisotropy is defined as the ratio of the difference between the emission intensity parallel to the polarization of the electric vector of the exciting light (I_{II}) and that perpendicular ($I_{\perp}$) to that vector, divided by the total intensity:

$$< r > = \frac{I_{\parallel} - I_{\perp}}{I_{\parallel} + 2I_{\perp}} \qquad (1)$$

where I_{II} and $I_{\perp}$ are the fluorescence intensities of the vertically (II) and horizontally ($\perp$) polarized emission, when the sample is excited with vertically polarized light (74-76).

The most frequently used optical set-up for measuring steady-state fluorescence anisotropy is the L-format method (74), which uses a single emission channel (74). To analyze the steady-state fluorescence anisotropy, parallel and perpendicular fluorescence emission components are measured in all four possible combinations of vertical or horizontal alignment, I_{VV}, I_{VH}, I_{HV}, and I_{HH} (Figure 11). The anisotropy is calculated according to:

$$< r > = \frac{Ivv - GIvH}{Ivv + G2IvH} \qquad (2)$$

where I_{VV} is fluorescence intensity measured with vertically polarized excitation and vertically polarized emission, I_{VH} is fluorescence

intensity measured with vertically polarized excitation and horizontally polarized emission.

$$G = \frac{I_{HV}}{I_{HH}} \qquad (3)$$

is the grating factor - a correction for the instrument response to transmission of vertically or horizontally polarized light at a particular emission wavelength, where I_{HV} corresponds to horizontally polarized excitation and vertically polarized emission , and I_{HH} corresponds to horizontally polarized excitation and horizontally polarized emission.

The transition moments for absorption and emission have fixed orientations within each fluorophore, and the relative angle between these moments influences the maximum measured anisotropy. Several processes (for example, rotational diffusion, energy transfer) can decrease the measured anisotropy to values lower than the maximum values. The most common is rotational diffusion. Such diffusion occurs during the lifetime of the excited state and displaces the emission dipole of the fluorophore. When rotational diffusion is the only significant process that results in the loss of anisotropy, the measured anisotropy is given by the Perrin equation relating fluorescence anisotropy to the rotational correlation time (ϕ) of the fluorophore:

$$r = \frac{r_0}{1+(\tau/\phi)} \qquad (4)$$

where r_0 is the anisotropy measured in the absence of rotational diffusion, ϕ is the rotationalcorrelation time for the diffusion process, and τ is fluorescence life-time of the fluorophore.

The rotational correlation time of the fluorophore is given by:

$$\phi = \frac{\eta V}{RT} \qquad (5)$$

where η is the viscosity of the solution, T is the absolute temperature, V is the volume of the rotating unit, and R is the universal gas constant.

The limiting or fundamental emission anisotropy value (r_0) for a particular fluorescent probe depends on the angle between the absorption and emission transition dipoles (73). A maximum anisotropy value of 0.4 is observed when the absorption and emission dipoles are colinear, and when there are no processes which result in depolarization (74). The limits for r_0 values are $-0.2 \leq r_0 \leq 0.4$, and the values outside this range are artifactual (74).

Due to different hydrodynamic properties, a high-molecular-weight species normally rotates in solution more slowly than a lower-molecular-weight species (76). Therefore, on photoselection with

polarized light, for a high-molecular-weight fluorophore-labeled species the emitted light will remain polarized due to hindered rotational motions (76). This dependence of emitted-light depolarization on the size of fluorophore-labeled macromolecules and macromolecule-macromolecule complexes permits the use of fluorescence anisotropy for studies of protein-DNA interactions (76). Binding of a protein to the fluorescently labeled oligonucleotide causes a decrease in the rotational rate of the probe due to the increased rotational restrictions arising from the size of the oligonucleotide-protein complex as compared to that of the free oligonucleotide (75). As a consequence, the fluorescence emission anisotropy value for the bound fluorophore is increased.

1.2.2 Advantages of Polarized Fluorescence Methods

Fluorescence anisotropy studies offer a convenient method for obtaining information about rotational dynamics of a fluorophore. In this study fluorescence anisotropy is used to determine apparent binding affinities of HIV-1 integrase for a series of model DNA substrates. Due to the highly asymmetric shape of oligonucleotides, rotation about the long axis of DNA (spinning) probably dominates the measured fluorescent anisotropy of labeled DNA molecules. This

mode of rotation is restricted upon protein binding. Thus a measurable change in the emission anisotropy will be observed.

The fluorescence emission anisotropy is a rapid, reliable solution-based method for detecting, characterizing, and quantitating protein binding to DNA (75). Since it is a solution technique, the effect of changing solution conditions - pH, protein concentration and oligonucleotide concentration, temperature, salt concentration - can be readily investigated (75). Measurement of fluorescence anisotropies can provide true equilibrium measurements that do not require separation of free and bound species and permit analysis of weak interactions ($K_D = 10^{-6}$ to 10^{0} M) as well as strong interactions ($K_D = 10^{-10}$ to 10^{-6} M) (75,76). Fluorescence anisotropy also permits true solution assays without macromolecule immobilization, allows both equilibrium and kinetic assays, and does not require high-cost instrumentation (75,76).

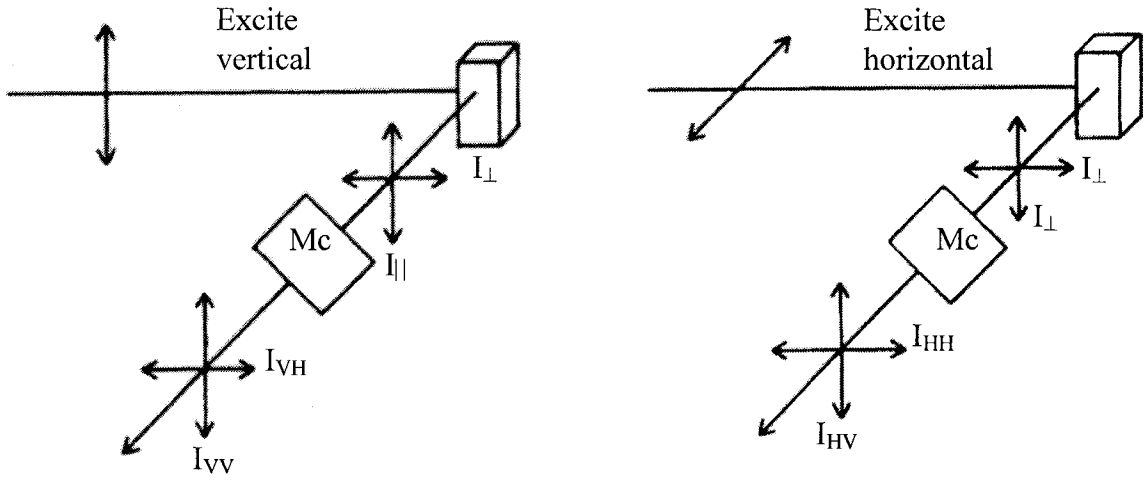

$$< r > = \frac{I_{||} - I_{\perp}}{I_{||} + 2I_{\perp}}$$

$$< r > = \frac{I_{VV} - GI_{VH}}{I_{VV} + 2GI_{VH}} \qquad G = \frac{I_{HV}}{I_{HH}}$$

Figure 11. Schematic diagram for L-format measurements of fluorescence anisotropy (74). The sample is excited with vertically polarized light (diagram on the left). After passing through the sample, vertically ($||$) and horizontally ($\perp$) polarized light pass through emission monochromator (Mc). The emission monochromator has different transmission efficiency for vertically and horizontally polarized light. Rotation of the emission polarizer can change the sensitivity of the emission channel. Thus, measured intensities (I_{VH} and I_{VV}) are biased by detection system. To take into consideration properties of the detection system, the G factor is measured using horizontally polarized excitation (diagram on the right). In this case, both horizontally and vertically polarized components are proportional to $I_{\perp}$, and therefore any difference in I_{HV} and I_{HH} must be due to the properties of the detection system. The steady-state fluorescence anisotropy can then be calculated from I_{VV}, I_{VH}, and G factor.

1.2.3 Fluorescent Probes Used in this Study

DNA bases are only slightly fluorescent and, therefore, extrinsic probes are commonly employed in fluorescence studies of DNA - protein interactions. A variety of fluorescent probes are available for DNA studies. Some fluorophores are larger than, and structurally different, from purines and pyrimidines, and are attached to the DNA on a linker arm. While such probes do not disrupt tertiary structure of DNA, they are often far from the sites of the specific DNA interactions under investigation.

Fluorescent nucleoside analogues used as DNA probes provide researchers with more direct approaches in DNA studies. It is possible to incorporate these probes into oligonucleotides through a deoxyribose linkage because they are similar in structure and size to native purines. Positioning of these probes within the oligonucleotide structure makes them sensitive to changes in the surrounding oligonucleotide structure as the oligonucleotide interacts with other molecules. One of the first nucleoside analogues developed, 2- amino purine (2-AP), provided a useful means for detecting protein-DNA interactions (77,78). The nucleoside analogue, 1,N^6- ethenoadenosine, is another probe used in DNA studies, particularly to study interactions between neighboring bases (77,78).

Recently a new class of nucleoside analogues based on pteridine structures has been developed (77-80). These are highly fluorescent guanosine analogs, which show sensitivity of their fluorescence properties as they become incorporated into the oligonucleotide structure. Altered fluorescence signals of the pteridine-containing labeled oligonucleotides as they interact with a protein can be measured through fluorescence anisotropy. Since independent movement of the probe is minimized, the interpretation of fluorescence emission anisotropy measurements to study DNA – protein interactions is significantly less complex (77,79).

The current studies of protein-DNA interactions use two fluorescent pteridine nucleoside analogs, 3-MI [3-methyl-8- (2-deoxy-(-D-ribofuranosyl) isoxanthopterin] and 6-MI [6-methyl-8- (2-deoxy-(-D-ribofuranosyl) isoxanthopterin] (Figure 13). Structural and fluorescence characteristics of the probes are discussed in the following section.

a. Compatibility of 3-MI and 6-MI with Oligonucleotide Structure

3-MI (Figure 13 A) is highly fluorescent in solution with a relative quantum yield Φ equal to 0.88 (78). The probe is stable enough to undergo automated DNA synthesis and can be incorporated

into an oligonucleotide sequence in place of guanine (77,79). Incorporation of 3-MI into an oligonucleotide significantly reduces the fluorescence intensity of the probe suggesting that 3-MI is sensitive to its local environment and is involved in base stacking interactions (78, 81). Bases adjacent to 3-MI in an oligonucleotide sequence were noted to influence the fluorescence yield of the probe; purines (adenine and guanine) adjacent to the flourophore quench the fluorescence intensity of 3-MI more than pyrimidines (thymine and cytosine) (78,80). Upon annealing of single stranded oligonucleotides containing 3-MI, further but not substantial fluorescence quenching is observed due to base pairing, suggesting that 3-MI is more involved in base stacking interactions that base pairing interactions (77-79). Melting temperature studies described elsewhere (77) and in this work (Results, section 3.1.1) suggest that 3-MI does not form base pairs with cytosine on the complementary strand in the double stranded oligonucleotide. Melting temperature depression corresponds to a single base mismatch for 3-MI containing oligonucleotides (77, section 3.1.1).

6-MI (Figure 13 A) is a guanine analog with relative quantum yield of 0.70 in solution and structurally and photochemically similar to 3-MI. They differ in structure by placement of a methyl group; the

methyl group at 3-position in 3-MI does not allow hydrogen bond formation to complementary stranded cytosine whereas 6-MI has a hydrogen at position 3 allowing hydrogen bond formation (Figure 13). Similar to 3-MI, incorporation of 6-MI into an oligonucleotide quenches its fluorescence intensity suggesting that the probe is involved in base stacking interactions (77-79). Upon annealing of single strand oligonucleotides containing 6-MI, further fluorescence quenching is observed due to base pairing (77-79). A greater quenching effect upon annealing is seen for 6-MI labeled oligonucleotides than for 3-MI labeled oligonucleotides, suggesting that the probe is more involved in base pairing than 3-MI (77-79). The involvement of 6-MI in base pairing is further supported by thermal stability studies (77, results: section 3.1.1).

It has been noted that changes in the local structure of the pteridine-containing oligonucleotides can be followed by monitoring changes in fluorescence properties (78,80-83). For example, Wojtuszewski *et al.* observe that an increase in fluorescence intensities of the 3-MI containing oligonucleotides observed upon protein binding result from reduction in base stacking interactions and increase in solvent exposure of the probe (81). In another example, Roca *et al.* describe an increase in the fluorescence intensity of 6-MI

that results from the change in the fluorophore environment such as exposure to the nonpolar binding site or the partial destacking of bases (82).

The work in this thesis is based upon observation of changes in the steady-state emission fluorescence anisotropy of the fluorophore (3-MI) covalently incorporated into oligonucleotide sequence. The model fluorescent oligonucleotides are used in the binding studies with HIV-1 integrase. 6-MI labeled oligonucleotides are used in the studies to provide additional support for data obtained with the oligonucleotides incorporating 3-MI. The following section describes the model oligonucleotides and experimental design.

b. Model Fluorescent Oligonucleotides for Binding Studies with HIV-1 Integrase

Model oligonucleotides used in this study are designed to resemble either U5 or U3 viral DNA ends (Figure 12). The oligonucleotides have sequences identical to the outermost 21 base pairs of U5 or U3 terminus (21- mers) of the HIV-1 genome, or a combination of both (41- mers) (Table 2). Fluorescent pteridine nucleoside analogs, 3-MI or 6-MI (Figure 13), are site-specifically incorporated into oligonucleotide sequences (Table 2). The presence

of the fluorescent probe (3-MI or 6-MI) as part of the oligonucleotide sequence allows quantitative measurements of interactions between HIV-1 integrase and model oligonucleotides with the probe inserted in specific positions. The role of individual bases in the interaction between HIV-1 integrase and the viral DNA ends can then be investigated. In the approach discussed here we have used changes in the fluorescence emission anisotropy of fluorophore (3-MI or 6-MI) covalently incorporated into oligonucleotide sequences to provide direct insight into binding interactions between HIV-1 integrase and model oligonucleotides. The observed steady state anisotropy is related to the rotational movement of the macromolecule. Since formation of the protein-DNA complex increases the molecular mass (decreases rotational diffusion), a corresponding increase in anisotropy values is expected on complex formation.

Hawkins et al. first described a 3'-processing assay for HIV-1 integrase using 3-MI labeled oligonucleotide as a substrate (15). The activity assay provides a means to monitor real time HIV-1 integrase activity at 37°C. The 3'-processing activity of HIV-1 integrase is reduced at lower temperatures. At 20°C HIV-1 integrase 3'-processing activity is greatly reduced or undetectable. Thus, binding of HIV-1 integrase to the model oligonucleotides can be investigated

without complications from the protein's catalytic activity. In a control experiment we established that reduction to this temperature does not cause conformational change of the HIV-1 integrase, making binding studies at 20°C relevant to the catalytic activity of the protein at 37°C.

Schematic Representation of Linear HIV-1 DNA

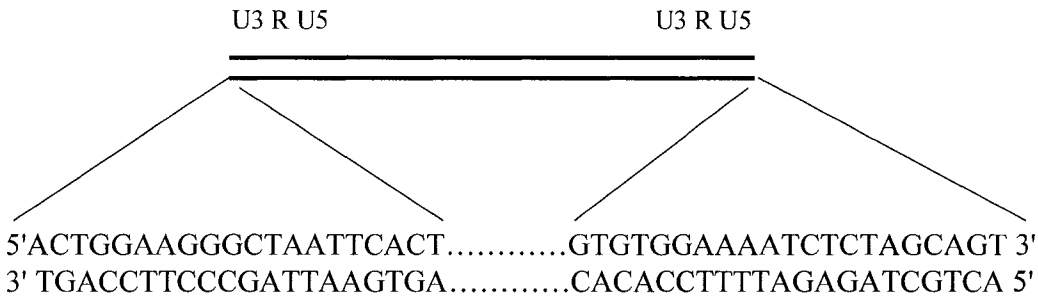

Figure 12. Model oligonucleotide sequences are based on the outermost 21 base pairs of U5 or U3 terminus of HIV-1 linear DNA. P. Hindmarsh and J. Leis. Retroviral DNA integration. Microbiology and Molecular Biology Reviews. 1999, 63(4): 836 - 843.

Table 2.
Base sequence of Single-Stranded Oligonucleotides Without (LTR) and With (PTER) 3-MI (**F**) and/or 6-MI (**F**) Substituted for Guanosine (G) at Various Positions

Name	Oligonucleotide sequence
U5 or U3 based 21bases long labeled oligonucleotides	
PTER2U5	5'-GTG TGG AAA ATC TCT AGC A**F**T-3'
PTER19U5	5'-GT**F** TGG AAA ATC TCT AGC AGT-3'
PTER5U5	5'-GTG TGG AAA ATC TCT A**F**C AGT-3'
PTER14U5	5'-ACT GCT A**F**A GAT TTT CCA CAC-3'
PTER18U5	5'-ACT **F**CT AGA GAT TTT CCA CAC-3'
PTER2U3	5'-AG TGA ATT AGC CCT TCC A**F**T-3'
Random sequence labeled oligonucleotide	
PCR7.1	5'-ACC GCT GAA **F**GA GGA AGC A-3'
Non-cleavable labeled oligonucleotide	
PTER2NC	5'-GTG TGG AAA ATC TCT AG**T G**F**C**-3'
U3andU5 combining 41 bases long labeled oligonucleotides	
PTER2U5-PTER2U3	5'-ACT GCT AGA GAT TTT CCA CAC AGT GAA TTA GCC CTT CCA **F**T-3'
PTER2U3-PTER2U5	5'-ACT GGA AGG GCT AAT TCA CTG TGT GGA AAA TCT CTA GCA **F**T-3'
Complementary strands for U5 terminus 21-mers	
LTR4	5'-ACT GCT AGA GAT TTT CCA CAC-3'
LTR5	5'-GTG TGG AAA ATC TCT AGC AGT-3'
Complementary strand for U3 terminus 21-mer	
LTR3	5'-ACT GGA AGG GCT AAT TCA CT-3'
Complementary strand for random sequence oligonucleotide	
PCR7.1C	5'-TGC TTC CTC CTT CTG CGG T-3'
Complementary strand for non-cleavable oligonucleotide	
PTER2NCC	5'-GCC ACT AGA GAT TTT CCA CAC-3'
Complementary strands combining U3 and U5 sequences	
LTR3-LTR5	5'-ACT GGA AGG GCT AAT TCA CTG TGT GGA AAA TCT CTA G CA GT-3'
LTR4-LTR2	5'-ACT GCT AGA GAT TTT CCA CAC AGT GAA TTA GCC CTT CC A GT-3'

A

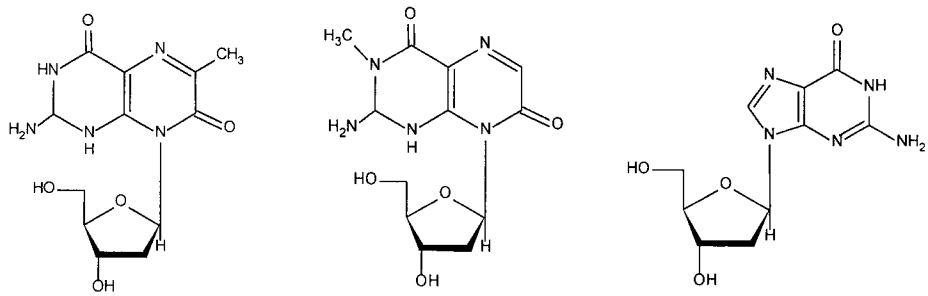

6-MI **3-MI** **G**

B

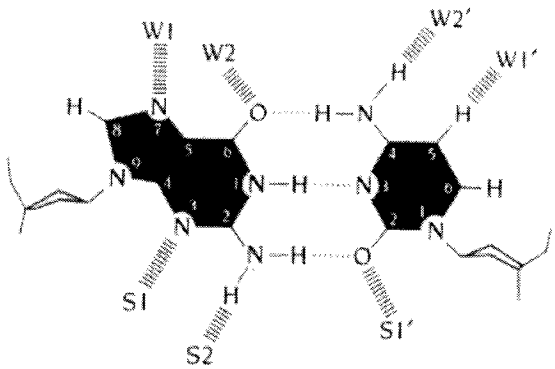

Guanine : Cytosine pair

Figure 13. **(A)** Structures of 3-methyl-8- (2-deoxy-(-D-ribofuranosyl) isoxanthopterin (**3-MI**), 6-methyl-8-(2-deoxy-(-D-ribofuranosyl) isoxanthopterin (**6-MI**), and guanosine (**G**). **(B)** Guanine: Cytosine base pair with hydrogen bonds formed between the bases. Also shown recognition sites at the edges of the base pair in the major groove: W1,W2, W2', and W1' and in the minor groove: S1,S2, and S1'. For GC pair, the major groove exposes a hydrogen bond acceptor, nitrogen 7 of guanine (N7, W1), another acceptor G O6 (W2), a hydrogen bond donor, C NH4 (W2'), and a hydrogen atom at C5 (W1'). In the minor groove for GC pair there is an acceptor G N3 (S1), a donor G NH2 (S2), and an acceptor C O2 (S1') (99).

1.3 Aims of the Study

Investigation of HIV-1 integrase-DNA interactions was carried out to enhance our understanding of the binding and selectivity of HIV-1 integrase for viral DNA. *In vitro* experiments are used to examine HIV-1 integrase interaction with short oligonucleotides in solution. Short oligonucleotides are designed to resemble viral DNA substrates of HIV-1 integrase with sequences identical to the 21 outermost base pairs of the U5 or U3 end of the viral DNA as described in Section 1.2.3 b. In particular, the studies are focused on investigation of possible contacts between bases in oligonucleotide sequences and HIV-1 integrase. Our interests focus on five positions along the length of 21 base pair long oligonucleotides. Availability of fluorescent probes that can be site specifically inserted into oligonucleotide sequences allow us, employing steady state fluorescence anisotropy measurements, to study interactions of HIV-1 integrase with model oligonucleotides in a solution based experimental set up to determine:

1) If binding affinity differences can be detected among five positions of the U5 double stranded model oligonucleotides: three positions of the plus strand and two positions of the minus strand;

2) If binding affinity preferences can be detected for double stranded *versus* single stranded U5 model oligonucleotides;
3) If differences can be observed in binding affinity between 21 base pair long U5 model olgonucleotide and U3 model oligonucleotide, the effect on binding affinity is also investigated with longer oligonucleotides (41 base pair long);
4) If there is a divalent cation preference by HIV-1 integrase in the experimental binding system used: in particular, effectiveness of manganese, magnesium, and zinc cations is investigated.

Chapter 2: MATERIALS AND METHODS

2.1 Synthesis and Purification of Fluorescent Oligonucleotides

All single-stranded oligonucleotides containing 3-MI or 6-MI were synthesized as described previously (79). Oligonucleotides were purified using a 20 % denaturing polyacrylamide gel, visualized by UV shadowing, and eluted from the gel by electroelution (Schleicher and Schuell, Concord, NH) followed by ethanol precipitation. Purified oligonucleotides were stored at -70°C either as a pellet or dissolved in 10 mM Tris, pH 7.5, with 10 mM NaCl. The concentration of oligonucleotides was estimated from the absorbance at 260 nm using extinction coefficients calculated by the method described by Brown et al. (84).

2.1.1 Hybridizations and DNA Melting Studies

Complementary oligonucleotide strands were annealed to form double-stranded oligonucleotides by mixing equimolar amounts of each strand in 10 mM Tris, pH 7.5, with 10 mM NaCl, heated at 85 °C for 5 minutes, and allowed to cool slowly to room temperature. Melting temperatures of double-stranded oligonucleotides were

measured by monitoring absorbance hyperchromicity at 260 nm in a Pharmacia Biotech Ultrospec 2000 spectrophotometer equipped with a Pharmacia Biotech Peltier temperature controller using quartz cuvettes with 0.3 cm optical path length. Melting profiles were measured in 10 mM Tris, pH 7.5, with 10 mM NaCl. The samples were heated from 30 °C to 80 °C in increments of 1°C. To avoid evaporation of the solvent, a layer of liquid paraffin was placed on the surface of the sample and the cuvette was tightly stopped with a Teflon plug and Parafilm. The melting temperatures (T_m) were estimated from the maximum of the first derivative curve of the absorbance at 260 nm versus temperature.

2.2 Purification and Characterization of HIV-1 Integrase

HIV-1 integrase carrying the N-terminal 6xHis affinity tag was a gift from Dr. Eugene Barsov (NCI, Frederick, Maryland). Full-length HIV-1 integrase was expressed in *E.coli* BL21(DE3)pLysS cells and purified as described elsewhere (85). The protein aliquots were stored at -70°C in the integrase storage buffer: 20mM N-2-hydroxyethylpiperazine-N'-ethanesulfonic acid (HEPES, pH 7.5),

1mM EDTA, 10mM 3-[(3-cholamidopropyl)dimethylammonio]-1-propanesulfonate (CHAPS), 570 mM NaCl.

Studies described by Hickman *et al.* show that the His-tag does not perturb the overall conformation of the IN^{50-212} protein (circular dichroism studies), tertiary structure (fluorescence studies), and the self-association properties of IN^{50-212} (analytical centrifugation). However, stimulation of the disintegration activity by His-tag was detected (65). His-tag appears to enhance the nonspecific DNA binding activity of IN^{50-212} (65). In contrast, Pemberton *et al.* argues that the presence of the His-tag in truncated protein, such as IN^{50-212} may be important in maintaining the native structure and activity of this domain, and does not influence nonspecific DNA binding (29). Pemberton and coworkers show that binding parameters of His-tagged full-length HIV-1 IN is similar to that of the processed integrase (29). Bushman *et al.* shows that His-tag has no influence on disintegration activity of full-length IN^{1-288}, or deletion mutants IN^{50-288}, IN^{50-263} (40). Therefore, the experiments described herein were conducted with the His-tagged full-length HIV-1 integrase.

Protein concentrations were determined based on absorbance at 280 nm using an extinction coefficient of 50470 $M^{-1}cm^{-1}$ (1.56 ml mg^{-1} cm^{-1}) per monomeric subunit (65).

For dilutions of stock HIV-1 integrase the following buffer was used: 20 mM HEPES pH 7.5, 1 mM EDTA, 1mM dithiothreitol (DTT), 570 mM NaCl.

Purity of HIV-1 integrase was verified by running 15% acrylamide 0.1% SDS-PAGE (Figure 14).

2.2.1 HIV-1 integrase Activity Assay

The HIV-1 integrase 3'-processing activity was tested routinely using a method previously described by Hawkins *et al.* (79). The system employs fluorescently labeled oligonucleotides where the fluorescent guanosine analog, 3-MI, is site-specifically inserted into the cleavage site of the double-stranded 21-mer U5 oligonucleotide substrate (77). Real-time 3'-processing activity of HIV-1 integrase is monitored at 37°C as an increase in fluorescence intensity due to cleavage of the 3'-terminal dinucleotide with guanine (G) substituted by 3-MI. The reaction mixture for the integrase assay contained 25 mM 3-morpholinopropanesulfonic acid (MOPS), pH 7.2, 7.5 mM

$MnCl_2$, 10mM 2-mercaptoethanol, 0.1 nM 3-MI-containing oligonucleotide substrate (PTER2U5:LTR4), and 285 nM (monomer) HIV-1 integrase in a total volume of 60 μl. The reaction mixture was incubated at 37°C. Activity was monitored by observing the increase in fluorescence intensity due to release of the 3-MI containing dinucleotide during 3'-processing: when incorporated the 21 base pair long oligonucleotide, the fluorescence intensity of 3-MI is quenched. Therefore, upon release of the probe as a part of dinucleotide product of 3'-processing reaction, an increase in fluorescence intensity is observed due to relief of quenching of 3-MI fluorescence. The samples were excited at 360 nm and emission was measured at 460 nm as a function of time. The reaction was carried out in $3\times3mm^2$ quartz cuvettes. Steady-state fluorescence intensities were monitored with a Fluorolog-tau3 spectrofluorometer (SPEX Industries, Edison, NJ) using a 450W xenon arc lamp as a light source, double excitation monochromator to minimize light scattering, and photon counting emission electronics. The sample temperature was maintained at 37°C with a circulating water bath (VWR Scientific Inc., Niles, IL).

2.3 Spectroscopic Methods for Binding Studies

The reaction solution for studies of HIV-1 IN-oligonucleotide binding using fluorescence emission anisotropy measurements contained 25 mM MOPS buffer at pH 7.2, 10 mM 2-mercaptoethanol, 7.5 mM $MnCl_2$, Millipore water, and a fixed concentration of the oligonucleotide substrate (0.1 nM) in a total volume of 58 μl. HIV-1 integrase diluted in buffer: 20 mM HEPES pH 7.5, 1 mM EDTA, 570 mM NaCl, was added in 0.5 μl (48 nM) aliquots. The final concentration of HIV-1 integrase was 714 nM (7.5 μl total volume added). Polarized fluorescence emission intensities were measured at 20 °C after each integrase addition and fluorescence emission anisotropy values were calculated according to equation 2. In this manner, the total volume increases 11.5% (58 → 65.5μl) for each titration experiment. In a control experiment for dilution effects, the fluorophore labeled substrate was titrated with HIV-1 integrase storage buffer and no significant decrease in fluorescence intensity was observed indicating no dilution effects on the fluorescence intensity values.

With solution viscosity staying constant throughout the titration, depolarization of the fluorescence intensity is predominantly influenced by rotational diffusion of the fluorophore and therefore

reflects its mobility. The greater the freedom of rotation of the fluorophore, the more depolarized is the emission (74). To analyze steady-state emission anisotropy that reflects changes in fluorescence polarization, parallel and perpendicular fluorescence emission components were measured in all four possible polarization combinations of vertical (v, 0°) or horizontal (h, 90°) alignment, I_{VV}, I_{VH}, I_{HV}, and I_{HH}, in L-format at 460 nm with excitation at 360 nm using a 450-W xenon arc lamp (SPEX, Fluorolog-τau3). For all emission anisotropy values, the equivalent parallel and perpendicular intensities of the background buffer solution were first subtracted from the corresponding measured polarized intensity values of the sample. The emission anisotropy was calculated according to formula 2:

$$< r > = \frac{I_{VV} - GI_{VH}}{I_{VV} + G2I_{VH}}$$

where I_{VV} is vertical intensity, I_{VH} is horizontal intensity, and $G = \frac{I_{HV}}{I_{HH}}$, is the grating factor, a correction for the instrument response to transmission of vertical or horizontal polarized light at a particular emission wavelength as described previously. Emission anisotropy values were calculated at each titration point from polarized

fluorescence intensity measurements with an integration time of 10 sec for each intensity measurement; each anisotropy point in the titration takes approximately 5 min for acquisition. Average emission anisotropy values of at least 3 separate binding experiments are reported as the final values.

The total fluorescence intensity (FI) was determined from the sum of polarized emission intensities as: $FI = I_{VV} + G2I_{VH}$. These values were used to determine the percent of the maximum fluorescence for each data point in the titration to follow any changes in intensity that may occur during protein binding to the labeled oligonucleotides.

All measurements were done at 20°C, and the sample temperature was maintained with a circulating water bath (VWR Scientific Inc., Niles, IL). $3\times3mm^2$ quartz cuvettes were used for the measurements.

2.3.1 Analysis of Binding Parameters

For a mixture of species with the same fluorescent intensity (lifetime) but different emission anisotropy values, the measured total anisotropy is the sum of the contributing mole fractions of each

individual anisotropic species (74). Thus, fluorescence anisotropy observed when free (f) and bound (b) forms are present is:

$$\langle r \rangle = F_f \langle r \rangle_f + F_b \langle r \rangle_b \qquad F_f + F_b = 1 \qquad (6)$$

where $\langle r \rangle_f$ and $\langle r \rangle_b$ are anisotropies of free and bound fluorescent labeled molecules respectively, and F_f is a fraction of the total fluorescent labeled molecules which is present in a free form, and F_b is a fraction of the total fluorescent labeled molecules which is present in bound form. Therefore, the fraction bound is:

$$F_b = \frac{\langle r \rangle - \langle r \rangle_f}{\langle r \rangle_b - \langle r \rangle_f} \qquad (7)$$

where $\langle r \rangle$ is a measured anisotropy in a mixture of free and bound fluorescent molecules.

In these studies, for the simple binding interaction between HIV-1 integrase (IN) and oligonucleotide (DNA) assuming independent single-site binding mechanism:

$$IN + DNA \Leftrightarrow IN\text{–}DNA$$

The dissociation constant will be:

$$K_D = \frac{[DNA][IN]}{[IN\text{–}DNA]}$$

$$[IN_t] = [IN] + [IN\text{–}DNA]$$

$$[DNA_t] = [DNA] + [IN\text{–}DNA]$$

$$K_D = \frac{([DNA_t] - [IN\text{–}DNA])([IN_t] - [IN\text{–}DNA])}{[IN\text{–}DNA]}$$

When $[IN] \cong [IN_t]$,

$$K_D = \frac{([DNA_t] - [IN\text{–}DNA])[IN]}{[IN\text{–}DNA]}$$

Solving for [IN–DNA],

$$[IN\text{–}DNA] = \frac{[DNA_t][IN]}{K_D + [IN]}$$

Thus,

$$F_b = \frac{< r > - < r >_f}{< r >_b - < r >_f} = \frac{[IN\text{–}DNA]}{[DNA_t]} = \frac{[IN]}{K_D + [IN]}$$

And

$$<r> = <r>_f + (<r>_b - <r>_f) \left[\frac{[IN]}{K_D + [IN]} \right] \qquad (8)$$

where <r> is the measured emission anisotropy at a particular total concentration of HIV-1 IN, $<r>_f$ is an anisotropy of free fluorescent labeled oligonucleotide prior to addition of HIV-1 IN, $<r>_b$ is an anisotropy of the oligonucleotide bound by HIV-1 IN, and K_D, the apparent dissociation constant, represents concentration of HIV-1 integrase monomers required to titrate the oligonucleotide substrate to half saturation (86-90).

Equation 8 is fitted to the binding data (anisotropy vs [IN]) by a nonlinear least-squares regression using program Sigma plot 7.0, giving initial parameter estimates for $\langle r \rangle_b$, $\langle r \rangle_f$, and K_D.

The quality of the fit was assessed by a correlation function (R^2), where values greater than 0.9 were judged as a good fit.

Analysis of binding parameters for random sequence oligonucleotide (PCR7.1)

For the random sequence oligonucleotide a multiple binding site expression (equation 9) was required to fit to the binding data. Equation 9 was fitted to the binding data by a nonlinear least-squares regression analysis using the program, Sigma plot 7.0.

$$\langle r \rangle = \langle r \rangle_f + (\langle r \rangle_b - \langle r \rangle_f)\left[\frac{1}{1+\left(\frac{[IN]}{K_D}\right)^b}\right] \qquad (9)$$

In the equation, $\langle r \rangle$ is the measured emission anisotropy at a particular total concentration of HIV-1 IN, $\langle r \rangle_f$ is the anisotropy of free fluorescent labeled oligonucleotide prior to addition of HIV-1 IN, $\langle r \rangle_b$ is the anisotropy of the oligonucleotide bound by HIV-1 IN, K_D is the apparent dissociation constant, and b represents number of the

binding sites (86-90). Initial parameters for $\langle r \rangle_b$, $\langle r \rangle_f$, and K_D were estimated from the fit. The quality of the fit was assessed by a correlation function (R^2), with $R^2 > 0.9$.

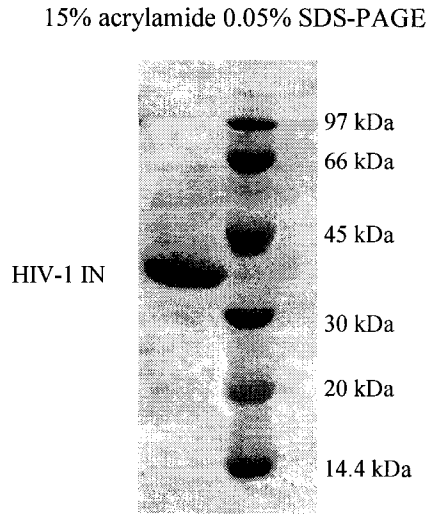

Figure 14. 15% acrylamide 0.05% SDS-PAGE of HIV-1 integrase at 100 °C. Shown are molecular calibration references: 97 kDa - phosphorylase b, 66kDa - bovine serum albumin, 45 kDa - ovalbumin, 30 kDa - carbonic anhydrase, 20 kDa - trypsin inhibitor, 14.4 kDa - α-lactalbumin. HIV-1 integrase migrates as a monomer (MW ≈ 32 kDa).

Chapter 3: RESULTS

3.1 Fluorescent Oligonucleotides as Substrates for HIV-1 Integrase

3.1.1 Thermal stability of Labeled Oligonucleotides

Thermal stabilities of probe-containing double stranded oligonucleotides were evaluated by determining melting temperatures. To determine melting temperatures of model oligonucleotides, the absorbance hyperchromicity was monitored at 260 nm as described in the Methods section. All melting curves showed typical sigmoidal behavior with only one apparent transition. Table 3 summarizes the melting temperatures (T_m) obtained. T_m values determined for the 3-MI-containing oligonucleotide (PTER2U5:LTR4(3-MI)) are depressed by approximately 7 °C relative to the control oligonucleotide of the same sequence that does not contain 3-MI. The temperature depression is comparable to a decrease in T_m associated with single base mismatch in duplex oligonucleotides of the same sequence and length suggesting that 3-MI does not participate in base pairing in double-stranded oligonucleotides (77). In contrast, T_m values for the 6-MI containing oligonucleotide (PTER2U5:LTR4(6-

MI)) were not depressed compared with the identical oligonucleotide containing no fluorophore suggesting that 6-MI may participate in base pairing (77).

Table 3.
Melting temperatures (T_m) of oligonucleotides with [1]fluorophore incorporated at position 2 and without fluorophore.

Oligonucleotide	[2] **T_m (°C) ± s.d.**
LTR5:LTR4 5'-GTG TGG AAA ATC TCT AGC A**G**T -3' 3'-CAC ACC TTT TAG AGA TCG TCA -5'	57.2 ± 0.7
PTER2U5:LTR4(3-MI) 5'-GTG TGG AAA ATC TCT AGC A**F**T -3' 3'-CAC ACC TTT TAG AGA TCG TCA -5'	50.3 ± 1.1
PTER2U5:LTR4(6-MI) 5'-GTG TGG AAA ATC TCT AGC A**F**T -3' 3'-CAC ACC TTT TAG AGA TCG TCA -5'	58.6 ± 0.7

[1]**F** shows position at which fluorophore, 3-MI or 6-MI, is incorporated.

[2]average T_m and standard deviations are calculated from a minimum of three trials of thermal denaturation for each double-stranded oligonucleotide.

3.1.2 HIV-1 Integrase 3'-processing Activity

Sequence specific endonucleolytic cleavage of a dinucleotide, 3'- processing, is the first reaction in the integration process. Using double-stranded oligonucleotide (21-mer) with the U5 terminus specific sequence of HIV-1 DNA as a substrate, HIV-1 integrase 3'-processing activity was monitored at 37°C. The fluorophore (3-MI) is site-specifically incorporated into the cleavage site of a double-stranded oligonucleotide substrate (PTER2U5:LTR4). Cleavage of the 3'-terminal dinucleotide containing 3-MI results in a measurable real time increase in fluorescence intensity (Figure 15). The activity is greatly reduced or undetectable at 20°C (Figure 15) allowing a study of HIV-1 integrase binding to model oligonucleotides without interference from 3'-processing catalytic activity at that temperature.

3'-processing activity was routinely tested using the U5 21-mer (PTER2U5:LTR4 3-MI) substrate to evaluate the integrity of HIV-1 integrase before collecting binding data.

A **HIV-1 integrase 3'- processing activity assay**

5' - GTGTGGAAAATCTCTAGCA**F**T - 3'

3' - CACACCTTTTAGAGATCGTCA - 5'

HIV-1 IN

5'- GTGTGGAAAATCTCTAGCA - 3' + **F**T - 3'

3'- CACACCTTTTAGAGATCGTCA - 5'

B

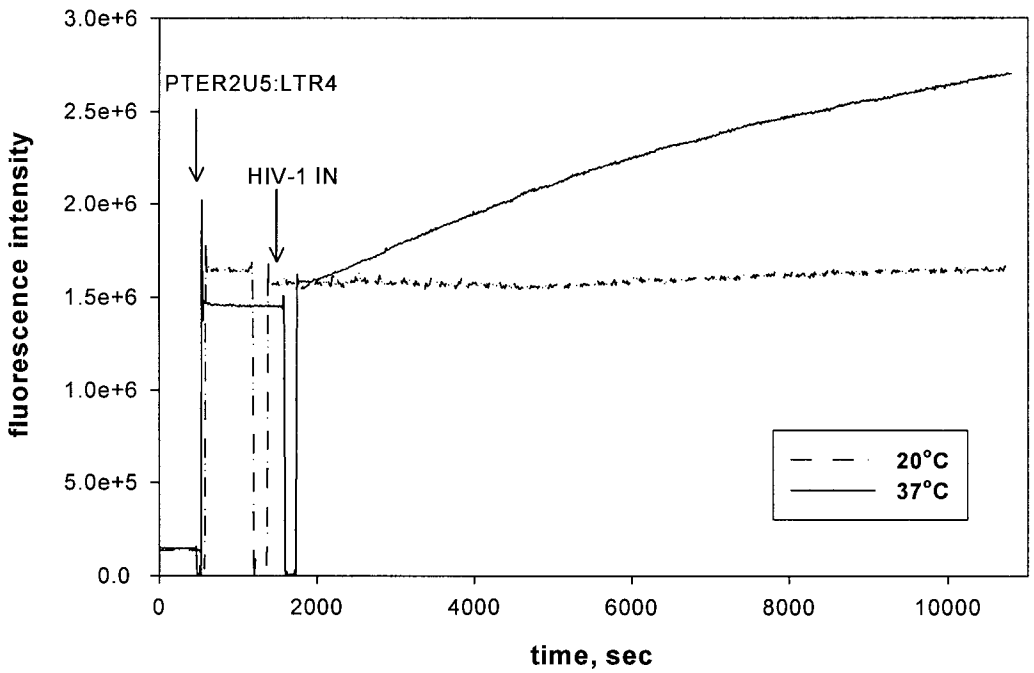

Figure 15. (A) schematic presentation of HIV-1 integrase 3-processing reaction with the fluorophore (**F**) position shown, (B) HIV-1 integrase activity assay. Fluorescence intensity of reaction mixture is monitored prior to addition of 3-MI labeled oligonucleotide (PTER2U5:LTR4). Fluorescence intensity of oligonucleotide in the reaction mixture is monitored before addition of HIV-1 IN and is constant. After addition of HIV-1 IN, the increase in fluorescence intensity is followed over time. Activity is monitored at 37 °C (solid line) and is greatly reduced at 20 °C (broken line).

3.1.3 Effect of Temperature Change on Oligonucleotide Binding

Because there is a possibility that changes in temperature may alter the conformation of HIV-1 integrase making binding studies at 20°C less relevant to the catalytic activity of the protein at 37°C, a control experiment was conducted using a non-cleavable substrate. In this experiment, binding affinities of HIV-1 integrase with non-cleavable substrate at 20°C and 37°C were compared. Complementary base-pair substitutions at positions 1,3, and 4 of the U5 21-mer (position 1: T/A →C/G, position 3: A/T → G/C, position 4: C/G → T/A) make the substrate unsuitable for 3'-processing by HIV-1 integrase (Table 2). Because of such sequence changes in the oligonucleotide, HIV-1 integrase was not able to process the non-cleavable substrate at 37°C. Thus, binding of HIV-1 IN to the non-cleavable substrate at 20°C and 37°C was compared without interference from catalytic activity (Figure 16). The binding data was fitted using equation 8. Similar K_D^{app} values obtained for the non-cleavable substrate at 20°C (255 ± 40 nM) and at 37°C (208 ± 52 nM) suggest that a change in temperature does not significantly affect the binding affinity of HIV-1 integrase, and therefore, does not appear to significantly affect the HIV-1 integrase conformation to the extent

that it influences the protein's binding to oligonucleotides in the system employed.

Non-cleavable substrate

5'- GTG TGG AAA ATC TCT AGT G*F*C -3'
3'- CAC ACC TTT TAG AGA TCA CCG -5'

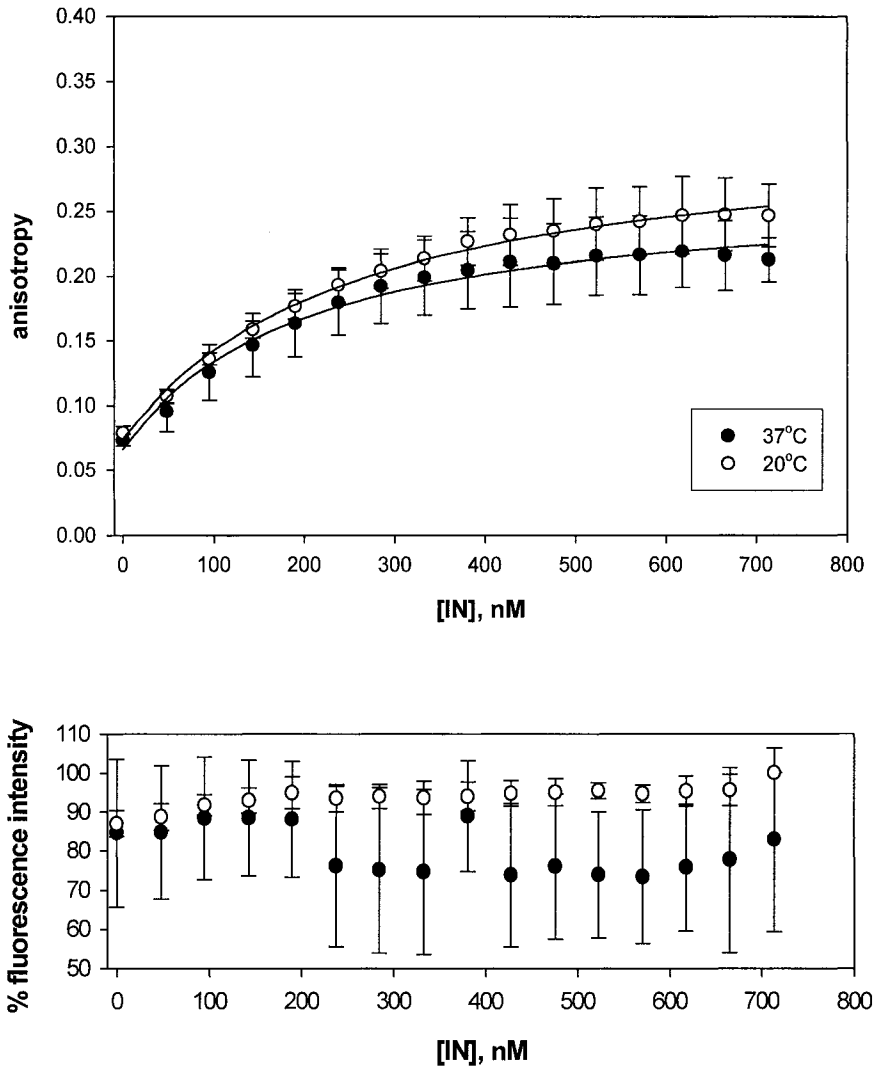

Figure 16. Binding of HIV-1 IN to the non-cleavable oligonucleotide. Anisotropy is measured as a function of total HIV-1 IN added to the binding reaction. Open circles represent binding at 20°C. Filled circles represent binding at 37°C. The concentration of the non-cleavable oligonucleotide is constant throughout the titration and is 0.1 nM. Concentration of HIV-1 IN added varies from 48 nM at the start of titration to 714 nM at the end of titration with HIV-1 IN added in 0.5 μl aliquots. Binding data are fitted using a nonlinear least squares regression to the equation described in the Methods, and the best fit is plotted as a solid line. The bottom panel shows the % fluorescence intensity as a function of HIV-1 IN concentration.

3.2. U5 Double Stranded Model Oligonucleotide Substrates

Binding affinities of HIV-1 integrase to several positions along U5 model double stranded oligonucleotides were investigated. As discussed previously, three sites for 3-MI on the plus strand of the U5 end model oligonucleotide were chosen: position 2 (oligonucleotide PTER2U5:LTR4), position 5 (oligonucleotide PTER5U5:LTR4), and position 19 (oligonucleotide PTER19U5:LTR4). In addition, two nucleotide positions on the minus strand of the U5 model oligonucleotide were investigated: position 4 (oligonucleotide PTER18U5:LTR5) and position 8 (oligonucleotide PTER14U5:LTR5).

The importance of the guanine bases at positions 2 and 5 on the plus strand, and position 4 on the minus strand for efficient HIV-1 integrase 3'-processing function with short oligonucleotides *in vitro* is well established in literature reports (14,48,46,66,91-97). Therefore, it is interesting to see if these same positions are also important for HIV-1 integrase contact during binding.

In addition, we chose to investigate the role of guanine bases located several bases away from the active end of the oligonucleotide. It is interesting to note if the observed binding affinity of HIV-1

integrase changes as the distance from the cleavage site increases. For PTER19U5:LTR4, position 19 of the plus strand is seventeen oligonucleotides away from the active end of the oligonucleotide. Therefore we investigated if there were any differences in binding affinities with the label at position 19 compared to binding with label at positions closer to the site of HIV-1 integrase 3'-processing. Similarly, position 8 of the minus strand is several bases removed from the active end of the U5 model oligonucleotide. Results of the binding studies are presented for each of the five positions of the double stranded U5 model oligonucleotides (sections 3.2.1-3.2.2) followed by the summary of the results for these five positions. Figure 17 shows each position along the U5 model oligonucleotide and corresponding oligonucleotide names with the probe in a particular position.

A

WT U5 oligonucleotide

B

Labeled U5 oligonucleotides

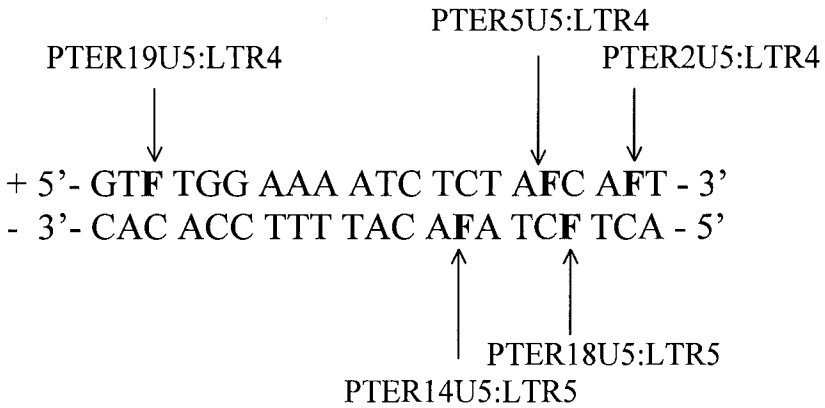

Figure 17. (**A**) Sequence of U5 21 base-pair long oligonucleotide. (**B**) Labeled oligonucleotides with position of fluorophore (**F**) presented.

3.2.1 Labeling of the Plus Strand

a. Studies with Label at the 3'-processing (position 2 from 3'-end)

Guanine at position 2 of the plus strand is at the cleavage site. The base is removed as a part of dinucleotide (GT) during the 3'-processing by HIV-1 integrase. Therefore, for efficient 3'-processing it is expected that this guanine plays a critical role in binding with HIV-1 integrase. Indeed, several reports have established, using base substitutions and mismatches, the importance of the presence of the guanine in position 2 of the DNA substrate for efficient HIV-1 IN-DNA complex formation, and 3'-processing and joining activities of HIV-1 integrase.

Mutations at position 2 reduce 3'-processing activity

Previous studies have shown that mutations at position 2 of the plus strand (PTER2U5:LTR4) significantly reduce 3'-processing activity (48,66). Specific cleavage at position 2 was reduced three fold by mutation (GT $\rightarrow$ CA) of the terminal two bases of the plus strand (66). When cytosine (C) or adenine (A) are substituted for guanine (G) at position 2, 3'-processing activity is reduced 50% and 70% respectively with manganese (Mn^{2+}) as a metal cofactor (48). More dramatic reduction (90%) in the rate of 3'-processing was observed

with magnesium (Mg^{2+}) as a metal cofactor for both substitutions (48). In contrast, substitution of guanine (G) with thymine (T) at position 2 of the plus strand resulted in 3'-processing activity comparable to wild-type substrate (48). Furthermore, substitution of G2 by T in the plus strand was also shown to slightly enhance integration (93).

The base at position 2 is involved in HIV-1 integrase – DNA complex formation

From UV cross-linking assay studies, Yoshinaga *et al.* have suggested that the terminal two nucleotides of the plus strand play an important role in the 3'-processing step by forming a pre-cleavage complex with HIV-1 integrase (91). Yoshinaga *et al.* also noticed that formation of complexes between HIV-1 IN and the U5 substrate missing two bases from the 5'end on the minus strand was similar to the formation of complexes between HIV-1 IN and the substrate with all bases present (91). Similarly, the absence of the two outermost bases on the minus strand did not result in reduction of the 3'-processing activity (91). Thus, it appears that the terminal two nucleotides from the 5'end of the minus strand do not play a critical

role in the formation of the complexes between HIV-1 IN and DNA or the 3'-processing of the plus strand (91). Deletion of these bases, however, greatly diminishes joining activity although complex formation appears to be similar to wild-type substrate (91).

Noncomplementary base pair substitutions at position 2 stimulate 3'-processing

In the substitution studies that compare complementary substitutions with noncomplementary base pair substitutions, complementary substitutions (G/C → A/T or G/C → T/A) in the second position resulted in a 3 to 5-fold reduction in the 3'-processing activity when compared to the wild-type substrate (94). Noncomplementary base pair substitutions (G/C → A/A or G/C → T/T) at the second position resulted in a 6 to 7-fold increase in 3'-processing activity compared to complementary substitution (94). Thus, substrates with noncomplementary base pair substitutions were better for 3'-processing reaction than the wild type substrate (94). The base at position 2 of the plus strand does not need to be matched to the complementary base of the minus strand for efficient 3'-processing activity (94). Thus, destabilization of the Watson-Crick base-pairing

in the position 2 as well as positions 1 and 3 of the U5 end by introduction of mismatched base pairs appears to enhance 3'-processing suggesting that these bases are unpaired during the reaction (94).

In summary, G → C or G → A mutations at position 2 of the plus strand result in reduced 3'-processing by HIV-1 integrase. G → T substitution at position 2 appears to be better tolerated by HIV-1 integrase. Mismatched base pair substitutions at position 2 appear to enhance 3'-processing by HIV-1 integrase.

Experimental results

3-MI at position 2 (PTER2U5:LTR4 3-MI)

For the binding studies, a fixed concentration (0.1 nM) of the U5 21 base pair long oligonucleotide with 3-MI incorporated at position 2 (PTER2U5:LTR4) was titrated with HIV-1 integrase and changes in the steady state emission anisotropy were monitored as a function of total HIV-1 IN concentration added at 20°C (Figure 18). The steady state fluorescence anisotropy increases in a hyperbolic fashion with each successive addition of HIV-1 integrase to the oligonucleotide in the binding reaction solution, and reaches a

saturation plateau at 400 nM integrase concentration. The hyperbolic nature of the concentration dependence of the binding suggests that the binding of HIV-1 integrase with PTER2U5:LTR4 proceeds via an independent, single-site binding mechanism. The EA data were fitted using equation 8 by a nonlinear least squares regression as described in Materials and Methods, and the apparent K_D value of 119 ± 21 nM was determined from the fit (Table 4). As shown in Figure 18 (open circles), under conditions where higher concentrations of the fluorescent oligonucleotide (1.0 nM) were titrated using the same concentration range for added HIV-1 integrase, the emission anisotropy values show an increase without reaching saturation. This surprising result may reflect altered oligonucleotide association in solution at those higher concentrations. Therefore, we chose to use a higher integrase to oligonucleotide molar ratio for these studies, which was achieved by addition of HIV-1 integrase (from 48 nM to 714 nM) to a fixed lower 0.1 nM oligonucleotide concentration. The corresponding fluorescence intensities for the same HIV-1 integrase :oligonucleotide mole ratios increased ~ 40 % with HIV-1 integrase binding (Figure 18) suggesting that a local conformational change of the oligonucleotide structure is involved during binding.

Conformational changes (such as bending and unwinding) can reduce base stacking interactions resulting in an increase in fluorescence intensity of the 3-MI probe (77).

In a control experiment, the effect of modification of the oligonucleotide by substitution of guanine in position 2 using 3-MI was assessed through a competition assay. There HIV-1 integrase was titrated into the binding solution containing equimolar concentrations of labeled (PTER2U5:LTR4) and unlabeled (LTR5:LTR4) oligonucleotides. The unlabeled oligonucleotide serves as a competitor for binding against the labeled oligonucleotide. Under conditions where HIV-1 integrase has a significantly different affinity for the unlabeled oligonucleotide over the fluorescently labeled one, the apparent binding constant will reflect the presence or absence of the unlabeled oligonucleotide. The measured binding curve (Figure 19) for the competition titration is slightly shifted to the right, as compared to the binding curve of the labeled oligonucleotide alone, suggesting a somewhat lower binding affinity for the labeled oligonucleotide. This is reflected in the value of the apparent dissociation constant. The K_D^{app} value of 222 ± 8 nM (Table 4) for the competition titration is twice the K_D^{app} value for the labeled

oligonucleotide alone suggesting that HIV-1 integrase can bind both the labeled and the unlabeled substrates with similar affinity and without preference.

6-MI at position 2(PTER2U5:LTR4 6MI)

Since 3-MI is not able to form proper Watson-Crick pair with the complementary cytosine base as shown by melting temperature results (Results, section 3.1.1; 77,79), studies with 6-MI in the second position were conducted to determine if there is any affect of the fluorophore on the efficiency of contact between HIV-1 integrase and position 2 of the DNA 21-mer. The resulting apparent K_D value of 282 ± 66 nM is 2.4 times greater than the K_D^{app} value of the corresponding 3-MI containing substrate (Figure 20, Table 4). These results suggest that the binding affinity of HIV-1 IN to position 2 of the DNA substrate is slightly greater for the mismatch pair (3-MI/C) than for the better matching pair (6-MI/C). Interestingly, the activity assay for HIV-1 integrase with the 6-MI substituted oligonucleotide substrate showed slower 3'-processing under conditions identical to those used for 3-MI labeled oligonucleotide. Thus, in addition to favored binding for mismatch, HIV-1 integrase may also favor unpaired bases at position 2 for efficient 3'-processing.

It is interesting to note that emission anisotropy values for 6-MI containing 21-mer PTER2U5:LTR4 free in solution (prior to the HIV-1 integrase addition) are higher (~ 0.2) than initial anisotropy values for the same oligonucleotide containing 3-MI (~ 0.07). The higher anisotropy values may reflect more restricted rotational freedom of the 6-MI fluorophore within the oligonucleotide. The overall anisotropy change upon HIV-1 integrase binding for 6-MI containing oligonucleotide is also different (Table 4). For 6-MI containing oligonucleotide anisotropy change (Δr) is 0.10 ± 0.01 units whereas Δr for the 3-MI containing oligonucleotide is 0.17 ± 0.03 units upon HIV-1 integrase binding (Table 4). Thus, 6-MI located at position 2 of the oligonucleotide bound by HIV-1 integrase appears to retain a higher degree of rotational freedom than 3-MI at position 2.

As observed for the 3-MI containing PTER2U5:LTR4, competition experiments employing the 6-MI labeled oligonucleotide revealed a binding curve (Figure 21) that is slightly shifted to the higher protein concentration ($K_D^{app} = 343 \pm 66$ nM) compared to that observed for the binding of 6-MI containing oligonucleotide only (282 $\pm$ 66 nM) titration. Thus, similarly to 3-MI labeled oligonucleotide, HIV-1 integrase does not appear to demonstrate any significant

preference for 6-MI labeled oligonucleotide over the corresponding unlabeled oligonucleotide.

PTER2U5:LTR4

5'- GTG TGG AAA ATC TCT AGC AFT -3'
3'- CAC ACC TTT TAG AGA TCG TCA -5'

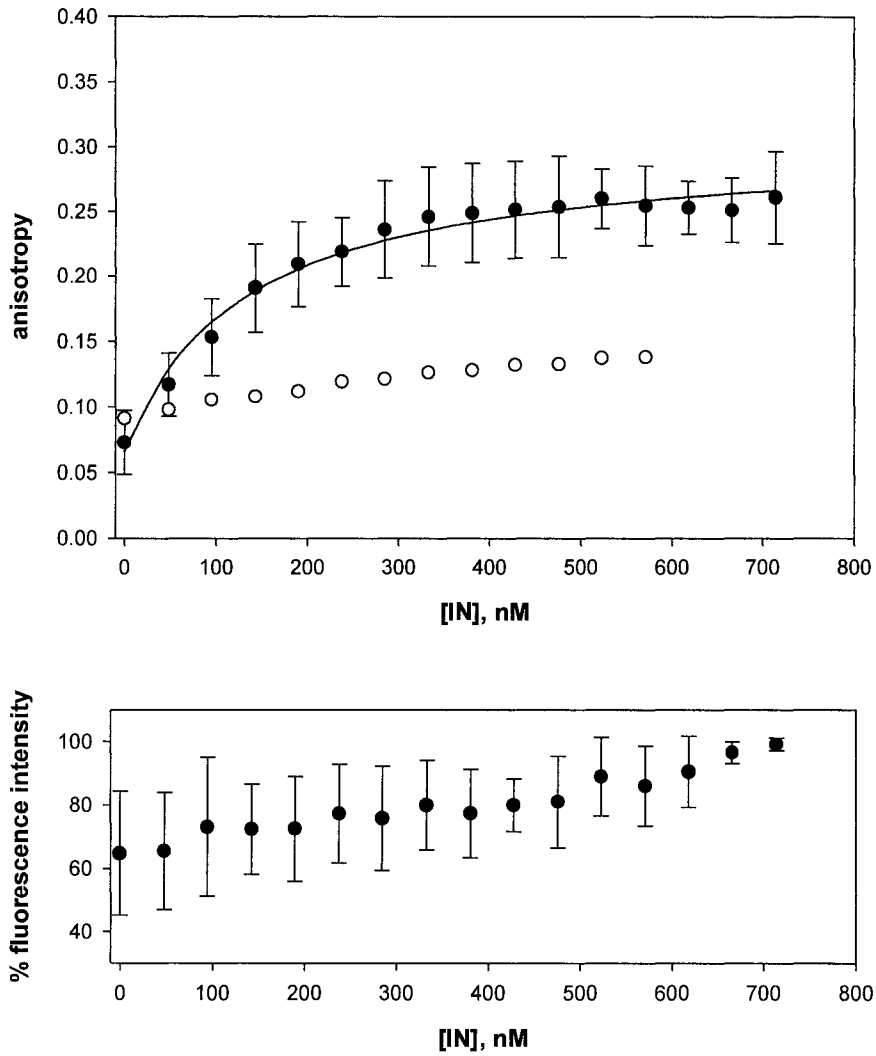

Figure 18. Binding of HIV-1 IN to the U5 model substrate labeled at position 2 of the plus strand (PTER2U5:LTR4). Top figure shows change in steady state emission anisotropy as a function of total HIV-1 IN concentration added. The concentration of HIV-1 IN added varies from 48 nM at the start of titration to 714 nM at the end of titration with HIV-1 IN added in 0.5 µl aliquots. Filled circles (•) represent binding data obtained with the concentration of PTER2U5:LTR4 oligonucleotide fixed throughout the titration at 0.1 nM. These binding data are fitted using a nonlinear least squares regression to the equation described in the Methods. The best fit is plotted as a solid line, and the apparent K_D value is obtained from the fit. Open circles (o) show data obtained where the concentration of PTER2U5:LTR4 oligonucleotide is fixed throughout the titration at 1.0 nM. The bottom panel shows the % fluorescence intensity as a function of HIV-1 IN concentration.

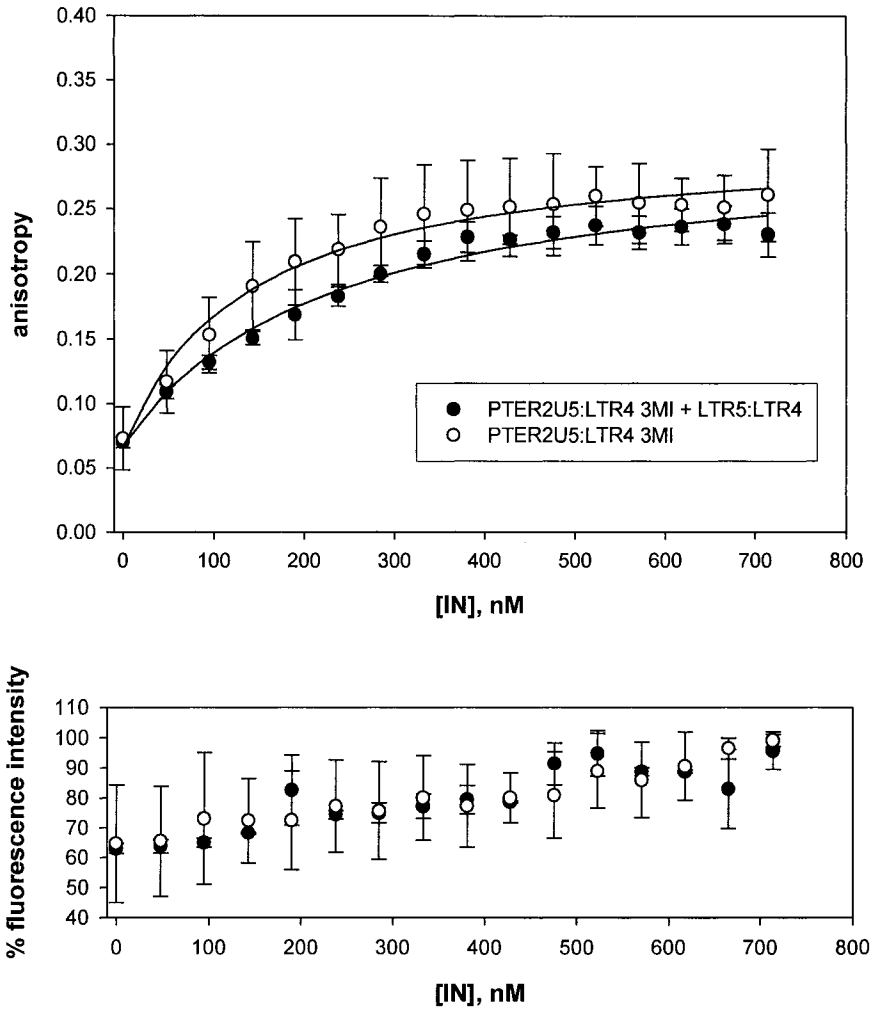

Figure 19. Equimolar concentrations of PTER2U5:LTR4 3MI and LTR5:LTR4 (0.1 nM each) are titrated with HIV-1 IN. Open circles represent binding data obtained for PTER2U5:LTR4 3MI titrated with HIV-1 IN. Filled circles represent binding data obtained for PTER2U5:LTR4 titrated with HIV-1 IN in the presence of LTR5:LTR4. Data are fitted as described in Methods. The best fits are shown as solid lines. The bottom panel shows the % fluorescence intensity as a function of HIV-1 IN concentration added.

Table 4.
Titration of U5 double stranded model oligonucleotides with HIV-1 integrase

oligonucleotide	$K_D^{app\ 1} \pm$ s.d.[2](nM)	$\Delta r \pm$ s.d.	$\langle r \rangle_{min} \pm$ s.d.
Non-cleavable 37°C	208 ± 52	0.14 ± 0.02	0.065 ± 0.005
Non-cleavable 20°C	255 ± 40	0.17 ± 0.02	0.074 ± 0.008
PTER2U5:LTR4 3MI	119 ± 21	0.17 ± 0.03	0.068 ± 0.026
PTER2U5:LTR4 3MI + LTR5:LTR4	222 ± 8	0.17 ± 0.02	0.067 ± 0.003
PTER2U5:LTR4 6MI	282 ± 66	0.10 ± 0.01	0.216 ± 0.005
PTER2U5:LTR4 6MI + LTR5:LTR4	343 ± 66	0.10 ± 0.01	0.205 ± 0.002
PTER5U5:LTR4	149 ± 15	0.23 ± 0.02	0.10 ± 0.012
Pre-cleaved	329 ± 68	0.21 ± 0.05	0.10 ± 0.008
PTER19U5:LTR4	156 ± 70	0.23 ± 0.06	0.086 ± 0.041
PTER14U5:LTR5	204 ± 75	0.15 ± 0.07	0.11 ± 0.02
PTER18U5:LTR5 3MI	408 ± 8	0.11 ± 0.04	0.093 ± 0.009
PTER18U5:LTR5 3MI + LTR5:LTR4	351 ± 49	0.08 ± 0.02	0.099 ± 0.003
PTER18U5:LTR5 6MI	270 ± 52	0.10 ± 0.01	0.23 ± 0.02
PTER18U5:LTR5 6MI + LTR5:LTR4	212 ± 53	0.12 ± 0.01	0.22 ± 0.01
PCR 7.1ds	260 ± 48	0.16 ± 0.01	0.090 ± 0.003

1- all apparent K_D values are averages of at least three separate experiments; 2- standard deviation

PTER2U5:LTR4 6MI

5'- GTG TGG AAA ATC TCT AGC AFT -3'
3'- CAC ACC TTT TAG AGA TCG TCA -5'

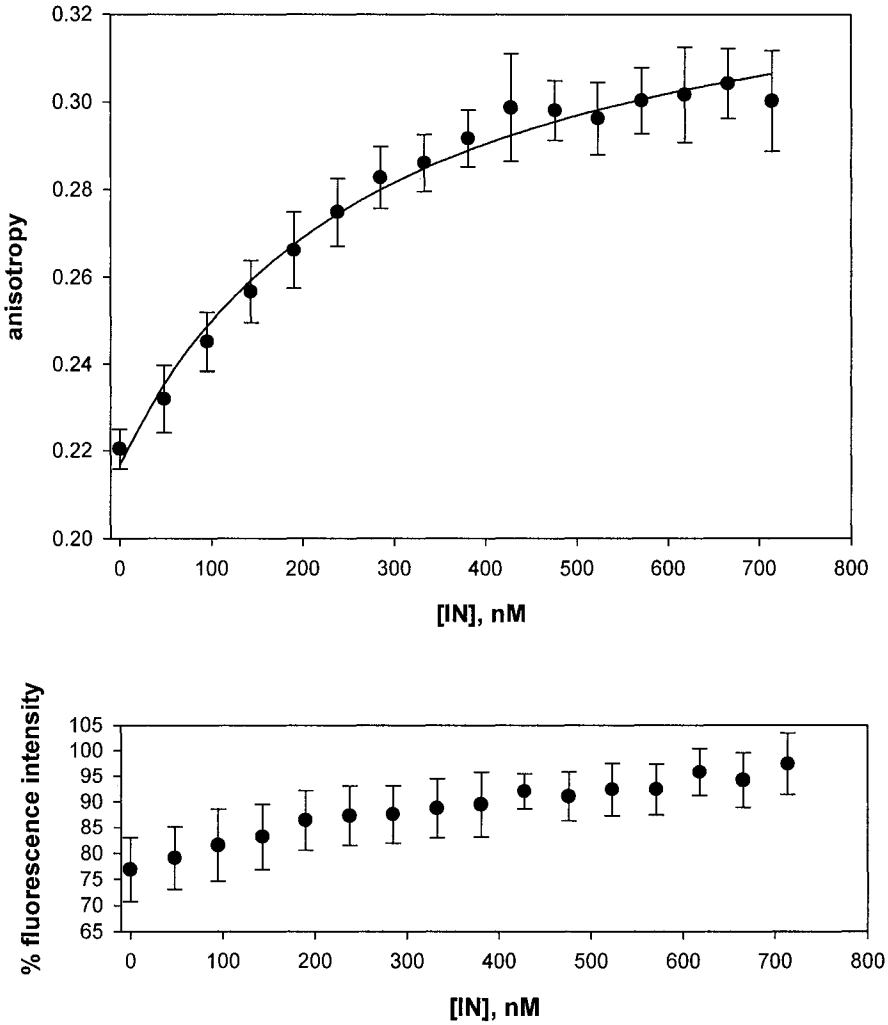

Figure 20. Titration of 6-MI labeled PTER2U5:LTR4 with HIV-1 IN. Top figure shows change in steady state emission anisotropy as a function of total HIV-1 IN concentration added. Concentration of HIV-1 IN added varies from 48 nM at the start of titration to 714 nM at the end of titration with HIV-1 IN added in 0.5 μl aliquots. The concentration of PTER2U5:LTR4 oligonucleotide was fixed throughout the titration at 0.1 nM. These binding data are fitted using a nonlinear least squares regression to the equation described in the Methods. The best fit is plotted as a solid line, and the apparent K_D value is obtained from the fit. The bottom panel shows the % fluorescence intensity as a function of HIV-1 IN concentration.

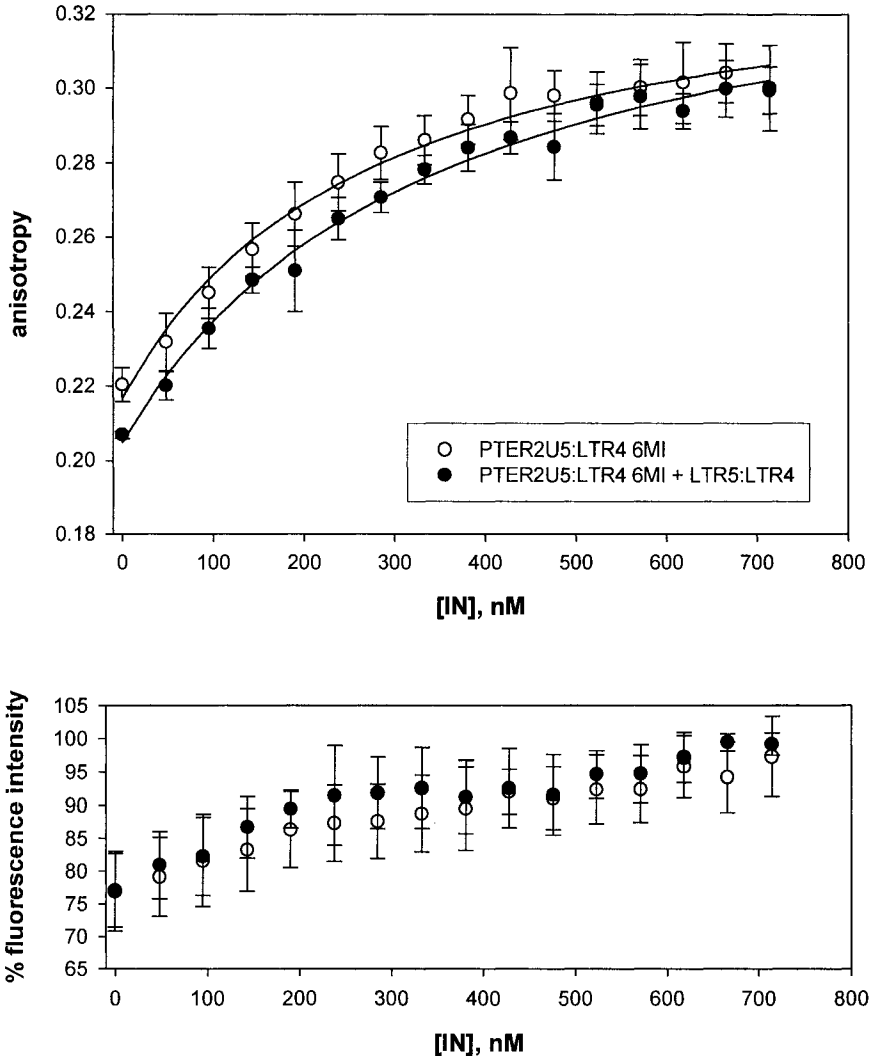

Figure 21. Equimolar concentrations of PTER2U5:LTR4 6MI and LTR5:LTR4 (0.1 nM each) are titrated with HIV-1 IN. Open circles represent binding data obtained for PTER2U5:LTR4 6MI titrated with HIV-1 IN. Filled circles represent binding data obtained for PTER2U5:LTR4 titrated with HIV-1 IN in the presence of LTR5:LTR4. Data are fitted as described in Methods. The best fits are shown as solid lines. The bottom panel shows the % fluorescence intensity as a function of HIV-1 IN concentration added.

Non-cleavable Substrate

A non-cleavable substrate, as first described in section 3.1.3, was used to establish the influence of any potential effects of temperature on the HIV-1 integrase interaction with DNA substrate. This non-cleavable substrate has 3-MI inserted at position 2 of the plus strand as for PTER2U5:LTR4, however, the 3-MI fluorophore in the second position is surrounded by base substitutions that differ form the wild type sequence (-CAFT-3'/-GTCA-5' is a wild type sequence versus -TGFC-3'/-ACCG-5' in the substituted sequence). An apparent K_D value of 255 ± 40 nM was determined from titration with HIV-1 IN at 20°C for the non-cleavable substrate, which represents a two fold weaker binding than for the PTER2U5:LTR4 substrate (Figure 16, Table 4). Hence, base substitutions at the cleavage site significantly affect the binding affinity of HIV-1 IN for the second position of the plus strand.

These results compare favorably with previous studies which reported that the U5 sequence with base substitutions similar to the non-cleavable substrate discussed here (-GCAGT-3'/-CGTCA-5'→-CGTGT-3'/-GCACA-5') also showed reduction in binding by HIV-1 integrase (35).

Summary

Figure 22 provides a summary of the experimentally determined K_D^{app} values and anisotropy changes for all oligonucleotides used in this study that have been labeled at position 2. The binding affinity of HIV-1 IN with 3-MI labeled PTER2U5:LTR4 is higher than for the 6-MI labeled PTER2U5:LTR4. Such results suggest the HIV-1 integrase may prefer unpaired bases at position 2 for both effective binding as well as for 3'-processing activity. Indeed the activity assay with 6-MI labeled oligonucleotide supports that view as the 6-MI labeled substrate is processed more slowly than the 3-MI labeled substrate.

The affinity for the non-cleavable substrate is lower suggesting involvement of bases next to position 2 in the interaction with HIV-1 integrase.

A larger change in anisotropy (Δr) upon HIV-1 integrase binding corresponds to a greater binding affinity (lower K_D^{app} values), suggesting more restricted freedom of movement of fluorophore.

Also observed is an increase in fluorescence intensity upon HIV-1 integrase binding for PTER2U5:LTR4 with 3-MI in position 2 of the plus strand (~ 40%) and for PTER2U5:LTR4 with 6-MI in

position 2 of the plus strand (~ 25%). A greater increase in fluorescence intensity for the 3-MI labeled position 2 corresponds to a lower K_D^{app} value. A local conformational change of the oligonucleotide upon protein binding can reduce base stacking or base pairing interactions resulting in an observed increase in the fluorescence intensity.

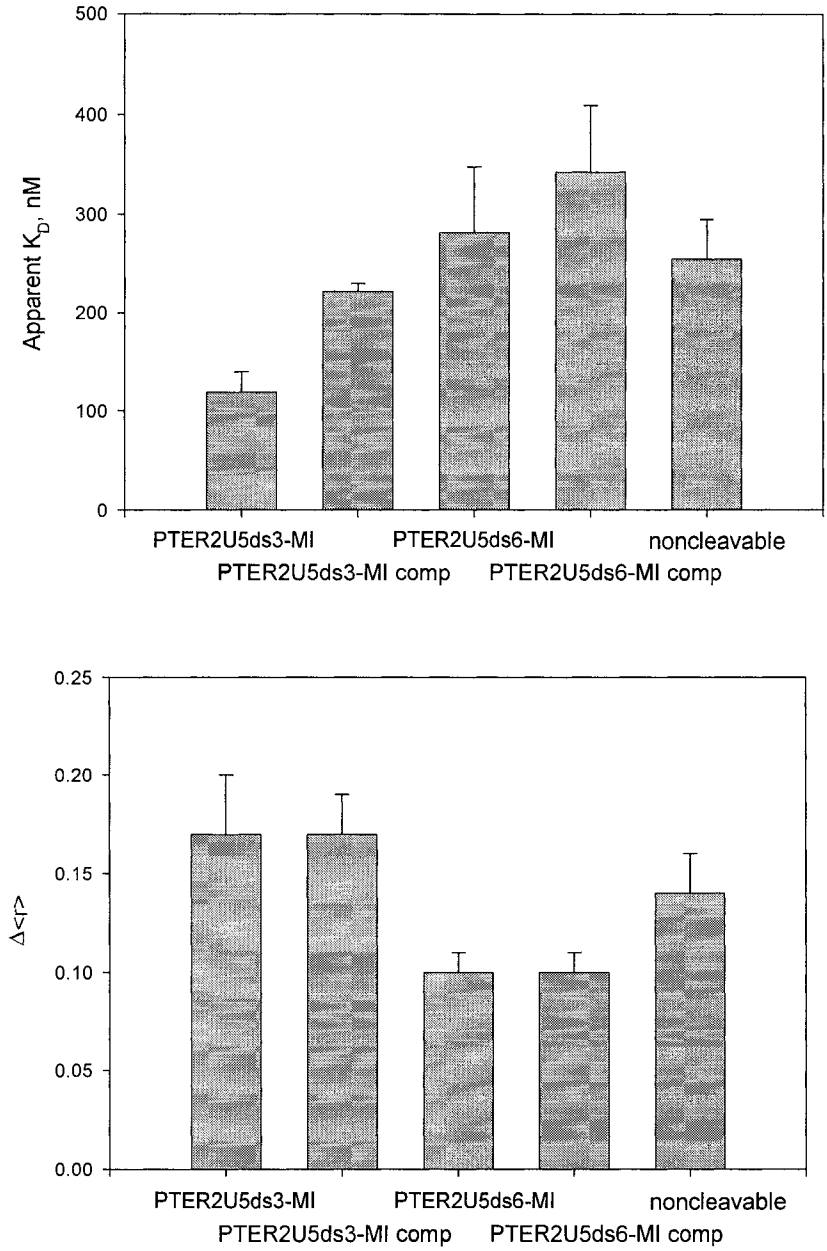

Figure 22. Top figure shows a comparison of apparent K_D values for double stranded oligonucleotide labeled at position 2 of the plus strand (PTER2U5:LTR4) with different probes (3MI vs 6MI), with and without competitor (PTER2U5ds3-MI vs PTER2U5ds3-MI comp, and PTER2U5ds6-MI vs PTER2U5ds6-MI comp). Also shown for comparison in the K_D^{app} value for the noncleavable substrate. The bottom panel summarizes overall anisotropy changes due to HIV-1 IN binding.

b. Studies with Label at Position 5 from 3'-end

Base substitutions at position 5 reduce 3'-processing activity

Previous missing-base analysis and base substitution studies have shown that the G base located at position 5 of the plus strand (Figure 17A) is critical for efficient 3'-processing and integration activities (92,93,95,97). For a G to T substitution in position 5 of the plus strand, a 5-fold reduction in 3'-processing activity in the presence of either Mn^{2+} or Mg^{2+} has been observed (48). With G to A and G to C substitutions a less dramatic reduction in 3'-processing activity was reported (48). Similarly, LaFemina *et al.* showed that substitution of a G base at position 5 with a C base on the plus strand had little effect on 3'-processing reaction (66). In contrast, their studies showed that a G to A substitution resulted in 30% reduction in the relative efficiency of 3'-processing and G to T substitution resulted in a 50% reduction of the 3'-processing efficiency by the protein (66).

Substitutions by nucleotide analogues reveal possible hydrogen bonding contact with HIV-1 integrase

Previous studies have investigated whether a lack in hydrogen bonding contacts in the minor or major groove (Figure 13B) at the G

at position 5 of the oligonucleotide influences the 3'-processing activity of HIV-1 integrase by substituting G(5) base with various nucleotide analogues (96). Such modified oligonucleotides were then tested in a 3'-processing assay (96). When the G base at position 5 of the plus strand was replaced with a nucleotide analogue that alters major (W2) and minor (S2) groove hydrogen bonding interactions, the 3'-processing activity of the substrate was similar to that determined for the wild-type U5 LTR (96). At the same time, replacement of G with a nucleotide analogue that places a very poor hydrogen bond acceptor at the major groove hydrogen bond site (W2) results in a 3.7-fold decrease in the rate of the 3'-processing reaction (96). Therefore, the major groove site (W2) at position 5 of the plus strand appears to be involved in bonding with a hydrogen bond donor from HIV-1 integrase (96).

In summary, previous studies suggest that base substitutions at position 5 of the plus strand from G to T or from G to A result in a considerable reduction in 3'-processing by HIV-1 integrase. G to C substitution produces less dramatic reduction in the 3'-processing. Nucleotide analogue substitutions at position 5 suggest involvement of guanine's major groove site W2 in hydrogen bonding with HIV-1

integrase for efficient 3'-processing reaction. Results of the previous studies define the importance of position 5 guanine of the plus strand for efficient catalytic activities of HIV-1 integrase. We were interested in quantifying binding interactions between HIV-1 integrase and model oligonucleotide fluorescently labeled at position 5.

Experimental results

Binding curves obtained for PTER5U5:LTR4 oligonucleotide with 3-MI at position 5 of the plus strand show hyperbolic character (Figure 23). From the fit of the binding data an apparent K_D value of 149 ± 15 nM was determined for HIV-1 IN binding to the oligonucleotide (Figure 23, Table 4), which is similar to that previously obtained for PTER2U5:LTR4 (3-MI in position 2). For higher oligonucleotide concentrations (1 nM) titration with HIV-1 integrase (Figure 23, open circles) showed non-saturation effect of the emission anisotropy values. To ensure saturation of oligonucleotide with protein, the oligonucleotide concentration used in the studies was fixed at 0.1 nM. Interestingly, for the oligonucleotide with the probe at position 5 of the plus strand fluorescence intensity increases (~ 30%) upon HIV-1 integrase binding suggesting changes in base

stacking interactions of the oligonucleotide on binding to the protein.

Pre-cleaved Substrate

In the 3'-processing reaction HIV-1 integrase produces a 5'-end overhang resulting from the loss of GT dinucleotide from the 3'-end of the plus strand of the viral DNA. This cleaved oligonucleotide is a substrate for the next step of integration process - strand transfer reaction- mediated by HIV-1 integrase.

Previous studies have shown that a pre-cleaved substrate does not form a complex with the HIV-1 IN; only nonspecific binding was detected with such a substrate (91). K_D values determined by surface plasmon resonance for a pre-cleaved substrate were 2-3 times higher than the K_D calculated for blunt-ended viral DNA (26).

In these studies a pre-cleaved substrate was prepared with a base sequence identical to PTER5U5:LTR4 with 3-MI substituted at position 5 of the plus strand. However, unlike PTER5U5:LTR4, the two outermost nucleotides of the plus strand are left out to form the pre-cleaved substrate. Figure 25 shows a comparison of apparent binding constants and anisotropy changes upon HIV-1 integrase binding for PTER5U5:LTR4 and the corresponding pre-cleaved

substrates. The apparent K_D was determined to be 329 ± 68 nM for the pre-cleaved substrate (Figure 24, Table 4) in contrast to the apparent K_D of 149 ± 15 nM for the 3'-processing substrate with 3-MI fluorophore in the same 5-position (PTER5U5:LTR5). It is apparent that removal of the dinucleotide from 21 base pair long oligonucleotide (as for pre-cleaved substrate) reduces the binding affinity of HIV-1 integrase two fold. Thus, it is clear that, following the 3'-processing reaction, position 5 from the 3' end of the plus strand of the substrate DNA appears to play a lesser role in HIV-1 integrase contact. Also the terminal dinucleotide may be important for the preferential recognition of unprocessed blunt ended viral DNA.

Anisotropy changes are the same for the probe in both oligonucleotide sequences upon HIV-1 integrase binding suggesting similar restrictions in freedom of movement of the probe. The fluorescence intensity increases ~ 30% for PTER5U5:LTR5 upon HIV-1 integrase binding. In contrast, a ~ 10% increase in fluorescence intensity is observed for pre-cleaved substrate. A local conformational change of the oligonucleotide upon protein binding can reduce base stacking or base pairing interactions resulting in an increase in fluorescence intensity.

PTER5U5:LTR4

5'- GTG TGG AAA ATC TCT AFC AGT -3'
3'- CAC ACC TTT TAG AGA TCG TCA -5'

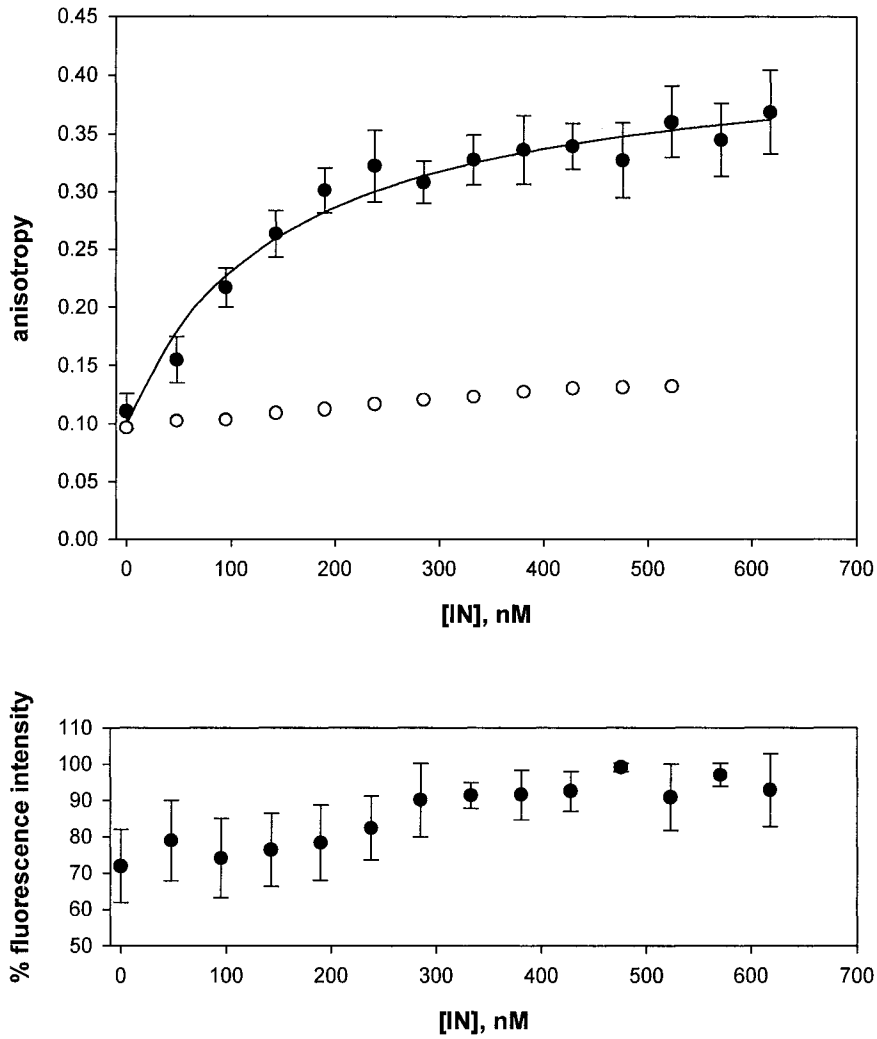

Figure 23. Binding of HIV-1 IN to the U5 model substrate labeled at position 5 of the plus strand (PTER5U5:LTR4). Top figure shows the change in steady state emission anisotropy as a function of total HIV-1 IN concentration added. Concentration of HIV-1 IN added varies from 48 nM at the start of titration to 714 nM at the end of titration with HIV-1 IN added in 0.5 µl aliquots. Filled circles represent binding data obtained with the concentration of PTER5U5:LTR4 oligonucleotide fixed throughout the titration at 0.1 nM. These binding data are fitted using a nonlinear least squares regression to the equation described in the Methods. The best fit is shown as a solid line, and the apparent K_D value is obtained from the fit. Open circles show data obtained with the concentration of PTER5U5:LTR4 oligonucleotide fixed throughout the titration at 1.0 nM. The bottom panel shows the % fluorescence intensity as a function of HIV-1 IN concentration.

5' - GTG TGG AAA ATC TCT A*F*C A -3'
3' - CAC ACC TTT TAG AGA TCG TCA - 3'

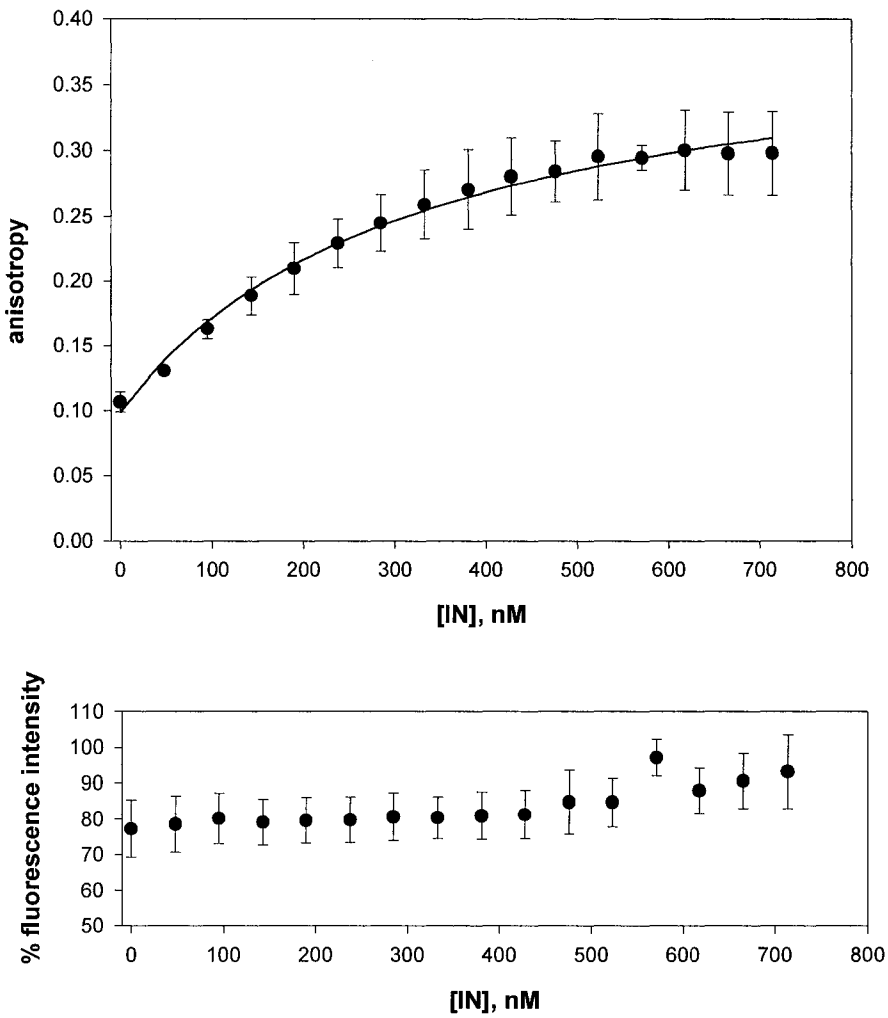

Figure 24. Titration of pre-cleaved PTER5U5:LTR4 3-MI with HIV-1 IN. Top figure shows the change in steady state emission anisotropy as a function of total HIV-1 IN concentration added. Concentration of HIV-1 IN added varies from 48 nM at the start of titration to 714 nM at the end of titration with HIV-1 IN added in 0.5 μl aliquots. The concentration of pre-cleaved PTER5U5:LTR4 oligonucleotide was fixed throughout the titration at 0.1 nM. These binding data are fitted using a nonlinear least squares regression to the equation described in the Methods. The best fit is shown as a solid line, and the apparent K_D value is obtained from the fit. The bottom panel shows the % fluorescence intensity as a function of HIV-1 IN concentration.

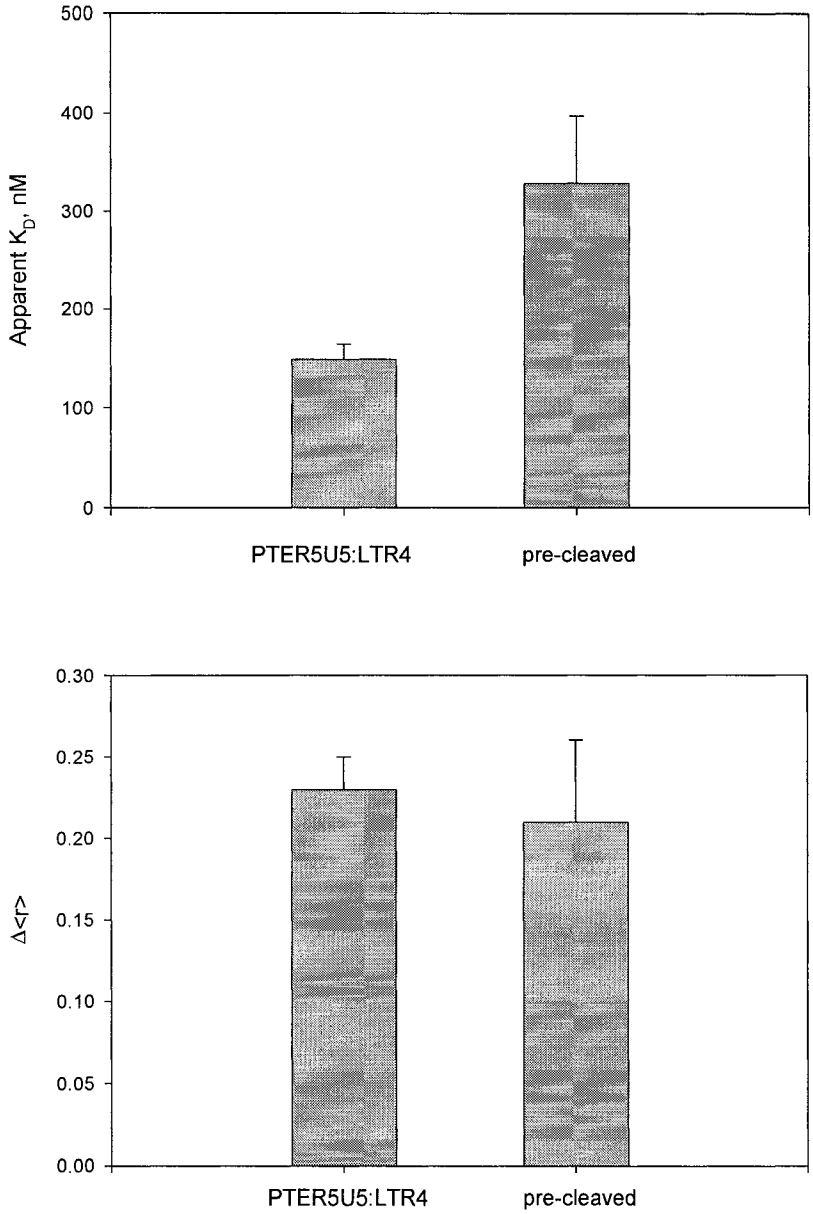

Figure 25. In the top figure, apparent K_D values are shown for the oligonucleotide labeled at position 5 of the plus strand (PTER5U5:LTR4) and is compared with the K_D^{app} value for oligonucleotide labeled at the same position but missing two terminal bases on the plus strand (pre-cleaved). Corresponding overall changes in anisotropy due to HIV-1 IN binding are shown in the bottom panel.

c. Studies with the Label at Position 19 from 3'-end

A literature survey suggests that guanine at position 19 of the plus strand plays a lesser role in determining the efficiency of HIV-1 integrase binding and catalytic activities with short oligonucleotides *in vitro*. This may not be unexpected as position 19 from the 3'end of the plus strand is far removed from the site of 3'-processing activity. Previous studies of the involvement of the guanine at position 19 in a concerted integration reaction carried out by HIV-1 IN are summarized below (98).

Role of guanine at position 19 in concerted integration

Employing a mini donor DNA (≈ 300 bp) containing U3 and U5 HIV-1 integrase recognition sequences at each end to study concerted DNA integration reactions *in vitro*, Brin *et al.* demonstrated that in addition to the conserved CA dinucleotide and surrounding sequence at the 3'end, positions 17 - 20 of the viral genome are also important for reconstituted concerted integration by HIV-1 IN (98). Indeed sequence analysis of concerted integration competent oligonucleotides showed that C and G were preferred at position 19 of the plus strand (84). Base substitutions at positions 18 (T → G) and 19

(G → A) significantly reduce the efficiency of the concerted DNA integration reaction compared with the wild type donor suggesting that these positions may be important for HIV-1 IN recognition of the donor substrate (98).

Although base pairs at positions 17 through 19 appear not to be required for 3'-processing or strand transfer reactions using short duplex oligonucleotide substrates *in vitro*, the bases may be needed for formation of concerted DNA integration complexes (98).

Experimental results

Using a fluorescently labeled 21 base pair long double stranded viral DNA sequence with 3-MI at position 19, we asked what the affect of position 19 is on the protein-oligonucleotide interaction. PTER19U5:LTR4 oligonucleotide has 3-MI at position 19 of the plus strand instead of guanine. The apparent K_D value was determined to be 156 ± 70 nM from hyperbolic binding data measured for PTER19U5:LTR4 with HIV-1 integrase (Figure 26). Also shown in Figure 24 are anisotropy values determined from titration of 1 nM PTER19U5:LTR4 with integrase (open circles). Similar to the data obtained for PTER2U5:LTR4 (Figure 18) and PTER5U5:LTR4

(Figure 23), anisotropy values do not reach a plateau with the higher (1 nM) concentration of PTER19U5:LTR4 substrate. Thus, for saturation conditions with HIV-1 IN, a 0.1 nM concentration of PTER19U5:LTR4 was used for the studies.

Our data suggests that the apparent binding affinity of HIV-1 integrase for position 19 labeled oligonucleotide is similar to apparent binding affinities to position 2 labeled oligonucleotide (PTER2U5:LTR4) and position 5 labeled oligonucleotide (PTER5U5:LTR4) of the plus strand (Table 4). Thus, HIV-1 integrase does not show considerable distinction between different positions of the plus strand on the U5 model double stranded oligonucleotide substrate.

PTER19U5:LTR4

5'- GTF TGG AAA ATC TCT AGC AGT -3'
3'- CAC ACC TTT TAG AGA TCG TCA -5'

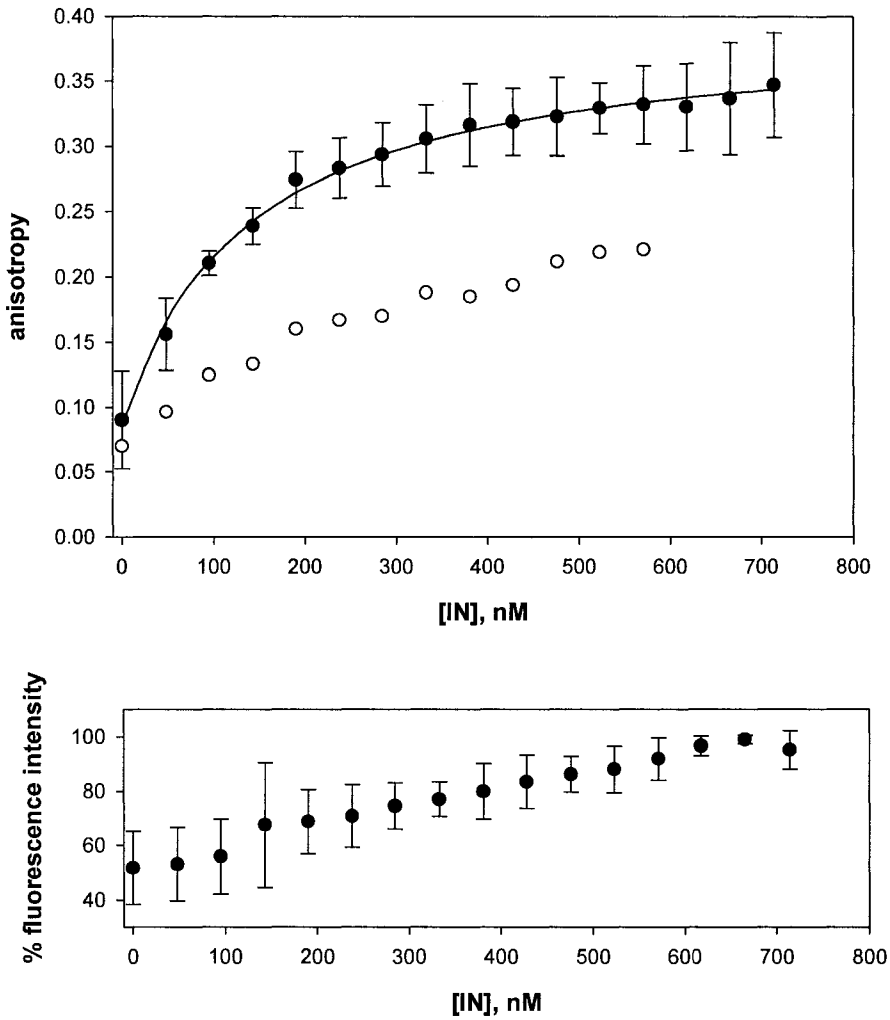

Figure 26. Binding of HIV-1 IN to the U5 model substrate labeled at position 19 of the plus strand (PTER19U5:LTR4). The top figure shows change in steady state emission anisotropy as a function of total HIV-1 IN concentration added. The concentration of HIV-1 IN added varies from 48 nM at the start of titration to 714 nM at the end of titration with HIV-1 IN added in 0.5 µl aliquots. Filled circles represent binding data obtained with the concentration of PTER19U5:LTR4 oligonucleotide fixed throughout the titration at 0.1 nM. These binding data are fitted using a nonlinear least squares regression to the equation described in the Methods. The best fit is plotted as a solid line, and the apparent K_D value is obtained from the fit. Open circles show data obtained with the concentration of PTER19U5:LTR4 oligonucleotide is fixed throughout the titration at 1.0 nM. The bottom panel shows the % fluorescence intensity as a function of HIV-1 IN concentration.

3.2.2 Labeling of the Minus Strand

a. Studies with the Label at Position 8 from the 5'-end

Mutations at position 8 do not influence HIV-1 integrase activity

Esposito *et al.*, using mutation studies, have suggested that the bases at position 8 of either the plus or minus strand of the viral DNA do not play any significant role in specificity of HIV-1 integrase interactions (36,48,92). Mutation at position 8 of the plus strand (C → G) of the oligonucleotide and corresponding mutation of complementary base in the minus strand (G → C) was cleaved by HIV-1 integrase at rates similar to those of corresponding wild type substrates suggesting that the base pair at position 8 is not influential in 3'-processing reaction (36,48). This hypothesis was further supported by C → A and C → T mutations, which also have no significant affect on the 3'-processing reaction (48).

Thus, from mutation studies the presence of guanine at position 8 of the minus strand in the U5 model oligonucleotide substrates does not appear to be required for efficient binding and 3'-processing by HIV-1 integrase. In the following study we asked whether interactions

between position 8 of the minus strand and HIV-1 integrase could be quantified in our *in vitro* system.

Experimental results

Binding studies with a U5 model fluorescent 21-mer oligonucleotide labeled at position 8 of the minus strand were performed using a complementary unlabeled plus strand. Binding data for this double stranded oligonucleotide labeled with 3-MI at position 8 of the minus strand was fitted as described in Materials and Methods (Figure 27). Similar to positions examined on the plus strand, the binding curve for the oligonucleotide with the probe at position 8 of the minus strand showed hyperbolic saturation (Figure 27). An apparent K_D value of 204 ± 75 nM was obtained for the oligonucleotide (Table 4), suggesting that HIV-1 IN binding affinity is reduced on the order of two fold for position 8 (PTER14U5:LTR5) *versus* position 2 of the plus strand (PTER2U5:LTR4). This reduced affinity is in agreement with previous mutation studies which suggest less integrity for this site for binding. For position 5 of the plus strand labeled oligonucleotide (PTER5U5:LTR4 K_D^{app} = 149 ± 15 nM) 1.5 times higher affinity is displayed by HIV-1integrase than for position 8 of the minus strand (PTER14U5:LTR5). So while a reduction in the

binding affinity is observed for positions more distant from the active end of the oligonucleotide for both plus and minus strands, the effect is greater for the minus strand. A large increase in fluorescence intensity (~ 50%) observed for PTER14U5:LTR5 upon HIV-1 integrase binding, which suggests a local conformational change of the oligonucleotide that reduces base stacking and base pairing interactions on binding with the protein.

PTER14U5:LTR5

5'-GTG TGG AAA ATC TCT AGC AGT-3'
3'-CAC ACC TTT TAG AFA TCG TCA-5'

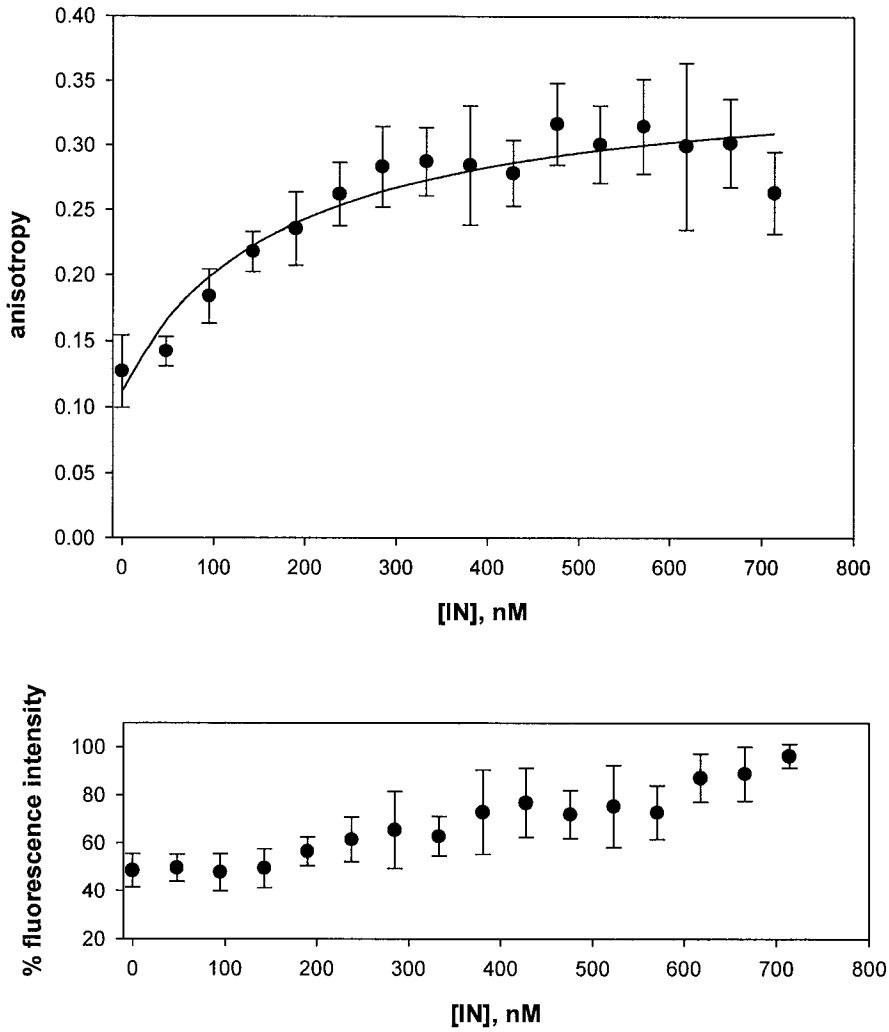

Figure 27. Binding of HIV-1 IN to the U5 model substrate labeled at position 8 of the minus strand (PTER14U5:LTR5). The top figure shows change in steady state emission anisotropy as a function of total HIV-1 IN concentration added. The concentration of HIV-1 IN added varies from 48 nM at the start of titration to 714 nM at the end of titration with HIV-1 IN added in 0.5 µl aliquots. The concentration of PTER14U5:LTR5 oligonucleotide was fixed throughout the titration at 0.1 nM. These binding data are fitted using a nonlinear least squares regression to the equation described in the Methods. The best fit is plotted as a solid line, and the apparent K_D value is obtained from the fit. The bottom panel shows the % fluorescence intensity as a function of HIV-1 IN concentration.

b. Studies with the Label at Position 4 from the 5'-end

CA/GT bases at positions 3 and 4 at the 3'end of U5 are conserved throughout all retroviral LTR sequences. Thus, the importance of base pair (C/G) at position 4 for binding and catalytic activities of HIV-1 integrase is not surprising. The conserved bases are recognized very specifically by HIV-1 integrase during 3'-processing reaction; integrase cleaves the phosphodiester bond immediately 3' to the adenine of the CA bases at the 3'-ends of the unintegrated retroviral DNA (14).

Base substitutions at position 4 result in reduction of binding and catalytic activities of HIV-1 integrase

Previous studies have shown that complementary base substitutions at position 4 result in a dramatic reduction of 3'-processing reaction (48,91). For mutants, C/G → A/T and C/G → T/A, almost no activity was observed and C/G → G/C showed 3'-processing activity 20-fold lower than for wild type levels in presence of Mg^{2+} (48). Less than 10% of wild type activity was retained in presence of Mn^{2+} for all three mutants (48). Scottoline *et al.* showed that complementary base pair substitution at position 4 (C/G → G/C)

also results in a drastic loss of the 3'-processing activity (94). Similarly, the C/G → T/A mutant showed almost no binding and very low 3'-processing and strand transfer activities (95). C/G → T/G and C/G → C/A mutants that have wild type sequence on only one of the strands, recovered 3'-processing and strand transfer activities, but were less active than wild type substrate (91). This same study showed that the 3'-processing activity of the C/G → T/G substrate is more efficient than that of the C/G → C/A substrate (91).

Two mismatched mutants also formed more non-specific binding complexes than wild type substrate or matched mutant (C/G → T/A) substrate (91). No pre-cleavage complex formation (sequence-specific binding prior to 3'-processing reaction) was observed with the mismatched substrates suggesting that both bases at the 4th position are important for the pre-cleavage complex formation (91). The C residue at position 4 of the plus strand and G residue at position 4 of the minus strand are very important for HIV-1 binding, with the G residue on the minus strand being more important than C (91).

Substitution of the C/G base pair by C/U (mismatch) abolished 3'-processing and decreased strand transfer by 89% (92). However,

binding to this mismatched substrate was not significantly affected suggesting that the decrease in the 3'-processing and strand transfer activities of HIV-1 IN is due to inhibition of catalysis and not to decreased DNA binding (92).

When G4 is mutated to A in the minus strand, both cleavage and integration activities are decreased, whereas a substitution of C4 to T in the plus strand does not influence IN activity (93). When C/G is mutated into either G/G or C/C, the integration activity is reduced by the mutated oligonucleotide in both strands (93). Cleavage activity was more affected by the substitution of the base in the minus strand (93). This indicates that G4 is essential for IN activity, whereas the C4 can be substituted by T but not by G (93).

Nucleotide analogues substitutions suggest hydrogen bond interactions between HIV-1 integrase and position 4 bases

Reported nucleotide analogue substitutions studies suggest strong hydrogen-bonding interactions in the major groove (W2) and minor groove (S2) at position 4 of the minus strand (Figure 13B), as demonstrated by the large reduction of 3'-processing activity when G is replaced by nucleotide analogues disturbing these interactions (96).

Additionally, only a moderate decrease in 3'-processing is observed when C is replaced by analogues that disrupt hydrogen bond interaction sites (96).

Cross-linking studies suggest that bases at position 4 may be contacted by HIV-1 integrase

Cross-linking studies show that amino acid residues 49-69 of the catalytic core domain of HIV-1 IN form primary cross links to the linker group immediately 3' to the conserved CA/TG base pairs; in addition, secondary cross-links from amino acids 139-152 of the catalytic core and, at a lower frequency, C-terminal cross-links with amino acids 271-288 (46) all suggest that position 4 and surrounding bases are involved in establishing contacts with HIV-1 integrase for efficient binding and catalytic activities.

Thus, it would be interesting to see how binding of HIV-1 IN to the double stranded oligonucleotide labeled at position 4 of the minus strand will be affected. Our method allows us to quantify and, from fluorescence intensity, to examine base stacking and H-bonding effects at this position.

Experimental results

3-MI at position 4 (PTER18U5:LTR5 3-MI)

As discussed, changes in steady state fluorescence anisotropy are monitored as a function of total HIV-1 IN concentration added to the fixed concentration (0.1 nM) of a 21 base pair long double stranded oligonucleotide with 3-MI at position 4 of the minus strand (PTER18U5:LTR5) (Figure 28). An increase in steady state fluorescence anisotropy values is observed with each successive addition of HIV-1 integrase to the oligonucleotide in the binding reaction until saturation is reached (Figure 28). The concentration dependence of the binding reaction corresponds to a hyperbolic function. From the fit (equation 8) the apparent K_D value was determined to be 408 ± 8 nM for PTER18U5:LTR5 (3-MI fluorophore at position 4 of the minus strand) (Table 4). In comparison to all positions that we have previously investigated, very weak binding is observed with PTER18U5:LTR5 labeled with 3-MI at position 4 of the minus strand.

To establish the effect of potential oligonucleotide modification (3-MI insertion) on the binding affinity of HIV-1 integrase to

PTER18U5:LTR4, in a control experiment unlabeled 21-mer oligonucleotide (LTR4:LTR5) was used as a competitor in the titration of 3-MI labeled PTER18U5:LTR4 with HIV-1 integrase. The K_D^{app} value determined was 351 ± 49 nM for the competition titration (Figure 29, Table 4). This result suggests that the fluorescent probe does not interfere to any great extent with HIV-1 integrase oligonucleotide interactions: addition of unlabeled oligonucleotide sequence (LTR4:LTR5) to the labeled oligonucleotide sequence (PTER18U5:LTR4) does not significantly alter the apparent binding affinity of the integrase for the DNA.

6-MI at position 4 (PTER18U5:LTR5 6-MI)

The surprisingly lower binding affinity observed with PTER18U5:LTR5 (position 4, minus strand) substrate may arise from perturbation of hydrogen bond interactions within the oligonucleotide at position 4 as a result of 3-MI substitution. Since reduced binding affinity can result from distortion of the oligonucleotide structure (3-MI creating single-base mismatch as discussed in the Introduction, section 1.2.3a), we examined the corresponding labeled oligonucleotide with 6-MI at position 4 of the minus strand. When 6-

MI, which is able to form H-bonds, is inserted into the oligonucleotide sequence (Table 4, Figure 30), the apparent K_D value (282 ± 66 nM) is reduced suggesting improvement in binding affinity for the protein to the oligonucleotide. This effect, presumably arises because 6-MI fits better within the oligonucleotide structure.

Enhanced binding affinity for the 6-MI containing oligonucleotide can be attributed to the improved hydrogen bonding between 6-MI and complementary cytosine (C). For position 4 of the minus strand any mismatch created by 3-MI is not well tolerated by HIV-1 integrase. This result shows excellent correspondence with mutation studies which show that replacement of G on the minus strand results in diminished binding and activity of the protein.

In a competition experiment with 6-MI substituted PTER18U5:LTR4, the K_D^{app} value was determined to be 212 ± 53 nM and is very similar to K_D^{app} value (270 ± 52 nM) obtained in the absence of the competitor (Table 4, Figure 31). Thus, HIV-1 integrase appears to display similar affinities for both the 6-MI labeled and unlabeled oligonucleotides.

Figure 32 summarizes the apparent binding constant values and anisotropy changes for HIV-1 integrase interactions where model

oligonucleotides where the fluorescent guanine analog (3-MI or 6-MI) has been inserted at position 4 of the minus strand sequence.

The presence of 6-MI in the oligonucleotide results in a 50 % increase in binding affinity in comparison to 3-MI. Competition studies using the corresponding unlabeled oligonucleotide sequence revealed that binding affinity of HIV-1 IN to the labeled oligonucleotide changes slightly (~12-20 % enhancement) in the presence of unlabeled sequence suggesting that these fluorescent probes (3-MI or 6-MI) do not significantly affect the specificity of HIV-1 integrase for the oligonucleotide.

Anisotropy changes (Δr) corresponding to 3-MI or 6-MI labeled PTER18U5:LTR5 are very similar implying that the probes have similar degrees of freedom of movement upon HIV-1 integrase binding.

Notable is the influence of HIV-1 integrase binding on fluorescence intensities of 3-MI and 6-MI labeled oligonucleotides. PTER18U5:LTR4 3-MI oligonucleotide demonstrated low binding affinity with HIV-1 integrase and the corresponding fluorescence intensity data is unchanged suggesting that contact between HIV-1 integrase and 3-MI incorporated at position 4 does not involve local

conformational changes (such as bending and unwinding) to the duplex oligonucleotide. In contrast, with 6-MI labeled oligonucleotide, there is an increase in fluorescence intensity upon HIV-1 integrase binding to the oligonucleotide suggesting that local conformational changes of the oligonucleotide may be involved in this interaction.

PTER18U5:LTR5

5'-GTG TGG AAA ATC TCT AGC AGT-3'
3'-CAC ACC TTT TAG AGA TCF TCA-5'

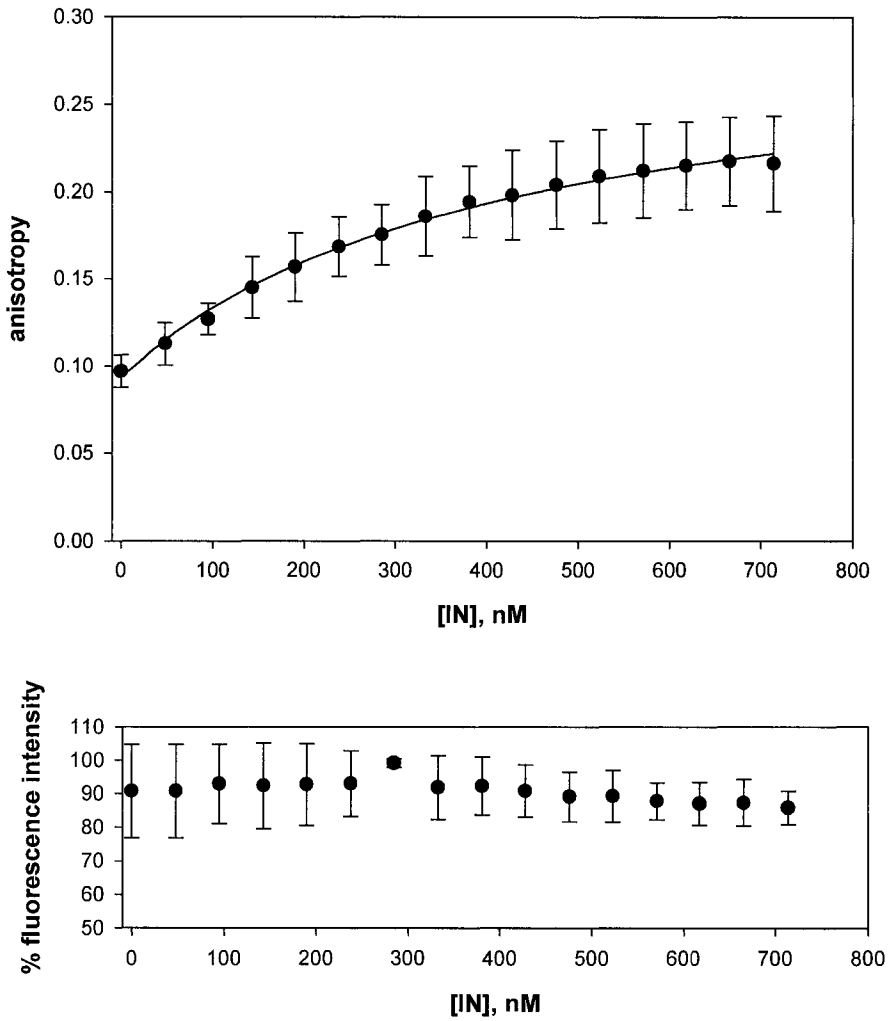

Figure 28. Binding of HIV-1 IN to the U5 model substrate labeled at position 4 of the minus strand (PTER18U5:LTR5 3-MI). Top figure shows change in steady state emission anisotropy as a function of total HIV-1 IN concentration added. Concentration of HIV-1 IN added varies from 48 nM at the start of titration to 714 nM at the end of titration with HIV-1 IN added in 0.5 µl aliquots. The concentration of PTER18U5:LTR5 oligonucleotide was fixed throughout the titration at 0.1 nM. These binding data are fitted using a nonlinear least squares regression to the equation described in the Methods. The best fit is plotted as a solid line, and the apparent K_D value is obtained from the fit. The bottom figure shows the % fluorescence intensity as a function of HIV-1 IN concentration.

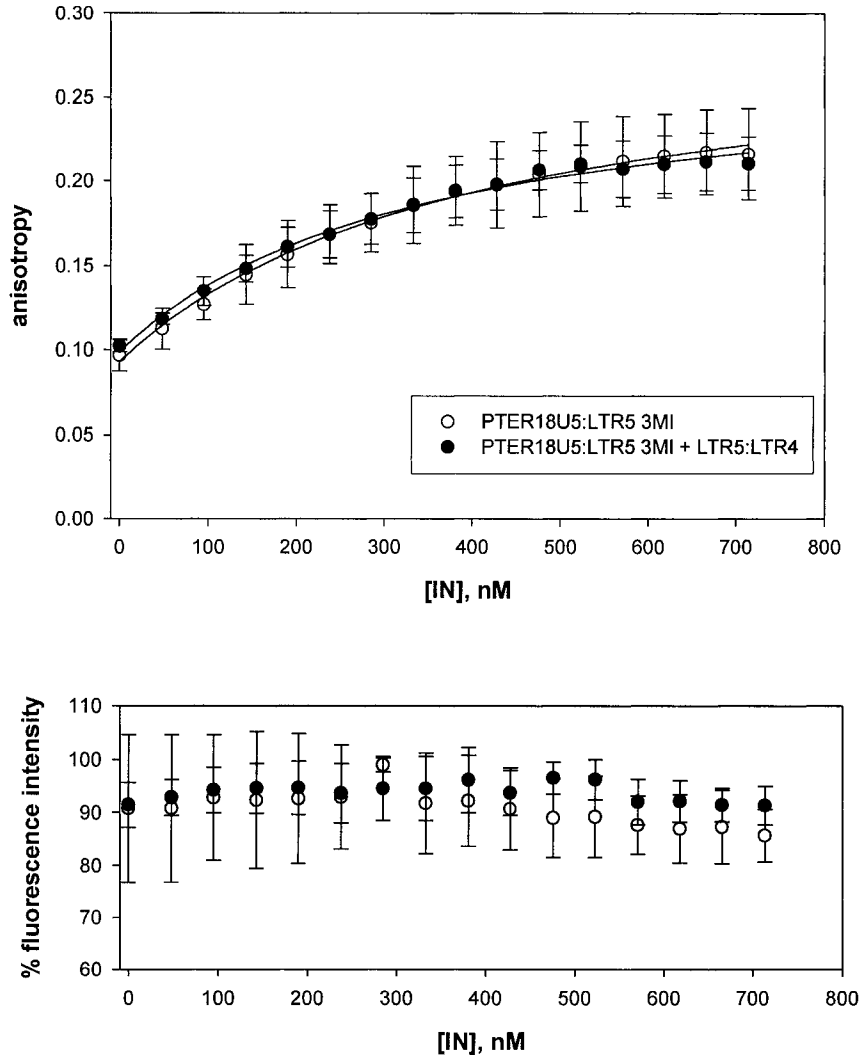

Figure 29. Equimolar concentrations of PTER18U5:LTR5 3MI and LTR5:LTR4 (0.1 nM each) are titrated with HIV-1 IN. Open circles represent binding data obtained for PTER18U5:LTR5 3MI titrated with HIV-1 IN. Filled circles represent binding data obtained for PTER18U5:LTR5 titrated with HIV-1 IN in the presence of LTR5:LTR4. Data are fitted as described in Methods, and the best fits are shown as solid lines. The bottom panel shows the % fluorescence intensity as a function of HIV-1 IN concentration added.

PTER18U5:LTR5

5'-GTG TGG AAA ATC TCT AGC AGT-3'
3'-CAC ACC TTT TAG AGA TCF TCA-5'

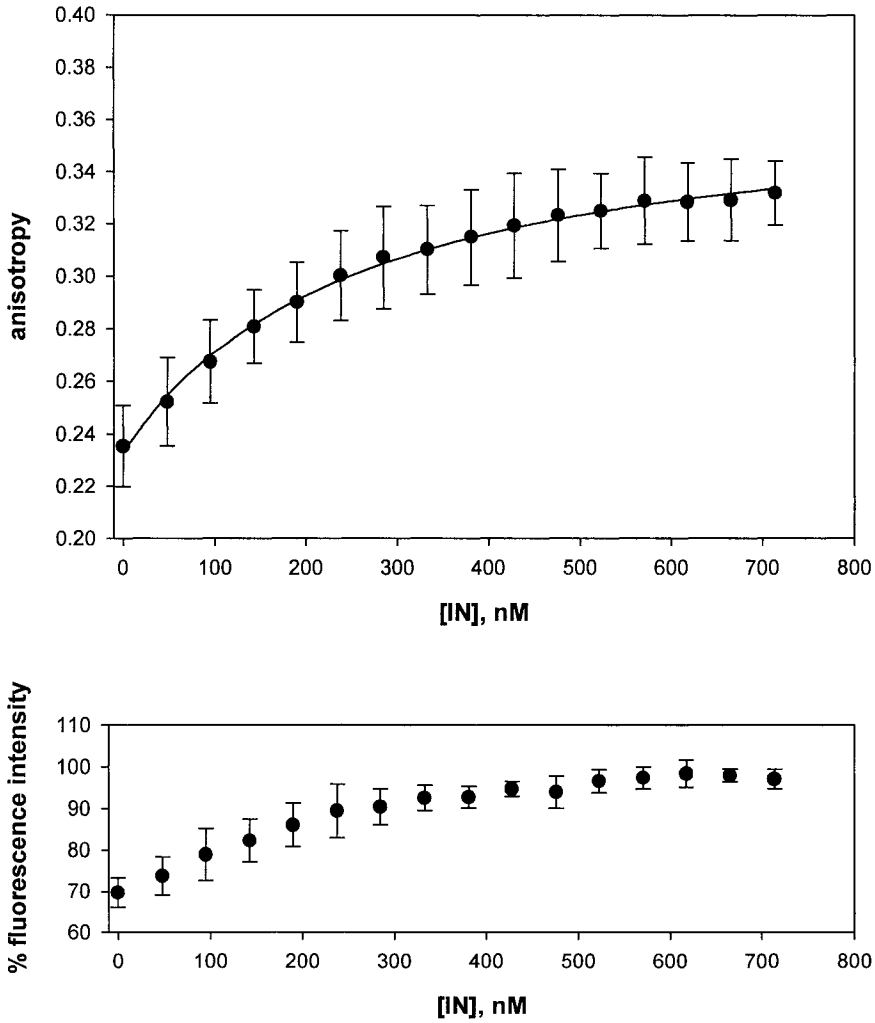

Figure 30. Titration of 6-MI labeled PTER18U5:LTR5 with HIV-1 IN. Top figure shows change in steady state emission anisotropy as a function of total HIV-1 IN concentration added. Concentration of HIV-1 IN added varies from 48 nM at the start of titration to 714 nM at the end of titration with HIV-1 IN added in 0.5 μl aliquots. The concentration of PTER18U5:LTR5 oligonucleotide was fixed throughout the titration at 0.1 nM. These binding data are fitted using a nonlinear least squares regression to the equation described in the Methods. The best fit is plotted as a solid line, and the apparent K_D value is obtained from the fit. The bottom panel shows the % fluorescence intensity as a function of HIV-1 IN concentration.

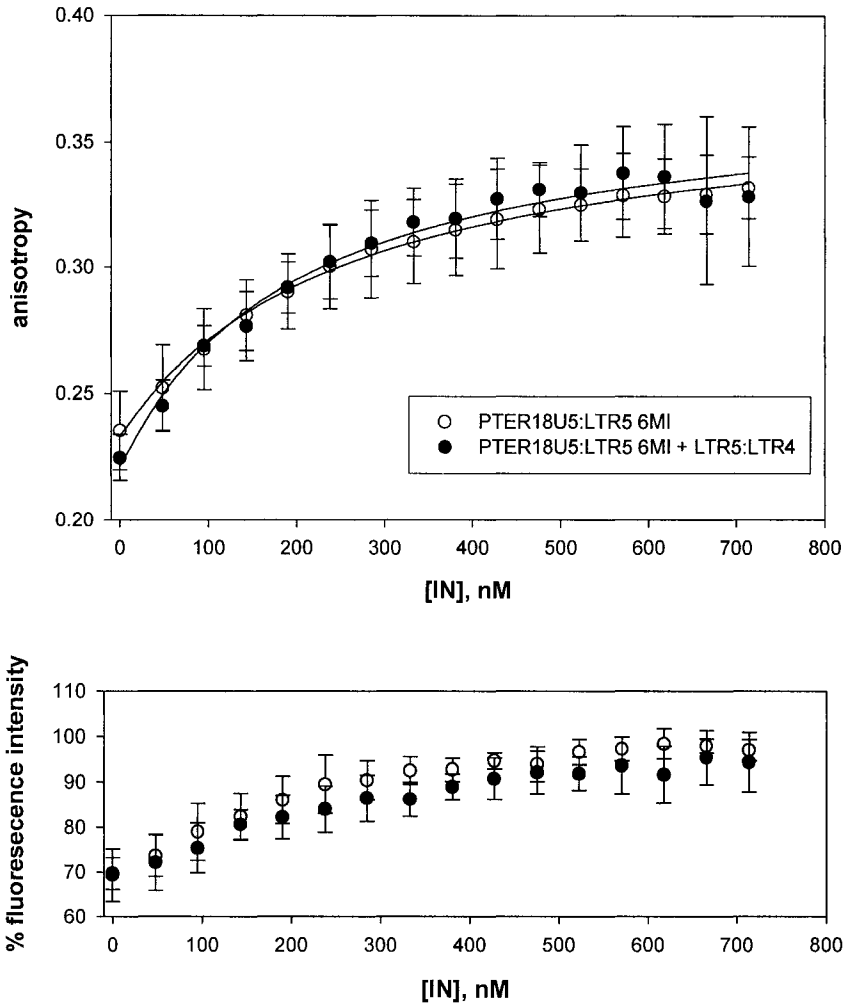

Figure 31. Equimolar concentrations of PTER18U5:LTR5 6MI and LTR5:LTR4 (0.1 nM each) are titrated with HIV-1 IN. Open circles represent binding data obtained for PTER18U5:LTR5 6MI titrated with HIV-1 IN. Filled circles represent binding data obtained for PTER18U5:LTR5 titrated with HIV-1 IN in the presence of LTR5:LTR4. Data are fitted as described in Methods, and the best fits are shown as solid lines. The bottom figure shows the % fluorescence intensity as a function of HIV-1 IN concentration added.

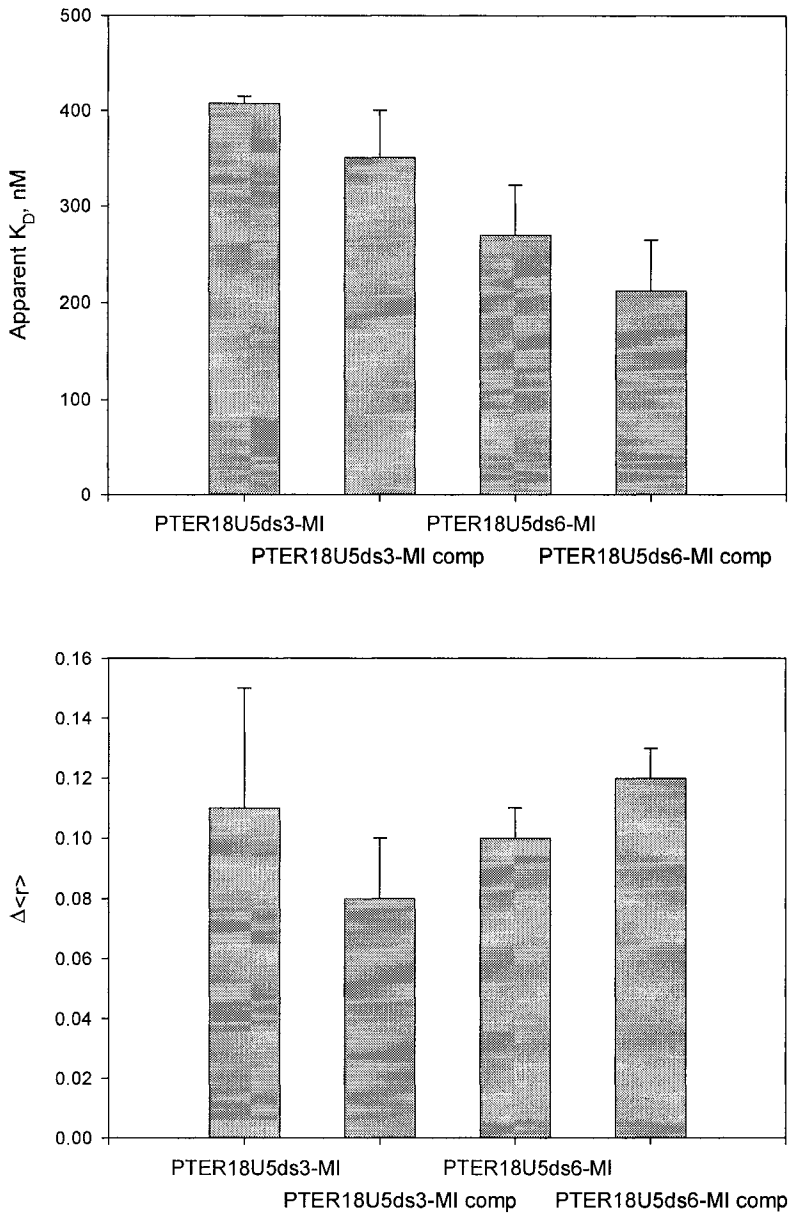

Figure 32. The top panel shows apparent K_D values for double stranded oligonucleotide labeled at position 4 of the minus strand (PTER18U5:LTR4) with different probes (3MI *vs* 6MI), with and without competitor (PTER18U5ds3-MI *vs* PTER18U5ds3-MI comp, and PTER18U5ds6-MI *vs* PTER18U5ds6-MI comp). The bottom panel summarizes the corresponding overall anisotropy changes due to HIV-1 IN binding.

Summary of results for HIV-1 integrase binding to U5 double stranded model oligonucleotide's various base positions

Figure 33 shows a summary of the values for apparent binding constants and anisotropy changes determined for various base positions along the 21 base pair long model oligonucleotide that mimic the U5 end of the viral DNA.

Positions 2 and 5 from the 3' processing end on the plus strand of the U5 double-stranded substrate show similar K_D^{app} values: PTER2U5:LTR4 119 ± 21 nM, PTER5U5:LTR4 149 ± 15 nM. Position 19, although removed from the 3'processing end, exhibits an apparent K_D value of 156 ± 70 nM that is close to the K_D^{app} value obtained for the position 5 labeled oligonucleotide (PTER5U5:LTR4). Apparent affinities of HIV-1 IN for the oligonucleotides do not appreciably depend on the position of the probe on the plus strand of U5 substrate. Indeed, PTER19U5:LTR4, where the fluorophore is located 19 base pairs away from cleavage site, shows a similar magnitude of binding affinity to the protein as observed for positions 2 and 5. Thus, with double stranded oligonucleotides positions 5 and 19 on the plus strand appear to be interacting with HIV-1IN with very similar affinities or specificity and only marginally tighter (~ 20 %)

interactions were determined at the cleavage site at position 2 of the plus strand (Figure 33).

In contrast, binding affinities for HIV-1 integrase observed for the minus strand of 21-mer duplex (Figure 33) differ significantly from the three positions investigated on the plus strand. In general we observed lower binding affinities for HIV-1 IN for the positions on the minus strand. This may reflect a greater integrity of the protein for oligonucleotide structure (as seen for 6-MI) and importance of minus strand for binding. In particular, HIV-1 integrase interacts with position 2 (plus strand) labeled oligonucleotide with an affinity twice that of position 8 (minus strand) labeled oligonucleotide (PTER2U5:LTR4 K_D^{app} = 119 ± 21 nM vs PTER14U5:LTR5 K_D^{app} = 204 ± 75 nM (Table 4)). In comparison to the oligonucleotide labeled at position 5 (PTER5U5:LTR4 K_D^{app} = 149 ± 15 nM), 1.5 times less affinity is displayed by HIV-1 integrase for the oligonucleotide labeled at position 8 (PTER14U5:LTR5). Less of a difference is observed between affinities for position 19 (PTER19U5:LTR4 K_D^{app} = 156 ± 70 nM) of the plus strand labeled oligonucleotide and PTER14U5:LTR5.

Interestingly, for our fluorescently labeled oligonucleotide,

position 4 of the minus strand appears to be contacted by HIV-1 IN with the least affinity (K_D^{app} = 408 ± 8 nM), while its importance for HIV-1 integrase binding and 3'-processing reaction has been firmly established in the literature using mutation and noncomplementary base replacement studies. This G base at position 4 of the minus strand has been shown to be critical for binding and 3'-processing of short duplex oligonucleotides by HIV-1 IN *in vitro*. Our data support the importance of the base position.

From the 3-MI-containing oligonucleotide melting temperature data shown here (Results, section 3.1.1) and elsewhere (77), it is clear that 3-MI substitution behaves similarly to a single base mismatch. 3-MI has the 3-position methyl group (Figure 13) and therefore hydrogen-bonding with a complementary base is reduced. Our reduced binding data obtained for position 4 on the minus strand, which displays the lowest affinity of all positions tested along the U5 double-stranded 21-mer (Figure 33), suggests that the fidelity of binding of HIV-1 IN for position 4 is critical and more demanding than for position 2 at the cleavage site. To assess the impact of reduced H-bonding we chose to examine 6-MI in position 4 of the minus strand. The 6-MI structure allows hydrogen bond formation to

the complementary base in the duplex oligonucleotide and the apparent K_D decreased to 270 ± 52 nM. Binding studies suggest that the oligonucleotide structure is critical, and that the oligonucleotide must form a helix structure to bind properly to HIV-1 IN. 6-MI improves hydrogen bonding to the complementary cytosine, improves ability of HIV-1 integrase to contact the position and, thus, some of the protein binding affinity is recovered. The 6-MI labeled oligonucleotide experiences some degree of conformational change upon HIV-1 integrase binding as indicated by an increase in fluorescence intensity and could result from the local bending or unwinding of the oligonucleotide (Figure 30). In the case of 3-MI (Figure 28) there is no conformational change as indicated by the lack of affect of the protein binding on fluorescence intensity.

In contrast, our previous investigation with substitution of 6-MI in position 2 of the plus strand resulted in a 2.4 fold decrease in affinity as compared with the corresponding oligonucleotide containing 3-MI (Figure 22). With respect to position 2 of the plus strand (PTER2U5:LTR4), distortion of oligonucleotide structure by 3-MI may be well tolerated by HIV-1 integrase because noncomplementary base pair substitutions at this position appear to

facilitate 3'-processing reaction.

When 6-MI is used as a probe, apparent K_D values determined for position 2 of the plus strand and position 4 of the minus strand become very similar (Table 4). Thus, the distinction between these two positions observed with 3-MI is not seen with 6-MI.

Also notable is the difference in anisotropy changes upon HIV-1 integrase binding to 6-MI containing PTER2U5:LTR4 oligonucleotide (0.10 ± 0.01) compared to 3-MI containing PTER2U5:LTR4 (0.17 ± 0.03) (Figure 22). 6-MI appears to retain greater freedom of movement than 3-MI in position 2 of the plus strand upon HIV-1 integrase binding. For position 4 of the minus strand anisotropy changes are very similar for 3-MI (0.11 ± 0.04) and 6-MI (0.10 ± 0.01) upon HIV-1 IN binding (Figure 32) suggesting that in this position both probes experience restriction in their movement similarly by contact with HIV-1 integrase.

The K_D^{app} value for pre-cleaved oligonucleotide, the substrate for the strand transfer reaction, is twice the K_D^{app} for the PTER5U5:LTR4 oligonucleotide, the substrate for the 3'-processing reaction (329 ± 68 nM vs 149 ± 15 nM) when both are labeled at position 5 of the plus strand with 3-MI (Figure 25). This result

suggests that position 5 of the plus strand is not important for contact by HIV-1 integrase in the pre-cleaved strand transfer substrate. Also the terminal dinucleotides that are absent in the pre-cleaved substrate may play a role in recognition of position 4 in blunt ended substrate.

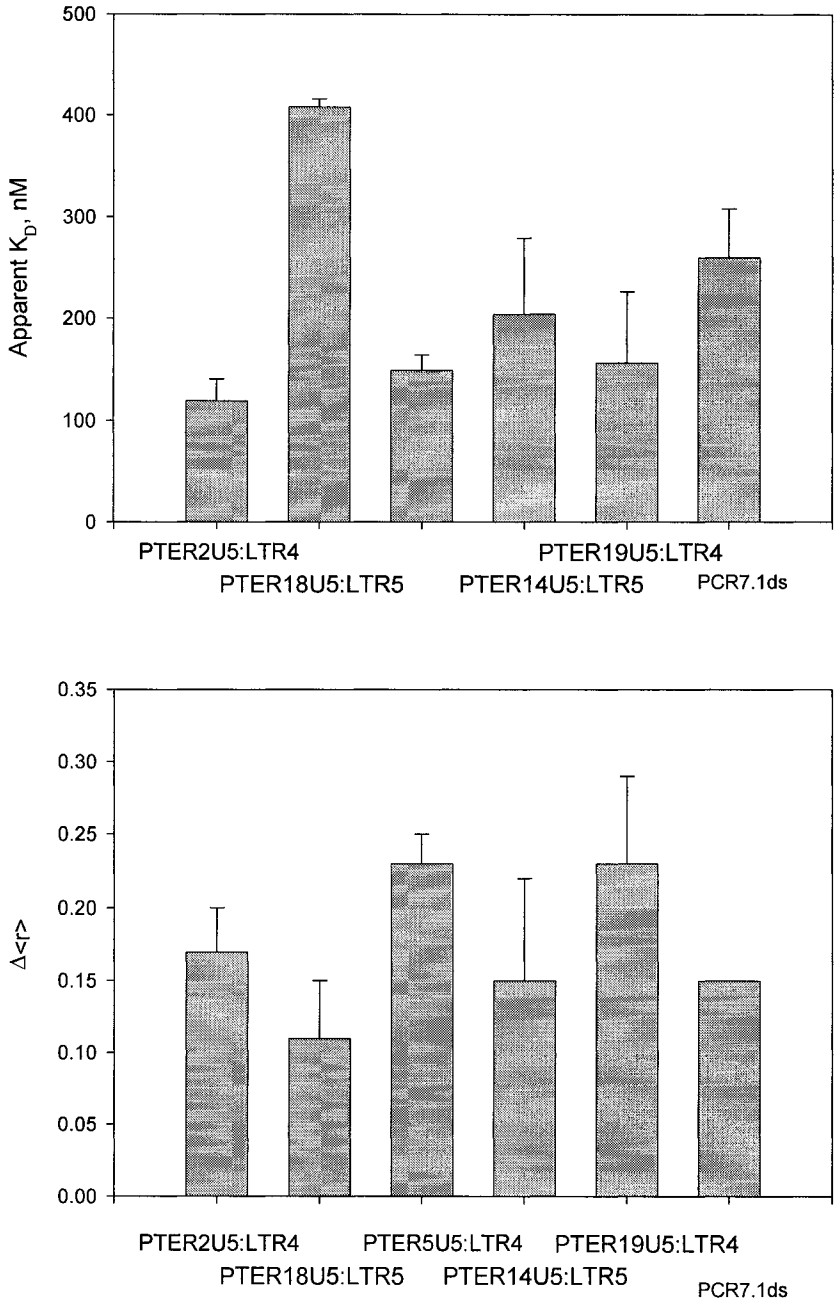

Figure 33. Top graph shows change of apparent K_D values determined for different positions of the probe (3-MI) within the double stranded model oligonucleotides. Bottom figure shows the corresponding overall changes in anisotropy due to HIV-1 IN binding.

3.3 U5 Single Stranded Model Oligonucleotide Substrates

Previous studies have suggested that HIV-1 IN displays similar apparent affinities for single and double stranded forms of the LTR and for nonspecific single-stranded DNA in UV cross-linking titrations (29). However, from results using an exonuclease protection assay it was inferred that HIV-1 integrase does not form stable complexes with single-stranded DNA in contrast to double-stranded DNA (29). As a consequence a different mechanism was proposed to be involved for binding of HIV-1 IN to single-stranded oligonucleotides (29).

Preferential binding of HIV-1 IN to the double-stranded substrate was suggested on the basis of dissociation constants obtained from inhibition of 3'-processing activity studies (99). Higher affinities were detected for specific double stranded oligonucleotides than for specific single stranded oligonucleotides (100). In this study binding affinities were determined from the ability of the single stranded oligonucleotides to compete with double-stranded substrates in the 3'-processing reaction (9,100).

Experimental results

From our fluorescence titration data of 3-MI labeled single stranded oligonucleotides, apparent K_D values revealed lower binding affinity for HIV-1 IN for single stranded nucleotides as compared to double stranded oligonucleotides (Table 5, Figures 34 - 38). Further there is no marked change in binding affinity dependent on the probe position along the single stranded oligonucleotides (Figure 39); all five positions tested appear to be interacting with HIV-1 integrase with similar weak affinities.

In addition, with single stranded oligonucleotides there is no distinction between plus strand and minus strand affinities. Single-stranded oligonucleotide with position 8 labeled has a K_D^{app} value (265 ± 170 nM) similar to K_D values obtained with positions on the plus single strand. Position 4 on the single minus strand is bound with an affinity similar (K_D^{app} = 290 ± 104 nM) to the three positions studied on the plus strand (PTER2U5, PTER5U5, PTER19U5) and one position on the minus strand (PTER14U5) of the single-stranded oligonucleotides.

Apparent K_D values for the five positions in single-stranded

substrate (Table 5) were two fold larger than for corresponding double-stranded oligonucleotides (Table 4). It is clear that HIV-1 IN prefers to bind with double-stranded oligonucleotides rather than single-stranded oligonucleotides.

Table 5.
Titration of 3-MI labeled U5 single stranded model oligonucleotides with HIV-1 integrase

oligonucleotide	$K_D^{app\,1} \pm$ s.d.[2](nM)	$\Delta r \pm$ s.d.[2]	$\langle r \rangle_{min} \pm$ s.d.[2]
PTER2U5	256 ± 59	0.15 ± 0.06	0.071 ± 0.010
PTER5U5	349 ± 61	0.13 ± 0.03	0.086 ± 0.001
PTER19U5	325 ± 84	0.10 ± 0.02	0.050 ± 0.007
PTER14U5	265 ± 170	0.16 ± 0.05	0.085 ± 0.004
PTER18U5	290 ± 104	0.08 ± 0.02	0.073 ± 0.005
PCR 7.1ss	290 ± 95	0.15 ± 0.05	0.085 ± 0.009

1- all values are averages of at least three separate experiments; 2- standard deviation

PTER2U5

5'-GTG TGG AAA ATC TCT AGC AFT-3'

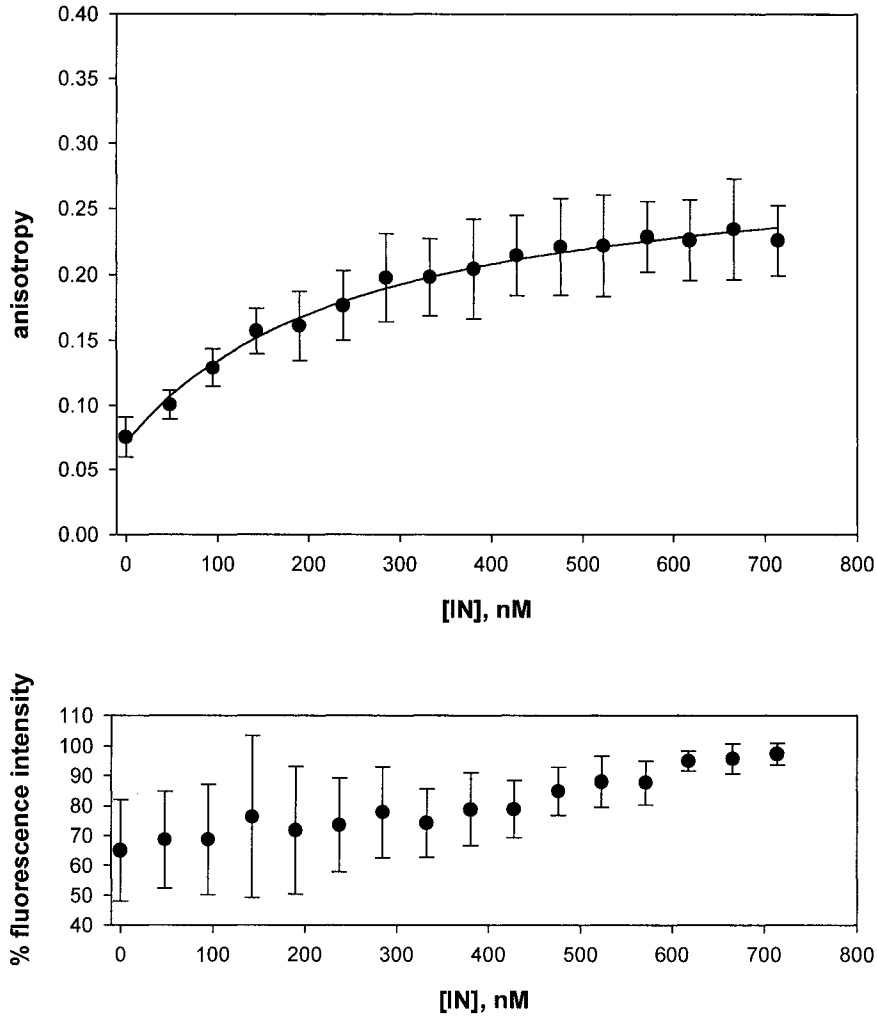

Figure 34. Binding of HIV-1 IN to the U5 single stranded (plus strand) model substrate labeled at position 2 (PTER2U5). Top figure shows change in steady state emission anisotropy as a function of total HIV-1 IN concentration added. Concentration of HIV-1 IN added varies from 48 nM at the start of titration to 714 nM at the end of titration with HIV-1 IN added in 0.5 µl aliquots. The concentration of PTER2U5 oligonucleotide was fixed throughout the titration at 0.1 nM. These binding data are fitted using a nonlinear least squares regression to the equation described in the Methods. The best fit is plotted as a solid line, and the apparent K_D value is obtained from the fit. The bottom panel shows the % fluorescence intensity as a function of HIV-1 IN concentration.

PTER5U5

5'-GTG TGG AAA ATC TCT AFC AGT-3'

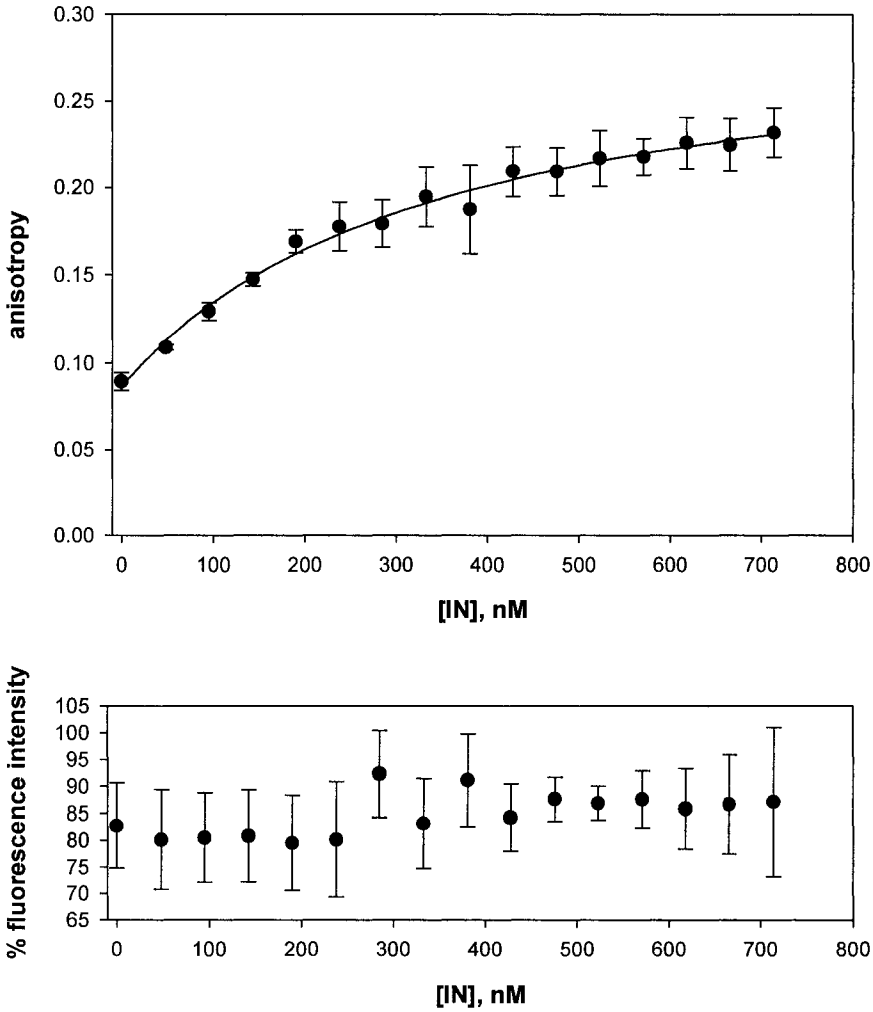

Figure 35. Binding of HIV-1 IN to the U5 single stranded (plus strand) model substrate labeled at position 5 (PTER5U5). Top figure shows change in steady state emission anisotropy as a function of total HIV-1 IN concentration added. Concentration of HIV-1 IN added varies from 48 nM at the start of titration to 714 nM at the end of titration with HIV-1 IN added in 0.5 μl aliquots. The concentration of PTER5U5 oligonucleotide was fixed throughout the titration at 0.1 nM. These binding data are fitted using a nonlinear least squares regression to the equation described in the Methods. The best fit is plotted as a solid line, and the apparent K_D value is obtained from the fit. The bottom panel shows the % fluorescence intensity as a function of HIV-1 IN concentration.

PTER19U5

5'-GTF TGG AAA ATC TCT AGC AGT-3'

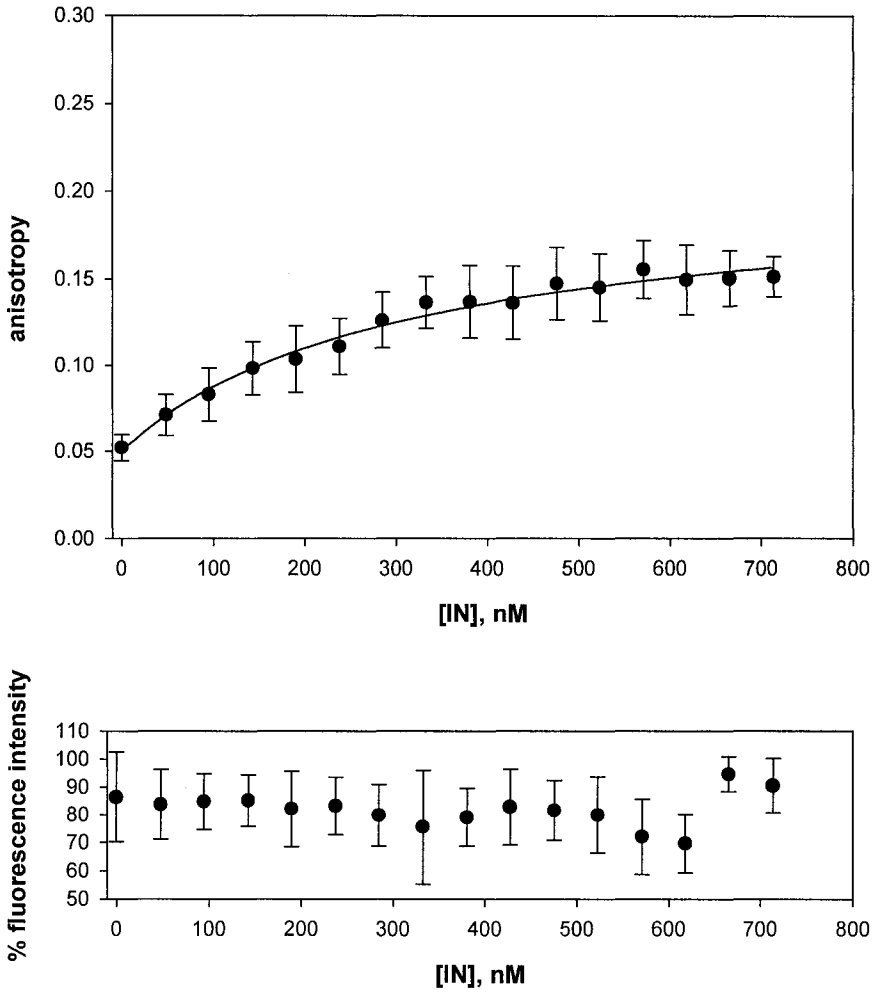

Figure 36. Binding of HIV-1 IN to the U5 single stranded (plus strand) model substrate labeled at position 19 (PTER19U5). Top figure shows change in steady state emission anisotropy as a function of total HIV-1 IN concentration added. Concentration of HIV-1 IN added varies from 48 nM at the start of titration to 714 nM at the end of titration with HIV-1 IN added in 0.5 µl aliquots. The concentration of PTER19U5 oligonucleotide was fixed throughout the titration at 0.1 nM. These binding data are fitted using a nonlinear least squares regression to the equation described in the Methods. The best fit is plotted as a solid line, and the apparent K_D value is obtained from the fit. The bottom panel shows the % fluorescence intensity as a function of HIV-1 IN concentration.

3'-CAC ACC TTT TAG AFA TCG TCA-5'

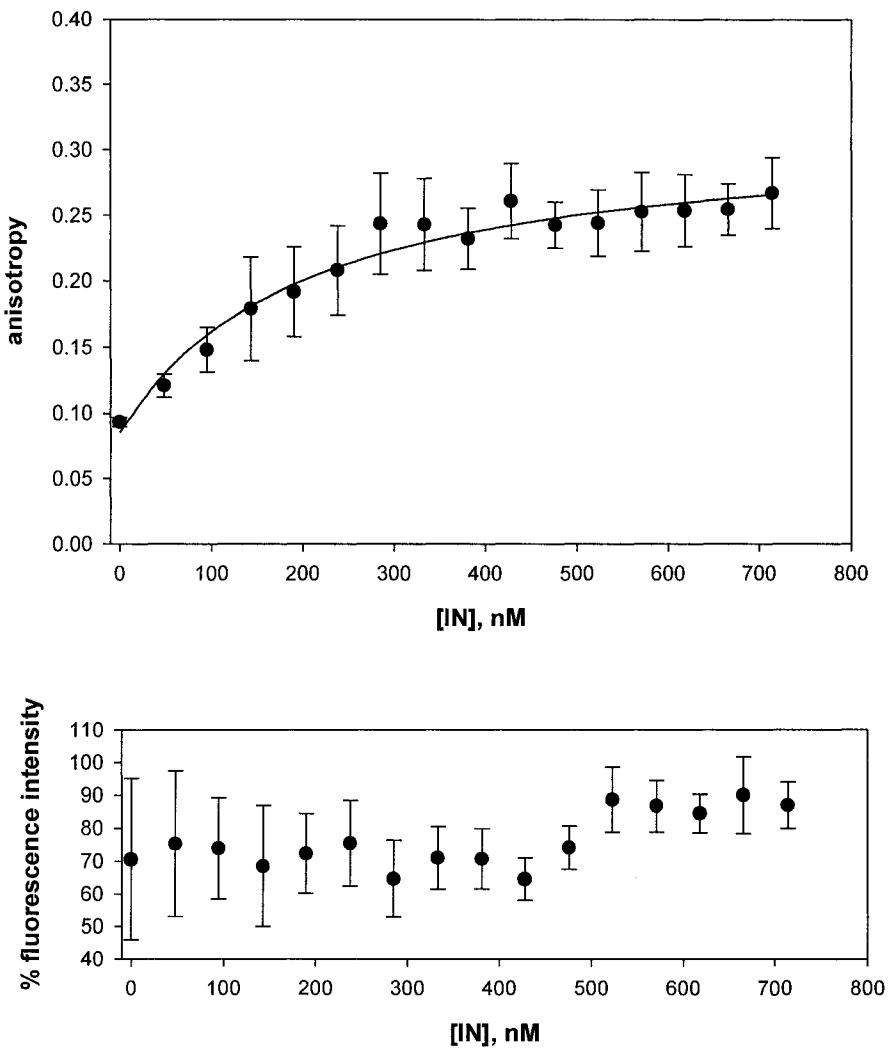

Figure 37. Binding of HIV-1 IN to the U5 single stranded (minus strand) model substrate labeled at position 8 (PTER14U5). Top figure shows change is steady state emission anisotropy as a function of total HIV-1 IN concentration added. Concentration of HIV-1 IN added varies from 48 nM at the start of titration to 714 nM at the end of titration with HIV-1 IN added in 0.5 µl aliquots. The concentration of PTER14U5 oligonucleotide was fixed throughout the titration at 0.1 nM. These binding data are fitted using a nonlinear least squares regression to the equation described in the Methods. The best fit is plotted as a solid line, and the apparent K_D value is obtained from the fit. The bottom panel shows the % fluorescence intensity as a function of HIV-1 IN concentration.

PTER18U5

3'-CAC ACC TTT TAG AGA TCF TCA-5'

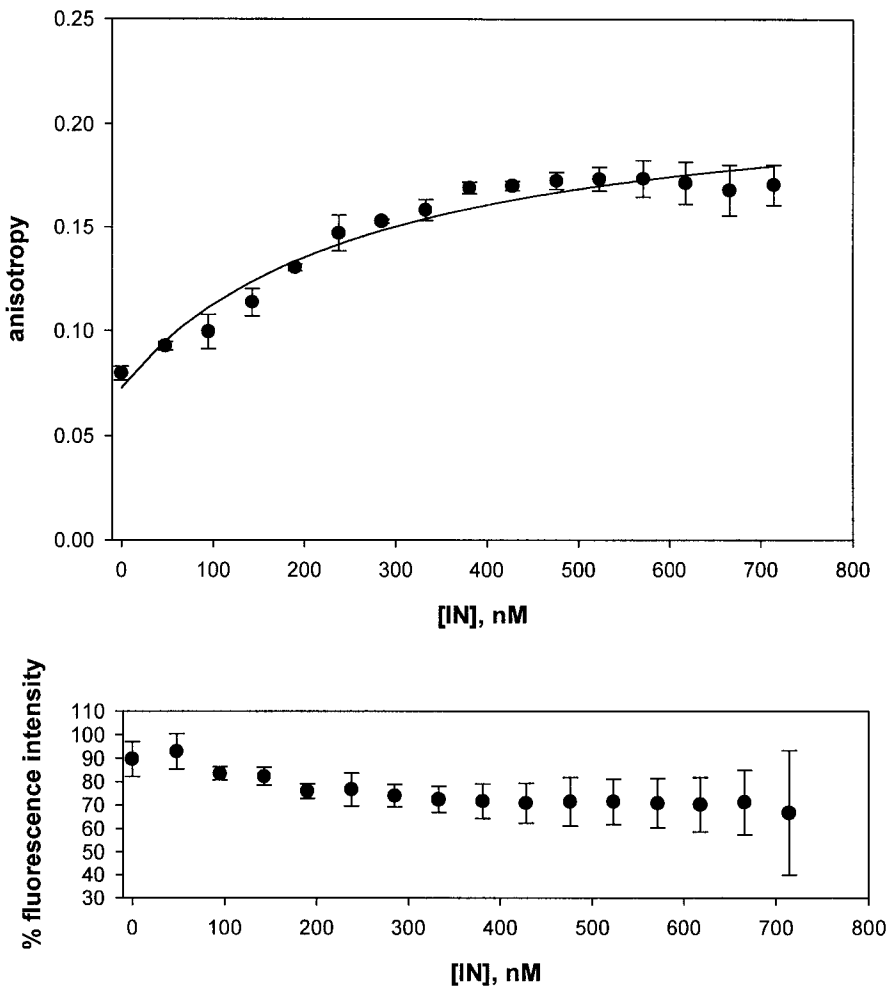

Figure 38. Binding of HIV-1 IN to the U5 single stranded (minus strand) model substrate labeled at position 4 (PTER18U5). Top figure shows change in steady state emission anisotropy as a function of total HIV-1 IN concentration added. Concentration of HIV-1 IN added varies from 48 nM at the start of titration to 714 nM at the end of titration with HIV-1 IN added in 0.5 µl aliquots. The concentration of PTER18U5 oligonucleotide was fixed throughout the titration at 0.1 nM. These binding data are fitted using a nonlinear least squares regression to the equation described in the Methods. The best fit is plotted as a solid line, and the apparent K_D value is obtained from the fit. The bottom panel shows the % fluorescence intensity as a function of HIV-1 IN concentration.

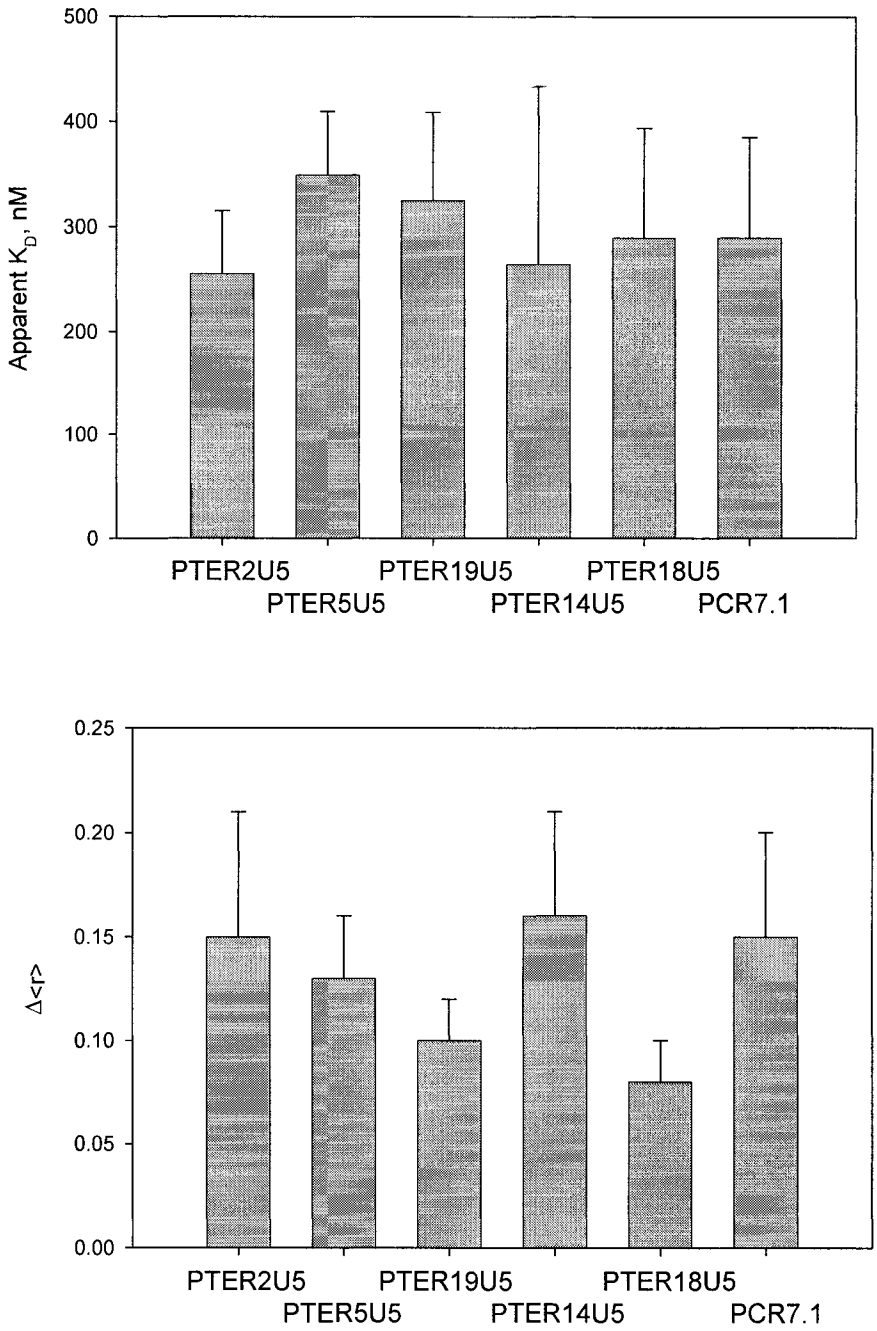

Figure 39. The top graph shows a summary of the apparent K_D values at various positions of the probe (3-MI) within the single stranded model oligonucleotides. The bottom graph shows the corresponding overall changes in anisotropy due to HIV-1 IN binding.

3.4 Random Sequence Double and Single Stranded Oligunucleotide Substrates

DNA is a natural substrate of HIV-1 integrase. Therefore, it is not unexpected that nucleotides, oligonucleotides, and polynucleotides interfere with HIV-1 IN activity. HIV-1 integrase is thought to interact with viral DNA in a sequence-dependent manner and with chromosomal DNA in a sequence-independent manner. Based on observations that HIV-1 IN binds short oligonucleotides *in vitro* without much specificity and yet is very specific in choosing the site of 3'-processing cut, proposed mechanisms suggest that HIV-1 IN binds to viral DNA nonspecifically at first. It then moves along the DNA to find specific sequence for 3'-processing reaction, and binds the sequence very specifically before proceeding with the 3'-processing reaction (18,91).

The ability of HIV-1integrase to bind oligonucleotides with viral and non-viral (random) sequences with similar affinities has been observed in *in vitro* experiments. In the following experiment, we investigate binding of HIV-1 IN to the random sequence short oligonucleotide labeled with 3-MI to determine how HIV-1 integrase interacts with a random sequence oligonucleotide in the described

experimental system.

Experimental results

A double stranded oligonucleotide 19 base pairs long with a random sequence was prepared and labeled with 3-MI. In contrast to labeled sequence specific double-stranded substrates, when titrated with HIV-1 integrase, the concentration dependence of the binding reaction for the random sequence oligonucleotide (PCR7.1ds) does not show a hyperbolic function which would be expected for an independent, single-site binding mechanism (Figure 40). Rather, the sigmoidal nature of the saturation curve indicates cooperative binding of HIV-1 integrase to double stranded PCR 7.1. While double stranded PCR 7.1 shows increased anisotropy when titrated with HIV-1 integrase, it is the only double-stranded oligonucleotide that shows a decrease in total fluorescence intensity upon HIV-1 integrase binding (Figure 40). The decrease in fluorescence intensity may be attributed to static fluorescence quenching through complex formation or changes in the lifetime of the fluorophore (dynamic quenching).

In contrast, binding of HIV-1 integrase to the random sequence single stranded oligonucleotide shows a hyperbolic saturation (Figure

41). The K_D^{app} values obtained (Table 4, Table 5) for double-stranded and single-stranded random sequence oligonucleotides were very comparable: PCR 7.1ds 260 ± 48 nM, PCR 7.1ss 290 ± 95 nM. Further, these random sequence oligonucleotides appear to bind with HIV-1 integrase with affinities similar to those determined for single-stranded U5 sequence specific oligonucleotides (Figure 39). Whereas HIV-1 integrase distinguishes between double-stranded and single-stranded U5 sequence specific oligonucleotides, the protein binds to random sequence oligonucleotides either double-stranded or single-stranded without distinction. Thus, the mechanism of binding to the random double stranded oligonucleotide may be different.

Although apparent binding affinity for random sequence double stranded oligonucleotide is not very different from the affinities for sequence specific double stranded oligonucleotides, PCR7.1 appears to undergo a change distinct from any other oligonucleotide upon HIV-1 integrase binding, suggesting the possibility of differences in interactions between HIV-1 integrase and random sequence duplex oligonucleotide.

PCR7.1

5'- ACC GCT GAA FGA GGA AGC A-3'
3'- TGG CGA CTT CCT CCT TCG T -5'

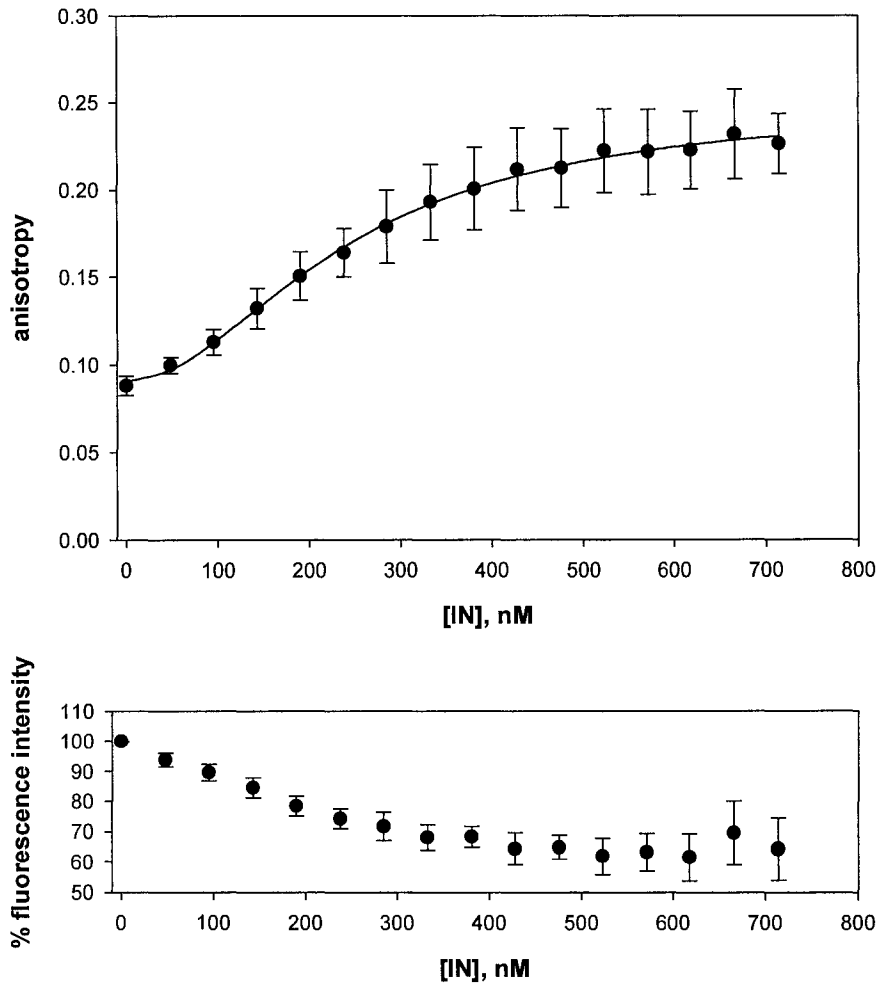

Figure 40. Binding of HIV-1 IN to the double-stranded random sequence oligonucleotide (PCR7.1). Top figure shows change in steady state emission anisotropy as a function of total HIV-1 IN concentration added. Concentration of HIV-1 IN added varies from 48 nM at the start of titration to 714 nM at the end of titration with HIV-1 IN added in 0.5 µl aliquots. Filled circles represent binding data obtained with the concentration of PCR7.1 oligonucleotide fixed throughout the titration at 0.1 nM. These binding data are fitted using a nonlinear least squares regression to the equation described in the Methods. The best fit is plotted as a solid line, and the apparent K_D value is obtained from the fit. The bottom panel shows the % fluorescence intensity as a function of HIV-1 IN concentration.

PCR7.1ss

5'- ACC GCT GAA FGA GGA AGC A-3'

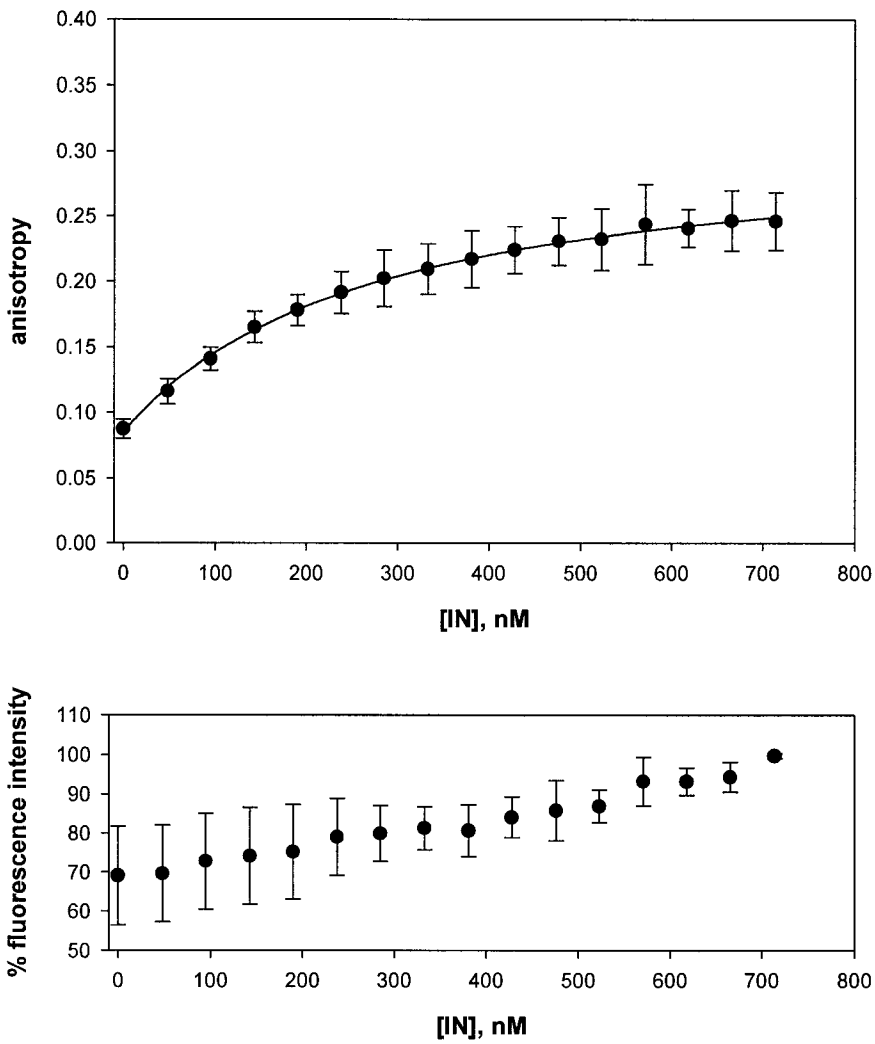

Figure 41. Binding of HIV-1 IN to single stranded random sequence oligonucleotide (PCR7.1ss). Top figure shows change in steady state emission anisotropy as a function of total HIV-1 IN concentration added. Concentration of HIV-1 IN added varies from 48 nM at the start of titration to 714 nM at the end of titration with HIV-1 IN added in 0.5 μl aliquots. The concentration of PCR7.1ss oligonucleotide was fixed throughout the titration at 0.1 nM. These binding data are fitted using a nonlinear least squares regression to the equation described in the Methods. The best fit is plotted as a solid line, and the apparent K_D value is obtained from the fit. The bottom panel shows the % fluorescence intensity as a function of HIV-1 IN concentration.

3.5 U3 Double and Single Stranded Model Oligonucleotide Substrates

HIV-1 integrase has been reported to exhibit different levels of activity with substrates derived from the two ends (U5 and U3 LTR) of unintegrated viral DNA *in vitro* (8,35,66). U5 LTR appears to be the more reactive end for *in vitro* 3'-processing and strand transfer assays using short 21 or 32 base pair oligonucleotides (8,66). In a gel mobility shift assay, wild type U5 LTR 21-mer was shown to compete effectively with U3 LTR 21-mer for HIV-1 integrase binding (35). The HIV-1 U5 IN recognition sequence has been reported to be almost nine times more efficient as a substrate for HIV-1 IN than the U3 IN recognition sequence in studies of concerted DNA integration by HIV-1 integrase with 310 bases substrates containing 20 base pairs from the U3 and U5 HIV-1 LTR termini at each end (95). The difference in activity between the two ends is proposed to be associated with the difference in the U3 and U5 sequences at positions 5 and 6 adjacent to the conserved CA dinucleotide (95). In HIV-1 U5, G and A are at positions 5 and 6 respectively, in the HIV-1 U3 LTR end these positions contain a C and a T respectively (95). When G and A are substituted into the U3 LTR termini, the activity of this IN

recognition sequence increases (95).

Experimental results

As a result of differences in activity between the U5 and U3 LTR ends we wanted to determine if HIV-1 integrase binding to double stranded oligonucleotides with the sequence of the U3 LTR shows a different affinity than when binding to the U5 LTR sequence using the model system. PTER2U3:LTR3 is an oligonucleotide we used as a model for the U3 LTR of HIV-1 genome and is 20 base pairs long (Figure 42). The U3 and U5 sequences differ at 8 base positions within the 20 base pair sequence (Figure 12). Data from titration of HIV-1 IN with the fluorescently labeled (3-MI) U3 LTR sequence showed a K_D^{app} value of 228 ± 40 nM (Figure 42). A slightly lower K_D^{app} value of 186 ± 18 nM was determined for the single stranded PTER2U3 substrate (Figure 43). Within experimental error, K_D^{app} values for single stranded U3 oligonucleotide and double stranded U3 oligonucleotide appear not to be significantly different (Table 6, Figure 44).

In contrast, the apparent binding affinity for the U3 double stranded model oligonucleotide (PTER2U3:LTR3) is 2 times lower

than the binding affinity previously measured for the U5 double stranded oligonucleotide (PTER2U5:LTR4) (Table 6, Figure 44).

Furthermore, no 3'-processing activity of HIV-1 integrase with PTER2U3:LTR3 as a substrate was detected on the time scale of 3'-processing activity observed with the U5 end substrate (PTER2U5:LTR4). Thus, the observed lower binding affinity of HIV-1 integrase for the U3 end appears to correspond with reduced 3'-processing activity for U3 model oligonucleotide in the described system.

Also shown in Figure 44 are anisotropy changes due to HIV-1 integrase binding. For single stranded U3 and U5 model oligonucleotides, the anisotropy changes are the same. Double stranded U3 oligonucleotide has a greater anisotropy change than double stranded U5 oligonucleotide, suggesting a greater reduction in independent movement of 3-MI in position 2 of the minus strand of U3 model oligonucleotide upon HIV-1 integrase binding.

Table 6.
Comparison between U5 and U3 model oligonucleotides

Oligonucleotide	$K_D^{app\,1} \pm$ s.d.[2] (nM)	$\langle r \rangle_{max} \pm$ s.d.	$\langle r \rangle_{min} \pm$ s.d.	$\Delta r \pm$ s.d.
PTER2U5:LTR4	119 ± 21	0.24 ± 0.01	0.07 ± 0.03	0.17 ± 0.03
PTER2U5	256 ± 59	0.22 ± 0.05	0.07 ± 0.01	0.15 ± 0.06
PTER2U3:LTR3	228 ± 40	0.27 ± 0.05	0.07 ± 0.005	0.21 ± 0.05
PTER2U3	186 ± 18	0.22 ± 0.02	0.07 ± 0.002	0.15 ± 0.03

1- all apparent K_D values are averages of at least three separate experiments; 2 - standard deviation

PTER2U3:LTR3

5' - AGT GAA TTA GCC CTT CCA FT - 3'
3' - TCA CTT AAT CGG GAA GGT CA - 5'

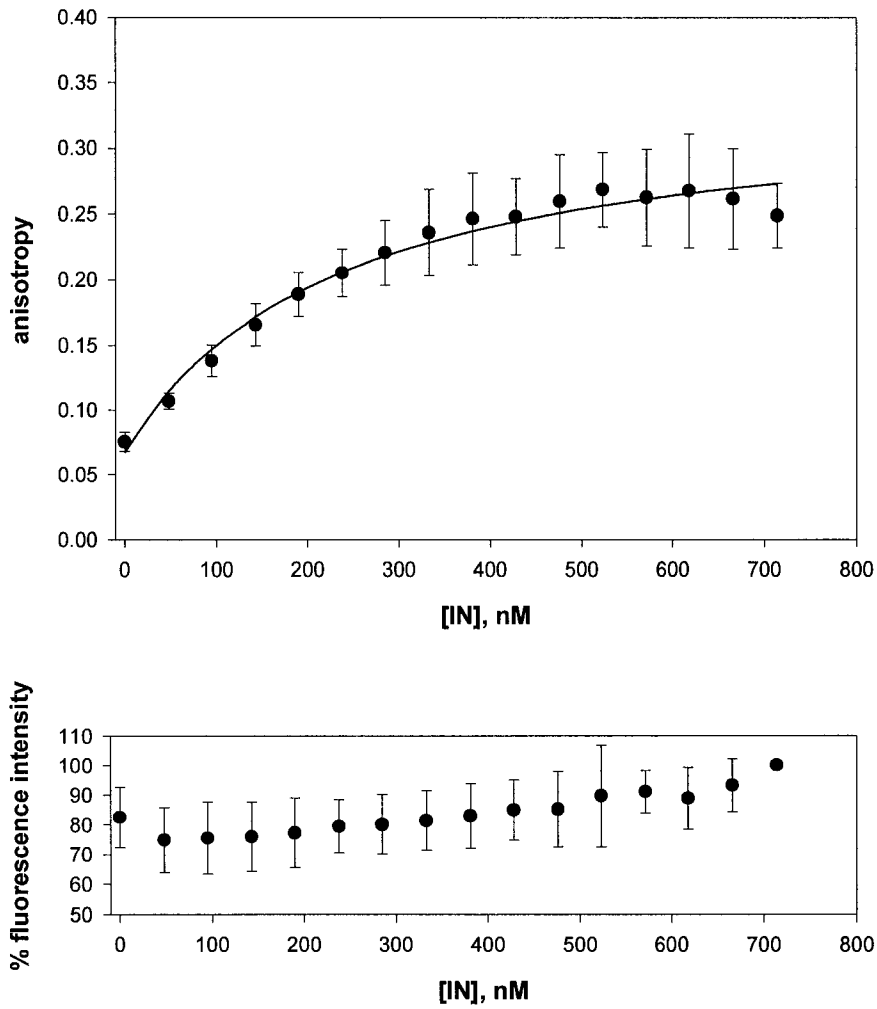

Figure 42. Binding of HIV-1 IN to theU3 model substrate labeled at position 2 of the minus strand (PTER2U3:LTR3). Top figure shows change in steady state emission anisotropy as a function of total HIV-1 IN concentration added. Concentration of HIV-1 IN added varies from 48 nM at the start of titration to 714 nM at the end of titration with HIV-1 IN added in 0.5 μl aliquots. The concentration of PTER2U3:LTR3 oligonucleotide was fixed throughout the titration at 0.1 nM. These binding data are fitted using a nonlinear least squares regression to the equation described in the Methods. The best fit is plotted as a solid line, and the apparent K_D value is obtained from the fit. The bottom panel shows the % fluorescence intensity as a function of HIV-1 IN concentration.

PTER2U3

5'- AGT GAA TTA GCC CTT CCA FT -3'

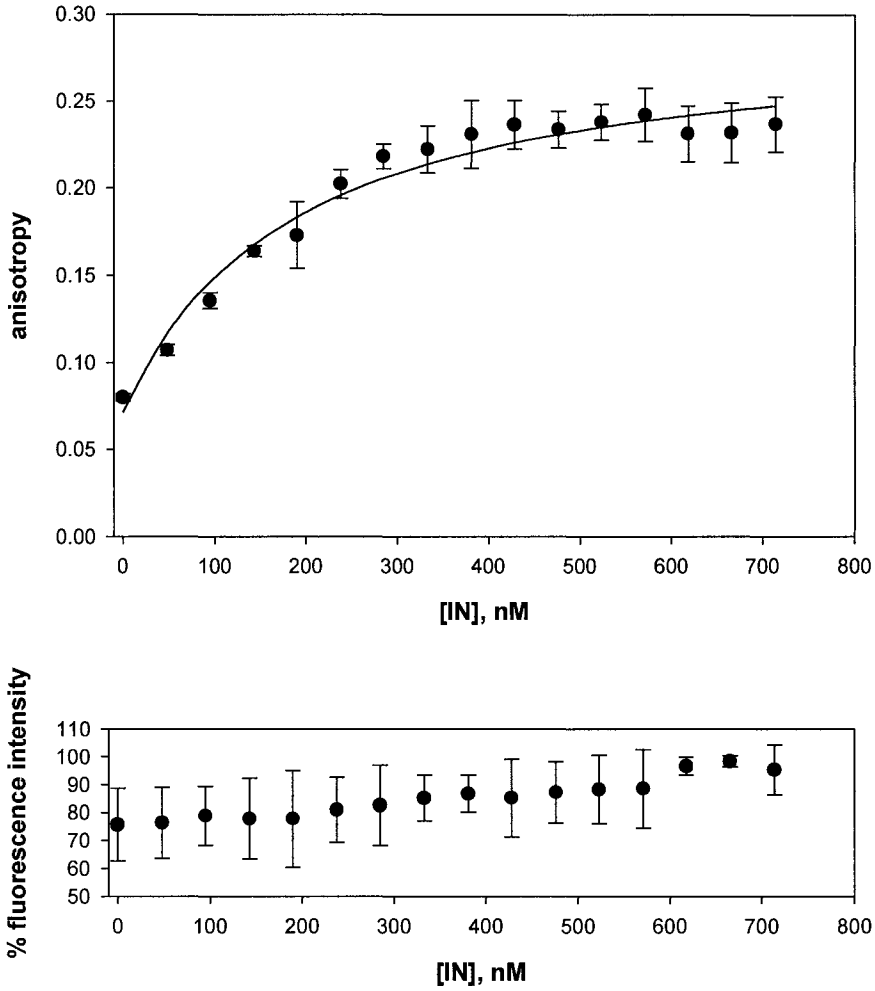

Figure 43. Binding of HIV-1 IN to theU3 single stranded (minus strand) model substrate labeled at position 2 (PTER2U3). Top figure shows change in steady state emission anisotropy as a function of total HIV-1 IN concentration added. Concentration of HIV-1 IN added varies from 48 nM at the start of titration to 714 nM at the end of titration with HIV-1 IN added in 0.5 μl aliquots. The concentration of PTER2U3 oligonucleotide was fixed throughout the titration at 0.1 nM. These binding data are fitted using a nonlinear least squares regression to the equation described in the Methods. The best fit is plotted as a solid line, and the apparent K_D value is obtained from the fit. The bottom figure shows the % fluorescence intensity as a function of HIV-1 IN concentration.

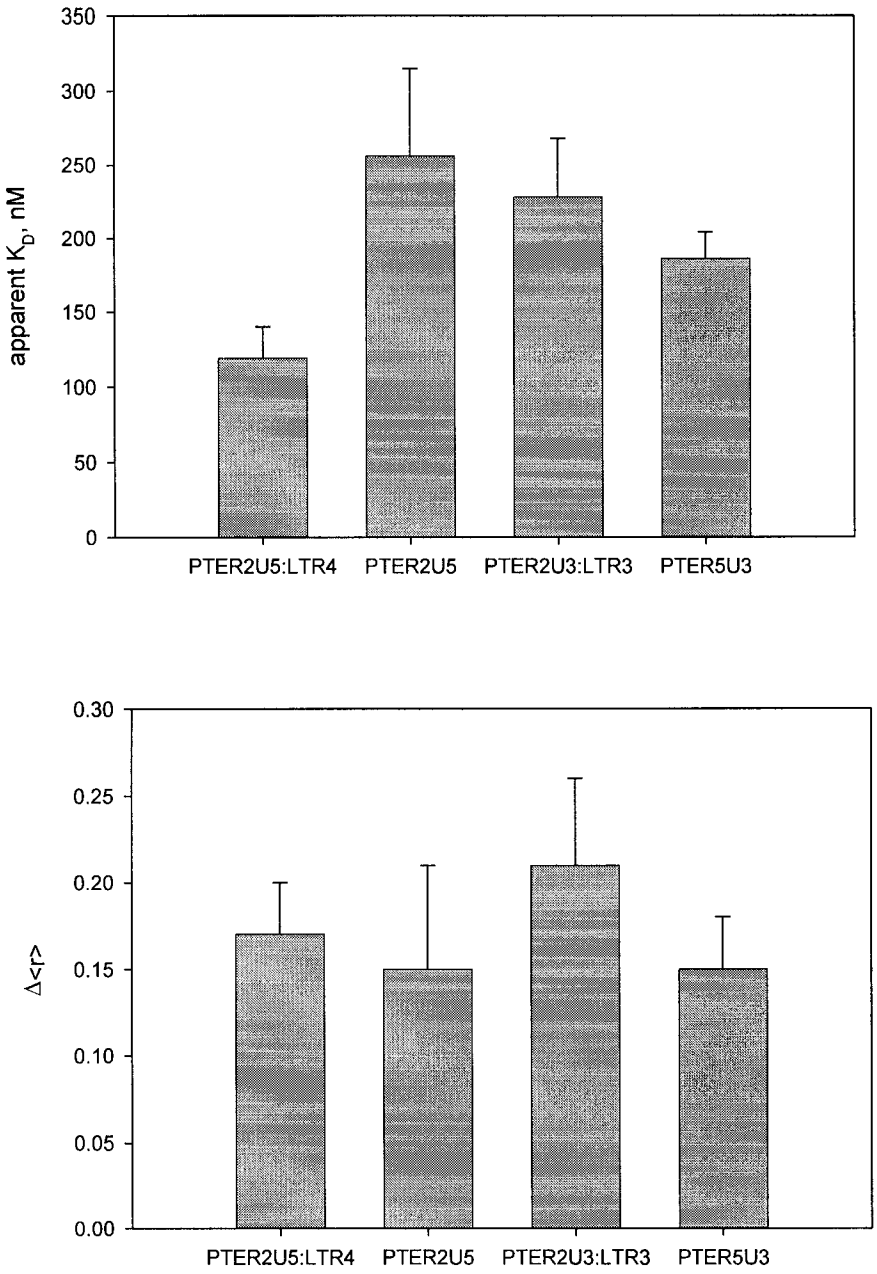

Figure 44. Top graph shows a comparison of the apparent K_D values for oligonucleotides with U5 or U3 sequences with the probe (3-MI) in the second position: double stranded U5 sequence oligonucleotide (PTER2U5:LTR4) vs double stranded U3 sequence oligonucleotide (PTER2U3:LTR3); single stranded U5 sequence oligonucleotide (PTER2U5) vs single stranded U3 sequence oligonucleotide (PTER2U3). The bottom graph shows the corresponding overall anisotropy changes.

3.6 U3-U5 41 base pair Oligonucleotide Substrate

Previous *in vitro* experiments have suggested that HIV-1 integrase interacts differently with longer substrates as compared to short (15-21 bp) oligonucleotide substrates. For example, investigations of the 3'-processing activity of this protein revealed that Mg^{2+}- dependent activity increases with increasing substrate length (24 to 29 bp), while Mn^{2+}- dependent 3'-processing activity was reduced (101). Longer substrates (35-bp DNA) were reported to have a higher specificity for HIV-IN as compared to shorter substrate (24-bp DNA) in the presence of either Mn^{2+} or Mg^{2+} (101). Also, the stability of HIV-1 integrase complexes with nonviral (random) sequence oligonucleotides were noted to increase with increasing length of DNA from 24 base pairs to 40 base pairs (26). Thus we proposed to determine the effects of longer oligonucleotide substrates on binding parameters of HIV-1 integrase in the described system.

Experimental results

Oligonucleotides of 41 base pairs used in our experiments were synthesized by combining sequences of U5 (21 base pair) and U3 (20 base pairs) ends. The 41 base pair double stranded oligonucleotide was labeled with 3-MI at position 2 of the U5 end (Figure 46), at

position 2 of the U3 end (Figure 45), and at position 2 of both U5 and U3 ends (Figure 47), thus providing three differently labeled oligonucleotides.

Binding studies with oligonucleotides that combine U5 and U3 sequences (41-mers) provide an alternative way to determine if HIV-1 integrase discriminates between the two ends when binding to the oligonucleotides. Table 7 summarizes the results of binding studies with these 41 base model oligonucleotides and displays the results obtained for the U5 and U3 short model oligonucleotides. The K_D^{app} value for U3 labeled 41-mer oligonucleotide is 399 ± 78 nM (Figure 45), and is similar to U5 labeled model oligonucleotide (369 nM) (Figure 46). It appears that HIV-1 integrase binds either DNA end (21 base pair long U5 end and 20 base pair long U3 end) in the 41-mers without apparent preference. The unlabeled end may compete with the labeled end for HIV-1 integrase binding. For the 41-mer with both U3 and U5 ends labeled, K_D^{app} value increases further (557 ± 61 nM) (Figure 47).

Lower binding affinities are observed with the 41-mer as compared to the 21-mer (Table 7). For the U3 labeled 41-mer K_D^{app} is determined to be 399 ± 78 nM, and is 2 times the K_D^{app} for U3 21-

mer. Similarly, for the U5 labeled 41-mer the K_D^{app} value is 3 times greater than for the U5 21-mer. And for 41-mer labeled at both ends, the K_D^{app} value increases even more (557 ± 61 nM). The U5 and U3 ends appear to compete with each other in binding and, thus, the apparent binding affinities obtained are the average binding affinities for U5 and U3 ends. Thus, it appears that the 0.1 nM oligonucleotide combining U5 and U3 sequences acts in the experimental system described as a 0.2 nM 21 base pairs long oligonucleotide. Longer substrates combining the U3 and U5 sequences appear to increase the number of potential binding sites therefore requiring higher concentrations of HIV-1 integrase to obtain the binding saturation comparable with shorter length oligonucleotides.

5'-ACT GGA AGG GCT AAT TCA CTG TGT GGA AAA TCT CTA GCA GT- 3'
3'-TFA CCT TCC CGA TTA AGT GAC ACA CCT TTT AGA GAT CGT CA - 5'

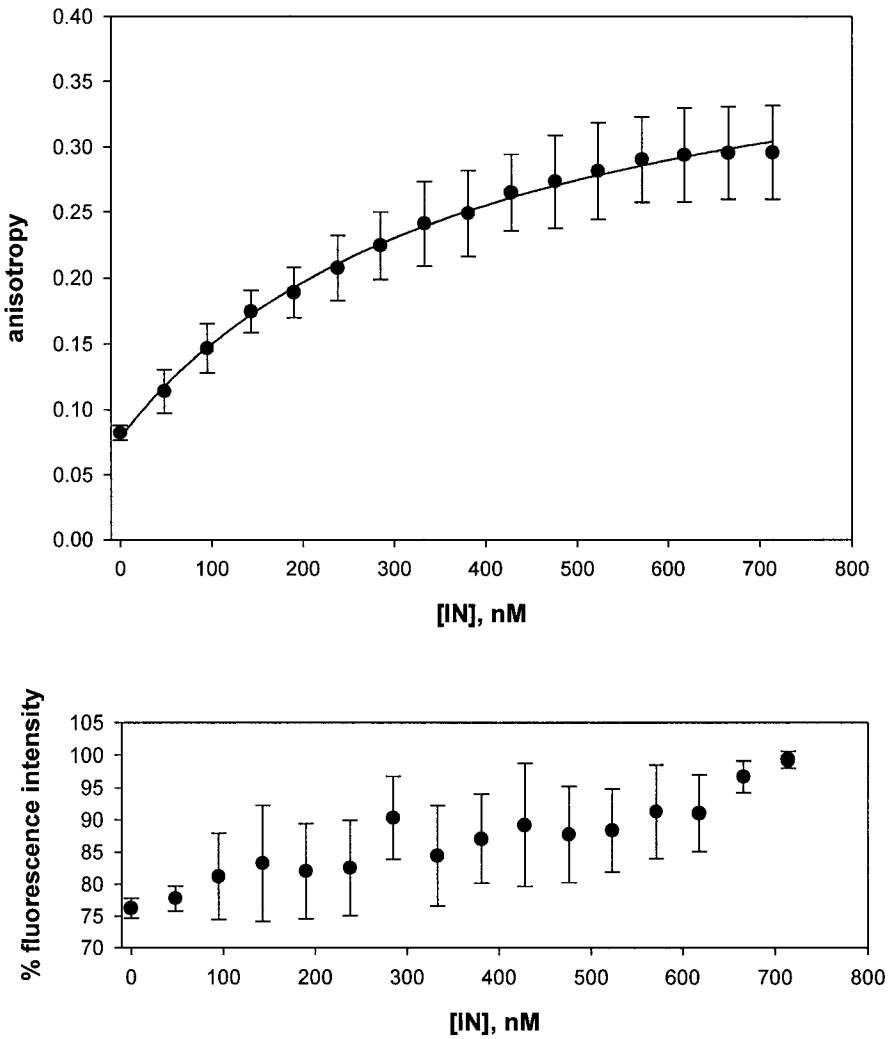

Figure 45. Binding of HIV-1 IN to the U3 labeled 41-mer model substrate. Top figure shows change in steady state emission anisotropy as a function of total HIV-1 IN concentration added. Concentration of HIV-1 IN added varies from 48 nM at the start of titration to 714 nM at the end of titration with HIV-1 IN added in 0.5 μl aliquots. The concentration of 41-mer oligonucleotide was fixed throughout the titration at 0.1 nM. These binding data are fitted using a nonlinear least squares regression to the equation described in the Methods. The best fit is plotted as a solid line, and the apparent K_D value is obtained from the fit. The bottom panel shows the % fluorescence intensity as a function of HIV-1 IN concentration.

5'-ACT GGA AGG GCT AAT TCA CTG TGT GGA AAA TCT CTA GCA FT- 3'
3'-TGA CCT TCC CGA TTA AGT GAC ACA CCT TTT AGA GAT CGT CA - 5'

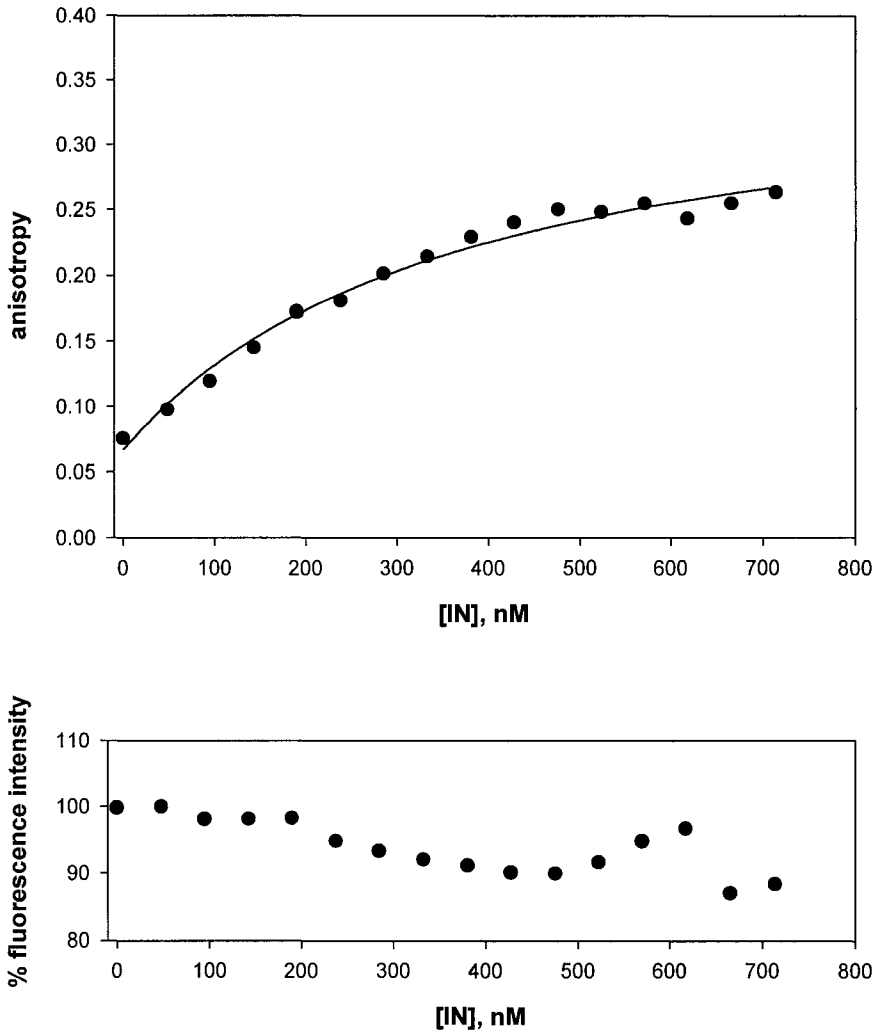

Figure 46. Binding of HIV-1 IN to the U5 labeled 41-mer model substrate. Top figure shows change in steady state emission anisotropy as a function of total HIV-1 IN concentration added. Concentration of HIV-1 IN added varies from 48 nM at the start of titration to 714 nM at the end of titration with HIV-1 IN added in 0.5 μl aliquots. The concentration of 41-mer oligonucleotide was fixed throughout the titration at 0.1 nM. These binding data are fitted using a nonlinear least squares regression to the equation described in the Methods. The best fit is plotted as a solid line, and the apparent K_D value is obtained from the fit. The bottom figure shows the % fluorescence intensity as a function of HIV-1 IN concentration.

5'-ACT GGA AGG GCT AAT TCA CTG TGT GGA AAA TCT CTA GCA FT- 3'
3'-TFA CCT TCC CGA TTA AGT GAC ACA CCT TTT AGA GAT CGT CA - 5'

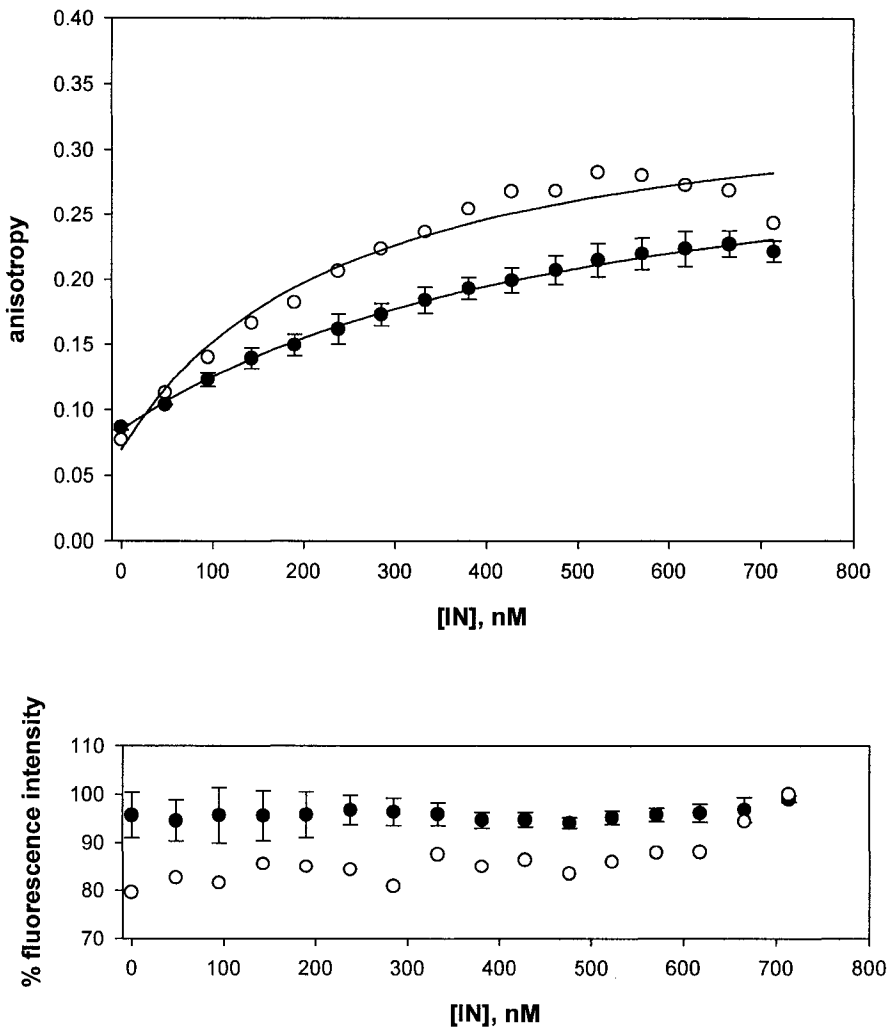

Figure 47. Binding of HIV-1 IN to the U5 and U3 labeled 41-mer model substrate. Top figure shows change in steady state emission anisotropy as a function of total HIV-1 IN concentration added. Concentration of HIV-1 IN added varies from 48 nM at the start of titration to 714 nM at the end of titration with HIV-1 IN added in 0.5 µl aliquots. Filled circles represent binding data obtained with the concentration of 41-mer oligonucleotide fixed throughout the titration at 0.1 nM. These binding data are fitted using a nonlinear least squares regression to the equation described in the Methods. The best fit is plotted as a solid line, and the apparent K_D value is obtained from the fit. Open circles show data obtained with the concentration of 41-mer oligonucleotide fixed throughout the titration at 0.05 nM. The bottom panel shows the % fluorescence intensity as a function of HIV-1 IN concentration.

Table 7.
41-mers vs 21-mers

oligonucleotide	K_D^{app} [1] ± s.d.[2](nM)	$\langle r \rangle_{max}$ ± s.d.	$\langle r \rangle_{min}$ ± s.d.	Δ $\langle r \rangle$ ± s.d.
U3 labeled 41-mer	399 ± 78	0.31 ± 0.04	0.08 ± 0.01	0.23 ± 0.03
U5 labeled 41-mer	369	0.30	0.07	0.23
U3-U5 labeled 41-mer	557 ± 61	0.27 ± 0.02	0.08 ± 0.01	0.19 ± 0.03
PTER2U5:LTR4	119 ± 21	0.24 ± 0.01	0.07 ± 0.03	0.17 ± 0.03
PTER2U3:LTR3	228 ± 40	0.27 ± 0.05	0.07 ± 0.01	0.21 ± 0.05

1- all apparent K_D values are averages of at least three separate experiments except for U5 labeled 41-mer; 2 - standard deviation

3.7 Role of Metal Cations on the Binding Process

With oligonucleotides being polyanions, protein-DNA interactions are governed to a large extent by the ionic strength of the solution in which interactions are being studied and by the presence of cations required for the productive protein-DNA interactions (1,102). In addition, electrostatic interactions between the phosphate backbone of oligonucleotides and interacting amino acids of proteins are thought to contribute considerably to the overall protein-DNA affinity (1,102).

As was described in Section 1.1.4, HIV-1 integrase shows a requirement for Mn^{2+} or Mg^{2+} for its catalytic activities. In general, considerably more activity is observed in the presence of Mn^{2+} than in the presence of Mg^{2+} for retroviral integrases *in vitro* (67,44,65,66). However, Mg^{2+} is generally assumed to be the biologically relevant cofactor because this cation is maintained at higher concentrations in the cytoplasm of living cells (9,30,64,68,69).

Divalent cations appear to play two roles in HIV-1 IN interaction with DNA: they participate in the formation of a stable IN-DNA complex and are required for efficient catalysis. It was noted that the initial complex between integrase and DNA can be formed

without divalent cations (Mn^{2+} or Mg^{2+}) (26,29,102). However, the binding of HIV-1 IN to DNA in the absence of divalent cations was determined to be unstable and nonspecific (29,37,102). Thus, assembly of a stable complex with viral LTR substrates has been shown to require divalent cations (37,38,61,102).

To gain some insight into the role of cations in the HIV-1 integrase interactions with model oligonucleotides, several experiments were conducted using the described system where a fixed concentration of oligonucleotide was titrated with HIV-1 integrase in the presence of cations that are thought to be important for its function. In particular, three cations were of interest: Mg^{2+}, Mn^{2+}, Zn^{2+}.

3.7.1 Studies with the Label at the 3'-processing Site (Position 2 from the 3'-end)

Binding studies using PTER2U5:LTR4 oligonucleotide were performed in the absence of divalent cation. Under these conditions, a small increase in emission anisotropy was observed, suggesting inefficient binding in the absence of cation (Figure 48). Similar binding affinities were observed when the concentration of NaCl corresponding to the ionic strength of 7.5 mM $MnCl_2$ was used in the

binding reaction (Figure 48). However, addition of Mn^{2+} to the system greatly stimulates binding (Figure 48). When the same oligonucleotides are titrated with HIV-1 integrase in the presence of 7.5 mM $MgCl_2$, some binding is detected as reflected by increases in anisotropy values, however the overall anisotropy change is too small to allow a meaningful determination of binding parameters (Figure 49). It was previously reported that addition of exogenous zinc to the 3'-processing reaction in the presence of Mg^{2+} enhances 3'-processing by HIV-1 integrase (39,70). Additionally, previous studies have shown that the enhancement of 3'processing activity by HIV-1 integrase was not observed for 3'-processing when zinc was added in the presence of Mn^{2+} (70). To see if addition of zinc can alter the binding interactions in this system, $ZnCl_2$ was added to the binding reaction together with manganese or magnesium. No measurable differences in binding interactions of HIV-1 integrase with the PTER2U5:LTR4 model substrate were detected when zinc cation was present in the binding reaction with magnesium or manganese (Figure 49).

3.7.2 Studies with the Random Sequence

Similarly, the effect of cation on binding interactions between HIV-1 integrase and oligonucleotide with nonviral (random) sequence were investigated for comparison to the oligonucleotides with specific sequence. For random sequence oligonucleotide, insignificant binding was observed without metals or in presence of NaCl (Figure 50). Magnesium alone or in presence of zinc does not stimulate binding between HIV-1 integrase and random sequence oligonucleotide in the described sysytem (Figure 51). Addition of zinc to manganese containing binding reaction appears to result in a linear increase in anisotropy as a function of HIV-1 IN concentration, and no saturation is observed as in the presence of manganese only (Figure 51). Thus, for PTER2U5:LTR4 with U5 specific sequence and PCR7.1ds with random sequence, we observed stimulation of the binding of HIV-1 integrase to the model oligonucleotides by Mn^{2+}.

3.7.3 Studies with the Label at Position 4 from the 5'-end of the Minus Strand

The effect of cations on HIV-1 IN binding to oligonucleotide labeled at position 4 of the minus strand was investigated. Previously we showed that HIV-1 integrase is sensitive to the presence of 3-MI at

this site for binding. Therefore, it was interesting to see if metal cations could influence the binding affinity between HIV-1 integrase and 3-MI labeled PTER18U5:LTR5. When PTER18U5:LTR5 3-MI was titrated with integrase in the presence of zinc and manganese, a greater increase in anisotropy values was observed upon HIV-1 integrase binding than in the presence of manganese only (Figure 52). For anisotropy data obtained in presence of manganese and zinc, an apparent K_D was determined. The value determined from the data fit is 306 nM, a 1.3 fold reduction from 408 ± 8 nM in the presence of manganese only. The presence of magnesium only, or magnesium with zinc does not produce any measurable differences in the interaction between HIV-1 IN and PTER18U5:LTR5 (Figure 52).

6-MI probe is better tolerated in PTER18U5:LTR5 by HIV-1 integrase for binding. A marginal increase in binding affinity of HIV-1 IN is observed with 6-MI labeled PTER18U5:LTR5 in the presence of manganese (Figure 53). The binding affinity in manganese and zinc containing binding reaction (205 nM) is similar to the binding affinity in the presence of manganese only (270 ± 52 nM).

3.7.4 U3-U5 41 base pair Oligonucleotide Substrates

It has been reported that HIV-1 integrase mediates the 3'-processing reaction with greater efficiency with longer substrates (35bp) in presence of magnesium than in presence of manganese (70). Therefore, we previously determined binding affinities for 41 base pair long oligonucleotides combining U3 and U5 sequences (section 3.6). As shown in Figure 54 for U3 labeled 41-mer and in Figure 55 for U3 and U5 labeled 41-mer, there were no stimulatory effects on HIV-1 integrase binding to 41base pair long double stranded oligonucleotides observed in presence of magnesium or magnesium and zinc.

Our results show that Mn^{2+} induced stronger effects than Mg^{2+} on the enhancement of HIV-1 IN binding to the model oligonucleotides.

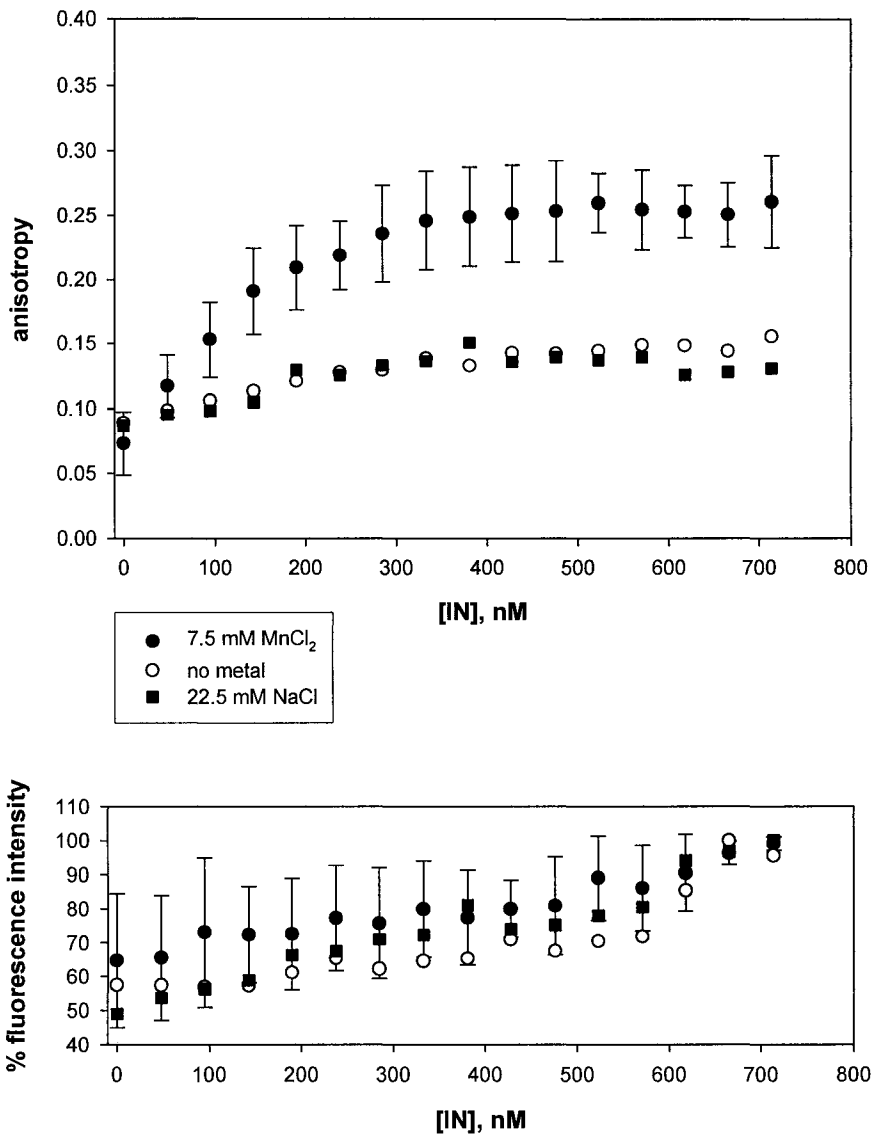

Figure 48. Titrations of PTER2U5:LTR4 with HIV-1 IN in the absence of divalent cation (open circle), with NaCl present creating ionic strength equivalent to 7.5 mM divalent cation (filled square) compared with binding curve obtained in presence of 7.5 mM Mn^{2+} (filled circle). Bottom figure shows the fluorescence intensity changes corresponding to the anisotropy data in the top figure.

PTER2U5:LTR4

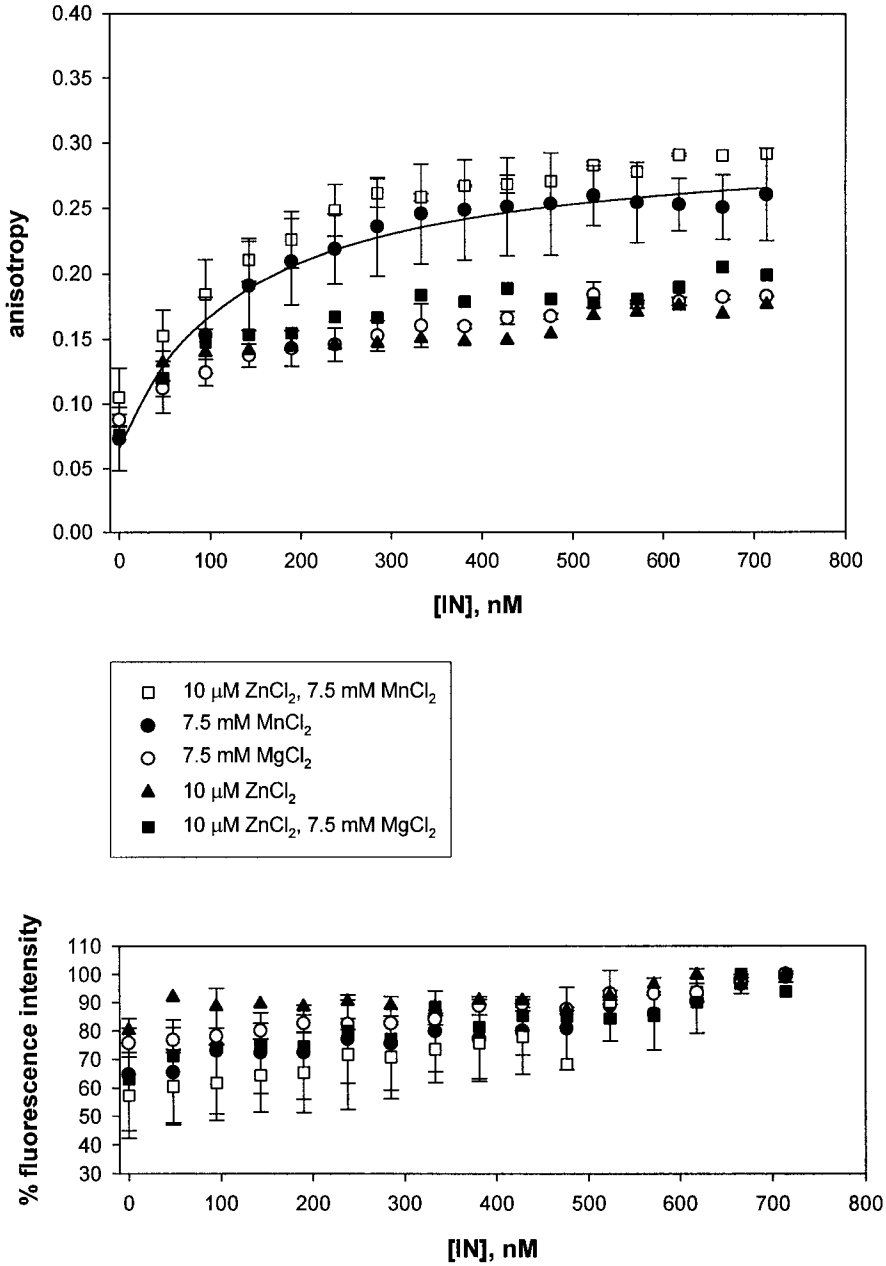

Figure 49. Titration of PTER2U5:LTR4 with HIV-1 IN in presence of 7.5 mM Mn^{2+} (filled circle) is compared to titrations in presence of 7.5 mM Mg^{2+} (open circle), 10 μM Zn^{2+} only(filled triangle), 10 μM Zn^{2+} and 7.5 mM Mn^{2+} (open square), 10 μM Zn^{2+} and 7.5 mM Mg^{2+} (filled square). Bottom figure shows the corresponding fluorescence intensities.

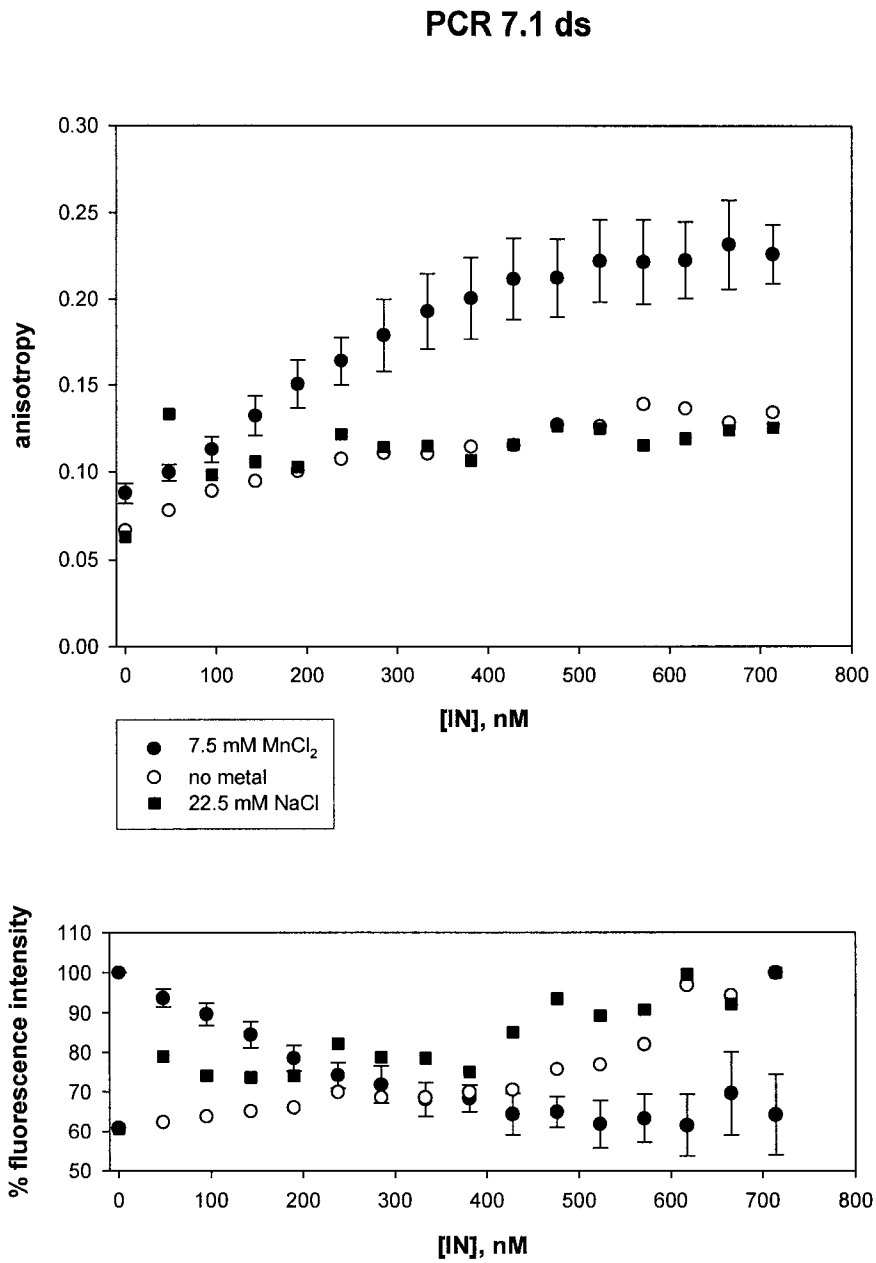

Figure 50. Titration of random sequence oligonucleotide with HIV-1 IN in the absence of divalent cation (open circle), with NaCl present creating ionic strength equivalent to 7.5 mM divalent cation (filled square) compared with binding curve obtained in presence of 7.5 mM Mn^{2+} (filled circle). Bottom figure shows the fluorescence intensity changes corresponding to the anisotropy data in the top figure.

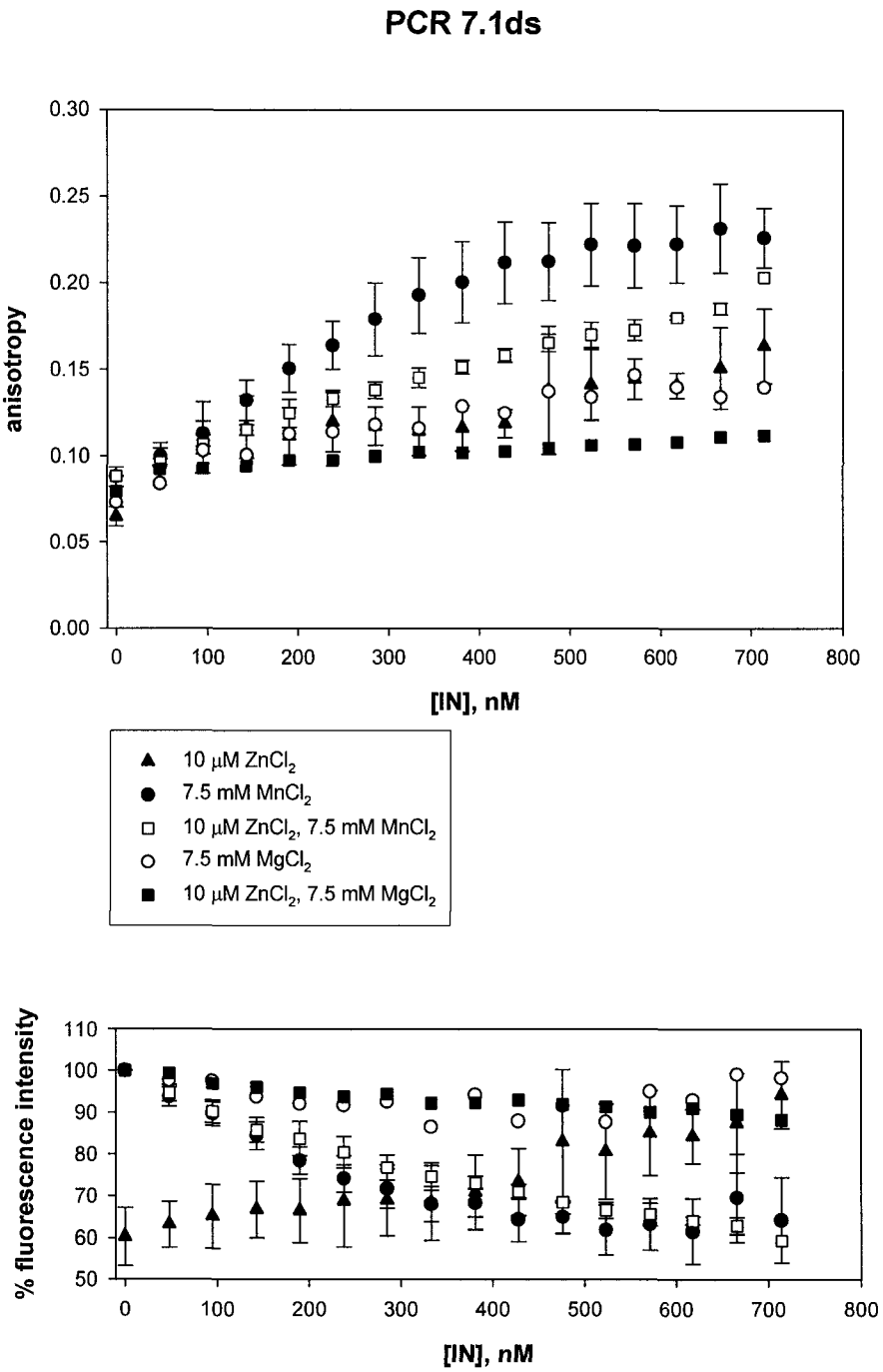

Figure 51. Titration of random sequence oligonucleotide with HIV-1 IN in presence of 7.5 mM Mn^{2+} (filled circle) is compared to titrations in presence of 7.5 mM Mg^{2+} (open circle), 10 μM Zn^{2+} only(filled triangle), 10 μM Zn^{2+} and 7.5 mM Mn^{2+} (open square), 10 μM Zn^{2+} and 7.5 mM Mg^{2+} (filled square). Bottom figure shows the corresponding fluorescence intensities.

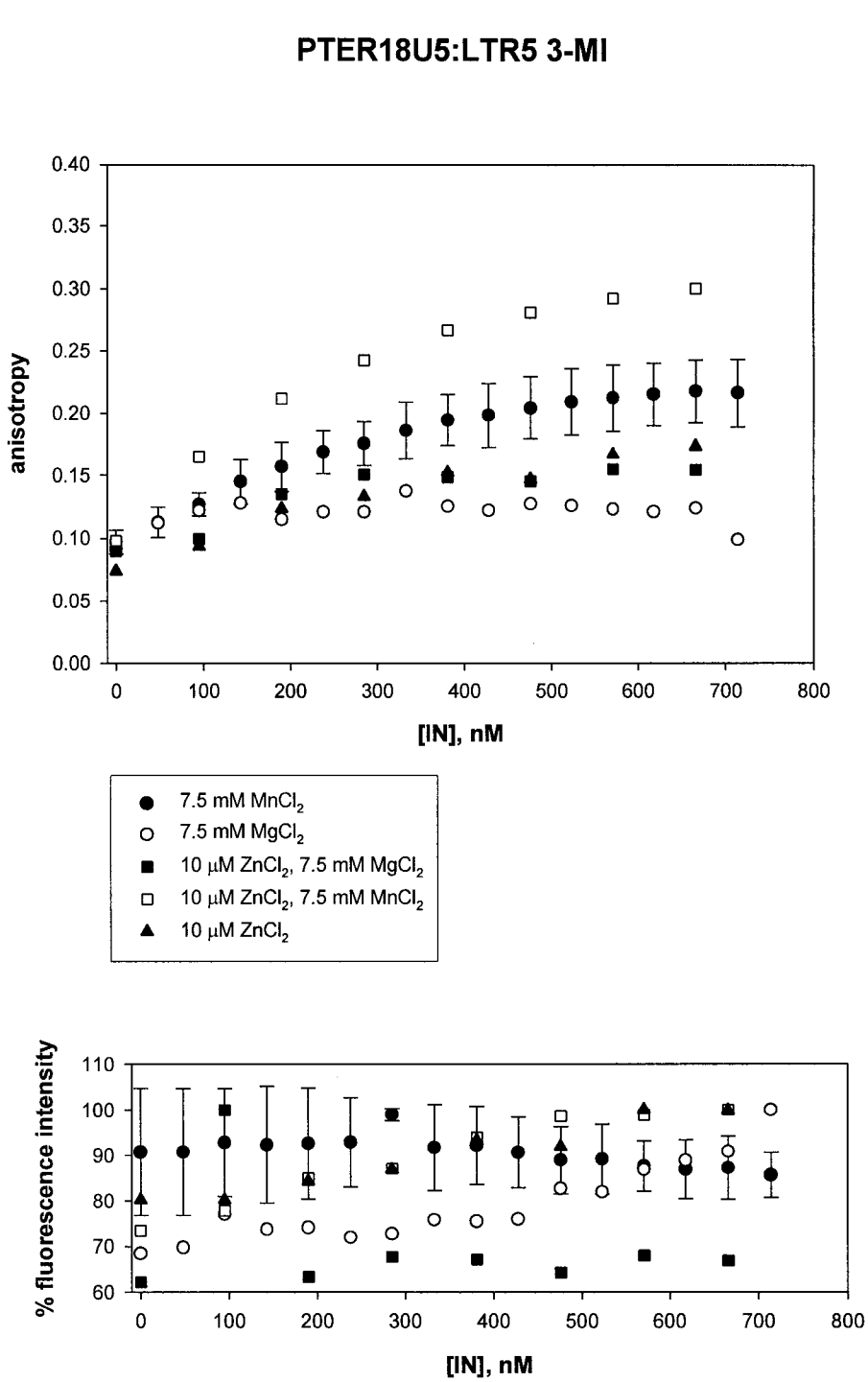

Figure 52. Titration of PTER18U5:LTR5 3-MI with HIV-1 IN in presence of 7.5 mM Mn^{2+} (filled circle) is compared to titrations in presence of 7.5 mM Mg^{2+} (open circle), 10 μM Zn^{2+} only (filled triangle), 10 μM Zn^{2+} and 7.5 mM Mn^{2+} open square), 10 μM Zn^{2+} and 7.5 mM Mg^{2+} (filled square). Bottom figure shows the corresponding fluorescence intensities.

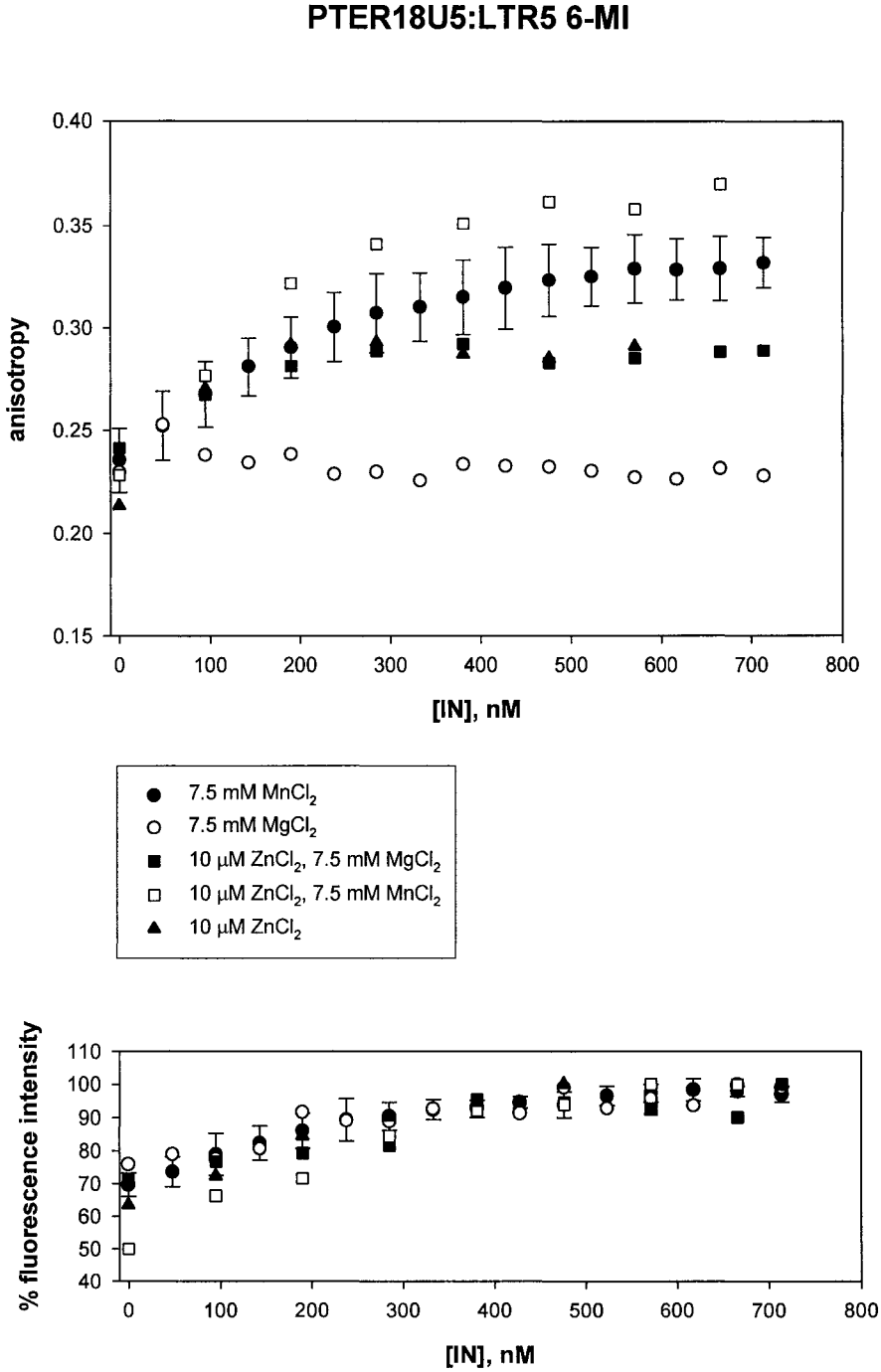

Figure 53. Titration of PTER18U5:LTR5 6-MI with HIV-1 IN in presence of 7.5 mM Mn^{2+} (filled circle) is compared to titrations in presence of 7.5 mM Mg^{2+} (open circle), 10 μM Zn^{2+} only (filled triangle), 10 μM Zn^{2+} and 7.5 mM Mn^{2+} (open square), 10 μM Zn^{2+} and 7.5 mM Mg^{2+} (filled square). Bottom figure shows the corresponding fluorescence intensities.

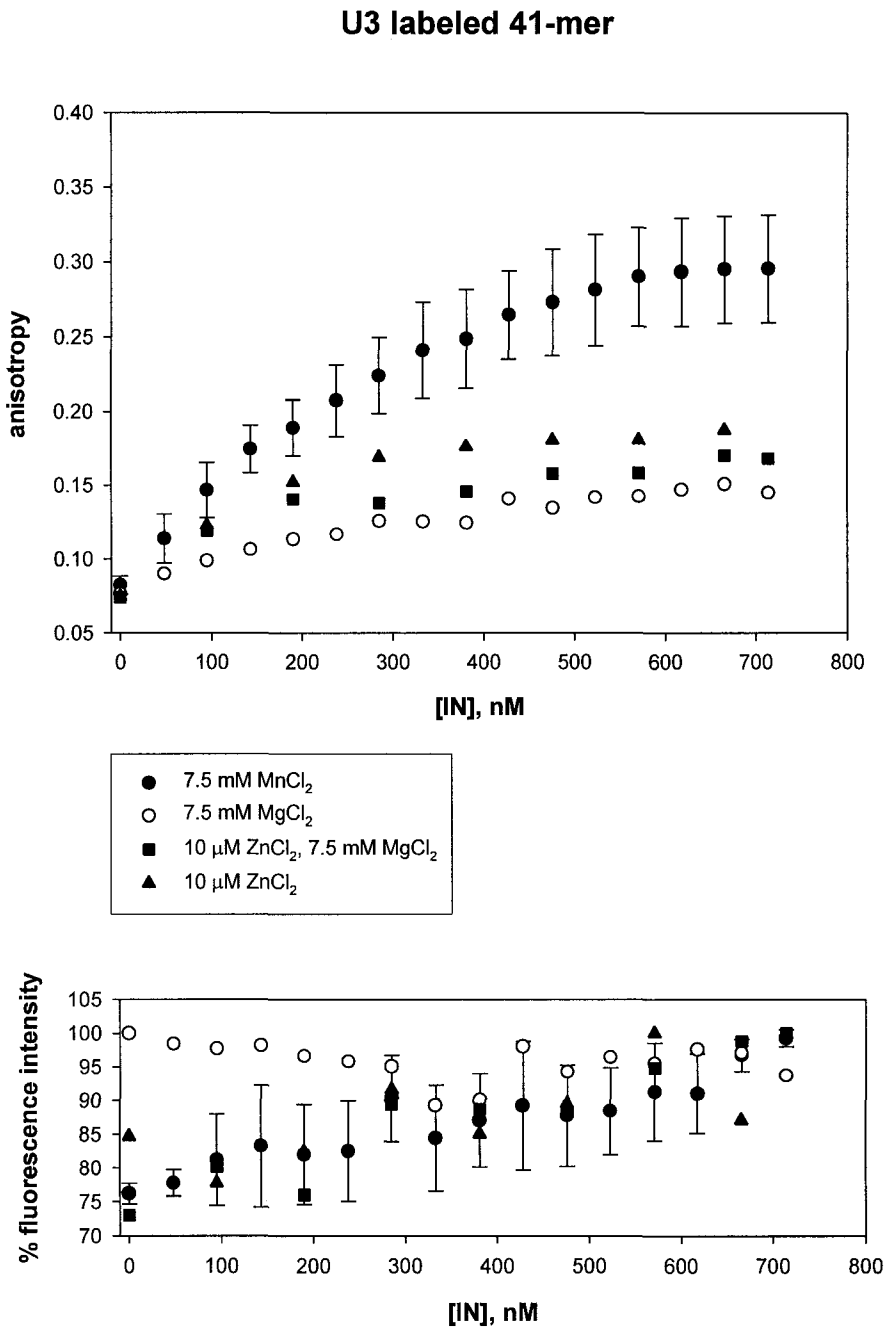

Figure 54. Titration of U3 labeled 41base pair long oligonucleotide with HIV-1 IN in presence of 7.5 mM Mn^{2+} (filled circle) is compared to titrations in presence of 7.5 mM Mg^{2+} (open circle), 10 μM Zn^{2+} only (filled triangle), 10 μM Zn^{2+} and 7.5 mM Mg^{2+} (filled square). Bottom figure shows corresponding fluorescence intensities.

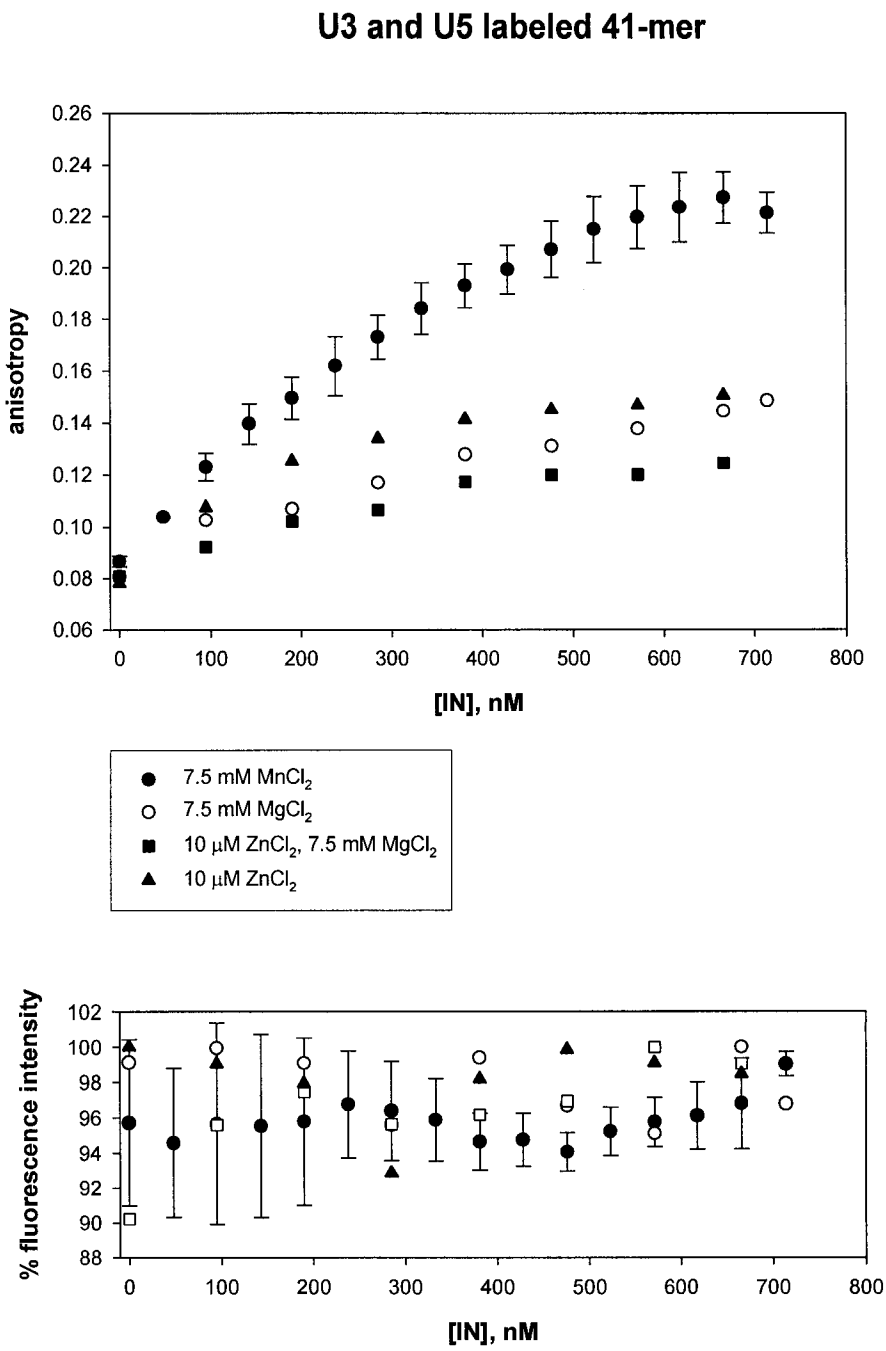

Figure 55. Titration of U3 and U5 labeled 41 base pair long oligonucleotide with HIV-1 IN in presence of 7.5 mM Mn^{2+} (filled circle) is compared to titrations in presence of 7.5 mM Mg^{2+} (open circle), 10 μM Zn^{2+} only (filled triangle), 10 μM Zn^{2+} and 7.5 mM Mg^{2+} (filled square). Bottom figure shows corresponding fluorescence intensities.

Chapter 4: CONCLUSION

An *in vitro* system has been described for the study of DNA-protein interactions between HIV-1 integrase and DNA substrates that utilizes purified HIV-1 IN protein, short synthetic viral fluorescent oligonucleotides, and divalent cations. This simple system offers a unique opportunity to investigate, in detail, the DNA sequence requirements for the HIV-1 integrase binding and provides, for the first time, quantification of these interactions at different positions along the synthetic oligonucleotide sequence.

While many biophysical approaches can be used to study DNA-protein interactions, this approach employs a convenient solution based method. Steady state fluorescence emission anisotropy measurements can provide insights into the affinity of binding of HIV-1 IN to short fluorescent oligonucleotides. Such measurements do not require separation of free and bound species and are not influenced by molecular immobilization effects, which may result in conformational alterations of the protein structure.

While previous mutation and base substitution studies have defined key viral DNA bases that are important for HIV-1 IN binding and catalytic functions, we have not found previous published studies

that quantify the binding affinities of HIV-1 integrase for different base positions along the length of varying model oligonucleotide substrates. The incorporation of fluorescent guanine analogs into these model viral sequences has provided us with the opportunity to determine the binding affinities of this protein towards a variety of base positions on both the plus and minus strands of DNA. In addition, this study has served to expand our general understanding of the applicability for 3-MI and 6-MI for DNA-protein studies. In particular, we have exploited fluorescence intensity and emission anisotropy changes for providing insights into conformational and binding information.

Interestingly, 3-MI in contrast to 6-MI demonstrates a larger overall anisotropy change (Δr) when comparing absolute emission anisotropy values of those fluorescent oligonucleotides free in solution *versus* bound to HIV-1 integrase. This suggests a greater sensitivity of this fluorophore to the imposed restricted rotational motions arising from DNA-protein binding. However, 3-MI is not known to participate in H-bonding to the cytosine on the complementary strand. In accordance with other studies (77,78,103), 6-MI demonstrates a better fit into the double stranded

oligonucleotide conformation and can form three hydrogen bonds with the complementary cytosine. In these studies, comparison of both probes has been used to establish effects of H-bonding interactions within the duplex oligonucleotide structure on binding with HIV-1 integrase.

As summarized in Figure 56, from a systematic analysis using steady-state fluorescence emission anisotropy binding data, we have determined quantitative binding differences displayed by HIV-1 integrase with the various base positions along model viral oligonucleotides (Figure 56). Apparent binding constants suggest, as might be expected, that double stranded specific sequences are the preferred substrate of HIV-1 integrase over corresponding single stranded specific sequences resulting in enhanced specificity of binding. Furthermore, double-stranded substrates with wild type sequences around the 3'-processing site (PTER2U5:LTR4) are preferred over the non-cleavable substrate with base substitutions close to the 3'-processing site. Our data suggests that base substitutions surrounding position 2 of the plus strand strongly influence the protein's binding affinity for that site, and therefore influence the 3' processing efficiency of the protein.

Additionally, apparent binding constants confirm that position 5 on the plus strand is bound with a greater affinity in the blunt ended (PTER5U5:LTR4) *versus* pre-cleaved oligonucleotide. This suggests that the strand transfer substrate (pre-cleaved oligonucleotide) has a lesser binding specificity and is not a good substrate for HIV-1 integrase (48). In general the efficiency of binding is stronger for the plus strand, but appears to be somewhat invariant to the absolute distance from the cleavage site.

The importance of the structural integrity of the duplex oligonucleotide in the region of position 4 of the minus strand for contact by HIV-1 integrase was established by employing both fluorescent probes, 3-MI and 6-MI. These probes, through differences in their H-bonding efficiencies with the complimentary strand, suggest that position 4 has a more stringent requirement for appropriate H-bonding and that disruption of such interactions, as in the presence of 3-MI can significantly impact the binding of HIV-1 integrase, and can serve as an important site for potential inhibitor design.

Our studies, showing that the relative activity of the U3 20-mer oligonucleotide sequence is less than for the U5 21-mer

oligonucleotide *in vitro* shows excellent agreement with previous literature reports. It would appear that the reduced activity of the protein correlates with the reduced binding affinity observed for the U3 oligonucleotide.

The effect of cation on the binding efficiency of HIV-1 integrase to model oligonucleotides shows that the manganese cation stimulates DNA-protein binding over magnesium cation. This result supports other *in vitro* experiments that employ short oligonucleotide substrates that have suggested that HIV-1 integrase prefers Mn^{2+} for its catalytic activity. This result is somewhat surprising in light of the fact that for HIV-1 IN and its substrates, the true cellular concentration of Mg^{2+} is greater than Mn^{2+}. This effect is believed to be associated with a stable complex formation that is formed using Mn^{2+} under *in vitro* conditions. Interestingly, the recessed ends of the endogenous viral DNA within core particles integrate efficiently *in vitro* with Mg^{2+} as the divalent cation (28).

While it is understood that these studies have focused on the use of an *in vitro* model, this simple system has provided further insights into the details of the DNA sequence requirements for HIV-1 IN binding. The biological relevance of the system may be further

improved by increasing the complexity of the model system: for example, using proteins involved in the pre-integration complex, along with the HIV-1 integrase. Such an approach can provide information on the influence that other proteins may have on the integrase-DNA interactions, and provide insights into designing competitors that can inhibit HIV-1 integrase binding.

In conclusion, by coupling the available HIV-1 IN structural data with the results of biochemical experiments, we can begin to picture how HIV-1 IN interacts with DNA on the molecular level (8). *In vitro* studies serve an important role in such studies, by furthering our understanding of the retroviral integration mechanism. Binding studies as discussed here are expected to add to the present body of knowledge focused on HIV-1 integrase-substrate interactions, binding specificity of the protein, and can provide insights into modeling HIV-1 integrase functions *in vivo*. Finally, a greater understanding of HIV-1 integrase interactions with its substrates can ultimately lead to the development of efficient inhibitors of this important protein.

U5 oligonucleotide

Figure 56. Summary of the roles of bases of U5 LTR in the binding reaction *in vitro*. Positions 2 and 5 on the plus strand are important in establishing binding contacts with HIV-1 IN prior to 3'-processing. Local oligonucleotide conformation at position 4 affects the manner in which IN recognizes and binds DNA substrate. HIV-1 IN also contacts position 8 of the minus strand and position 19 of the plus strand before 3'-processing reaction.

REFERENCES

1. H. Loodish, D. Baltimore, A. Berk, S.L. Zipursky, P. Matsudaira, J. Darnell. Molecular Cell Biology. 3rd ed. New York: W. H. Freeman and Company, 1997.

2. R.A. Weiss, Gulliver's travels in HIV land (2001), Nature 410, 963 - 967.

3. M. Chicurel, Probing HIV's elusive Activities within the host cell (2000), Science 290, 1876 - 1879.

4. M. Thomas and L. Brady, HIV-1 integrase: a target for AIDS therapeutics (1997), Trends in Biotech. Vol.15, 167-172.

5. M. Katzman and R. A. Katz, Substrate recognition by retroviral integrases (1999), Adv. Vir. Res. Vol.52, 371-395.

6. Y. Goldgur, R. Craigie, G. H. Cohen, T. Fujiwara, T. Yoshinaga, T. Fujishita, H. Sugimoto, T. Endo, H. Murai, and D. R. Davies, Structure of the HIV-1 integrase catalytic domain complexed with an inhibitor: A platform for antiviral drug design (1999), Proc. Natl. Acad. Sci. USA Vol.96, 13040-13043.

7. R. R. Drake, N. Neamati, H. Hong, A. A. Pilon, P. Sunthankar, S. D. Hume, G. W. A. Milne, and Y. Pommier, Identification of a nucleotide binding site in HIV-1 integrase (1998), Proc. Natl. Acad. Sci. USA Vol.95, 4170-4175.

8. D. Esposito and R. Craigie, HIV integrase structure and function (1999), Adv. Vir. Res. Vol.52, 319-333.

9. D. C. van Gent, Y. Elgersma, M. W. J. Bolk, C. Vink, and R. H. A. Plasterk, DNA binding properties of the integrase proteins of human immunodeficiency viruses types 1 and 2 (1991), Nucleic Acids Res. Vol. 19, 3821 - 3827.

10. K. Sayasith, G. Sauve, J. Yelle, Targeting HIV-1 integrase (2001), Expert Opin.Ther.Targets 5(4), 443 - 464.

11.H. Chen, S-Q Wei, and A. Engelman, Multiple integrase functions are required to form the native structure of the Human Immunodeficiency Virus type 1 intasome (1999), J. Biol. Chem. Vol. 274, 17358 - 17364.

12.M. Bouyac-Bertoia, J.D. Dvorin, R.A.M. Fouchier, Y. Jenkins, B.E. Meyer, L.I. Wu, M. Emerman, and M.H. Malim, HIV-1 infection requires a functional integrase NLS (2001), Mol. Cell 7, 1025 - 1035.

13.E. Tramontano, P. L. Colla, and Y-C. Cheng, Biochemical characterization of the HIV-1 integrase 3'-processing activity and its inhibition by phosphorothioate oligonucleotides (1998), Biochemistry Vol. 37, 7237-7243.

14.L.M. Skinner, M. Sudol, A.L. Harper, and M. Katzman, Nucleophile selection for the endonuclease activities of human, ovine, and avian retroviral integrases (2001), J. Biol. Chem. Vol. 276, 114 - 124.

15.S. Popov, M. Rexach, L. Ratner, G. Blobel, and M. Bukrinsky, Viral protein R regulates docking of the HIV-1 preintegration complex to the nuclear pore complex (1998), J. Biol. Chem. Vol. 273, 13347- 13352.

16. M. Bukrinsky, N. Sharova, T.L. McDonald, T. Pushkarskaya, W.G. Tarpley, and M. Stevenson, Association of integrase, matrix, and reverse transcriptase antigens of human immunodeficiency virus type 1 with viral nucleis acids following acute infection (1993), Proc. Natl. Acad. Sci. USA Vol. 90, 6125 - 6129.

17. M.I. Bukrinsky and O. K. Haffar, HIV-1 nuclear import: in search of a leader (1999), Frontiers in Bioscience 4, 772 - 781.

18.P. Cherepanov, D. Surratt, J. Toelen, W. Pluymers, J. Griffith, E. De Clercq, and Z. Debyser, Activity of recombinant HIV-1 integrase on mini-HIV DNA (1999), Nucleic Acid. Res. Vol. 27, 2202 - 2210.

19.P. Hindmarsh and J. Leis, Retroviral DNA integration (1999), Microbiol. Mol. Biol. Rev. Vol. 63, 836 - 843.

20.M.L. Holmes-Son, R.S. Appa, C.A. Chow, Molecular genetics and target site specificity of retroviral integration (2001), Adv.Genet. 43, 33 - 69.

21.E.A. Faust, A. Garg, L. Small, A. Acel, R. Wald, B. Udashkin, Enzymatic capability of HIS-tagged HIV-1 integrase using oligonucleotide disintegration substrates (1996), J. Biomedical Science 3, 254 - 265.

22.S.A. Chow, In vitro assays for activities of retroviral integrase (1997), Methods: A companion to Methods in Enzymology 12, 306 - 317.

23.E. Khan, J.P.G. Mack, R.A. Katz, J. Kulkosky and A.M. Skalka, Retroviral integrase domains: DNA binding and the recognition of LTR sequences (1991), Nucleic Acids Res. Vol. 19, 851- 860.

24.M.D. Andrake and A.M. Skalka, Retroviral integrase, putting pieces together (1996), J. Biol. Chem. Vol. 271, 19633 - 19636.

25.E.A. Faust, H. Triller, Stimulation of Human Flap Endonuclease 1 by Human immunodeficiency virus type1 integrase: possible role for flap endonuclease 1 in 5'-end processing of Human immunodeficiency virus type 1 integration intermediates (2002), J. Biomed. Sci. 9, 273 - 287.

26.J. Yi, E. Asante-Appiah, and A. M. Skalka, Divalent cations stimulate preferential recognition of a viral DNA end by HIV-1 integrase (1999), Biochemistry 38, 8458-8468.

27.K. S. Jones, J. Coleman, G.W. Merkel, T. M. Laue, and A.M. Skalka, Retroviral integrase functions as a multimer and can turn over catalytically (1992), J. Biol. Chem. Vol. 267, 16037-16040.

28.S. P. Lee, H.G. Kim, M. L. Censullo, and M.K. Han, Characterization of Mg^{2+} -dependent 3'-processing activity for HIV-1 integrase *in vitro*: real-time kinetic studies using

fluorescence resonance energy transfer (1995), Biochemistry Vol.34, 10205-10214.

29. I. K. Pemberton, M. Buckle, and H. Buc, The metal ion-induced cooperative binding of HIV-1integrase to DNA exhibits a marked preference for Mn (II) than Mg (II) (1996), J. Biol. Chem. Vol. 271, 1498-1506.

30. B. M. Nilsen, I. R. Haugan, K. Berg, L. Olsen, P.O. Brown, and D. E. Helland, Monoclonal antibodies against Human Immunodeficiency Virus type 1 integrase: Epitope mapping and differential effect on integrase activities in vitro (1996), J. Virol. Vol.70, 1580-1587.

31. E. Asante-Appiah and A. M. Skalka, HIV-1 integrase: structural organization, conformational changes, and catalysis (1999), Adv. Vir. Res. Vol.52, 351-369.

32. A. Wlodawer, Crystal structures of catalytic core domains of retroviral integrases and role of divalent cations in enzymatic activity (1999), Adv. Vir. Res. Vol.52, 335-350.

33. R. D. Lins, T.P. Straatsma, J. M. Briggs, Similarities in the HIV-1 and ASV integrase active sites upon metal cofactor binding (2000), Biopolymers Vol.53, 308-315.

34. A. Engelman, A. B. Hickman, and R. Craigie, The core and carboxyl-terminal domains of the integrase protein of Human Immunodeficiency Virus type 1 each contribute to nonspecific DNA binding (1994), J. Virol. Vol. 68, 5911-5917.

35. D. J. Hazuda, A. L. Wolfe, J.C. Hastings, H. L. Robbins, P. L. Graham, R. L. LaFemina, and E. A. Emini, Viral long terminal repeat substrate binding characteristics of the Human Immunodeficiency Virus type 1 integrase (1994), J. Biol. Chem. Vol. 269, 3999-4004.

36. M. Katzman and M. Sudol, Influence of subterminal viral DNA nucleotides on differential susceptibility to cleavage by Human

Immunodeficiency Virus Type 1 and Visna Virus integrases (1996), J. Virol. Vol.70, 9069-9073.

37. V. Ellison and P. O. Brown, A stable complex between integrase and viral DNA ends mediates human immunodeficiency virus integration in vitro (1994), Proc. Natl. Acad. Sci. USA Vol.91, 7316-7320.

38. A. L. Wolfe, P. J. Felock, J. C. Hastings, C. U. Blau, and D. J. Hazuda, The role of manganese in promoting multimerization and assembly of Human Immunodeficiency Virus type 1 integrase as a catalytically active complex on immobilized long terminal repeat substrates (1996), J. Virol. Vol. 70, 1442-1432.

39. R. Zheng, T. M. Jenkins, and R. Craigie, Zinc folds the N-terminal domain of HIV-1 integrase, promotes multimerization, and enhances catalytic activity (1996), Proc. Natl. Acad. Sci. USA Vol. 93, 13659- 13664.

40. F. D. Bushman, A. Engelman, I. Palmer, P. Wingfield, and R. Craigie, Domains of the integrase protein of human immunodeficiency virus type 1 responsible for polynucleotidyl transfer and zinc binding (1993), Proc. Natl. Acad. Sci. USA Vol. 90, 3428-3432.

41. D. J. Kim, S.K. Lee, Y. T. Oh, and C. G. Shin, Minimal Core Domain of HIV-1 Integrase for Biological Activity (2000), Mol. Cells Vol. 10, 96 - 101.

42. M. Cai, R. Zheng, M. Caffrey, R. Craigie, G.M. Clore and A.M. Gronenborn, Solution structure of the N-terminal zinc binding domain of HIV-1 integrase (1997), Nature Structural Biology 4, 567 - 577.

43. C.J. Burke, G. Sanyal, M.W. Bruner, J.A. Ryan, R.L. LaFemina, H.L. Robbins, A.S. Zeft, C.R. Middaugh, and M.G. Cordingley, Structural implication of spectroscopic characterization of a putative zinc finger peptide from HIV-1 integrase (1992), J.Biol.Chem. Vol. 267, 9639 - 9644.

44. S. P. Lee, J. Xiao, J. R. Knutson, M. S. Lewis, and M. K. Han, Zn^{2+} promotes the self-association of human immunodeficiency virus type 1 integrase in vitro (1997), Biochemistry 36, 173- 180.

45. K. A. Vincent, V. Ellison, S. A. Chow, and P. O. Brown, Characterization of human immunodeficiency virus type 1 integrase expressed in Escherichia coli and analysis of variants with amino-terminal mutations (1993), J. Virol. Vol. 67, 425- 437.

46. T.S. Heuter and P.O. Brown, Mapping features of HIV-1 integrase near selected sites on viral and target DNA molecules in an active enzyme-DNA complex by photo-cross-linking (1997), Biochemistry 36, 10655 - 10665.

47. F.M.I. Van den Ent, A. Vos, R.H.A. Plasterk, Dissecting the role the N-terminal domain of human immunodeficiency virus type 1 integrase by trans-complementation analysis (1999), J. Virol. Vol.73, 3176 - 3183.

48. D. Esposito and R. Craigie, Sequence specificity of viral end DNA binding by HIV-1 integrase reveals critical regions for protein-DNA interaction (1998), EMBO J. Vol.17, 5832-5843.

49. A. P. A. M. Eijkelenboom, R. Sprangers, K. Hard, R. A. Puras Lutzke, R. H. A. Plasterk, R. Boelens, and R. Kaptein, Refined solution structure of the C-terminal DNA-binding domain of hunam immunovirus-1 integrase (1999), Proteins: structure, Function, and Genetics 36, 556 - 564.

50. R.A. Puras Lutzke, C. Vink and R.H.A. Plasterk, Characterization of the minimal DNA-binding domain of the HIV integrase protein (1994), Nucleic Acids Res. Vol. 22, 4125 - 4131.

51. R. A. Puras Lutzke and R. H. A. Plasterk, Structure-based mutational analysis of the C-terminal DNA-binding domain of human immunodeficiency virus type 1 integrase: critical residues for protein oligomerization and DNA binding (1998), J. Virol. Vol. 72, 4841- 4848.

52. P.J. Lodi, J.A. Ernst, J. Kuszewski, A.B. Hickman, A. Engelman, R. Craigie, G.M. Clore, and A.M. Gronenborn , Solution structure of the DNA binding domain of HIV-1 integrase (1995), Biochemistry 34, 9826 - 9833.

53. A.P. Eijkelenboom, R.A. Lutzke, R. Boelens, R.H. Plasterk, R. Kaptein, and K. Hard, The DNA-binding domain of HIV-1 integrase has an SH3-like fold (1995), Nat. Struct. Biol. 2, 807-810.

54. T. M. Jenkins, A. Engelman, R. Ghilardo, and R. Graigie, A soluble active mutant of HIV-1 integrase (1996), J. Biol. Chem. Vol. 271, 7712 - 7718.

55. F. Dyda, A. B. Hickman, T. M. Jenkins, A. Engelman, R. Craigie, D. R. Davies, Crystal structure of the catalytic domain of HIV-1 integrase: similarity to other polynucleotidyl transferases (1994), Science Vol. 266, 1981- 1986.

56. J. C.-H. Chen, J. Krucinski, L. J. W. Miercke, J. S. Finer-Moore, A.H. Tang, A. D. Leavitt, and R. M. Stroud, Crystal structure of the HIV-1 integrase catalytic core and C-terminal donains: A model for viral DNA binding (2000), Proc. Natl. Acad. Sci. USA Vol. 97, 8233- 8238.

57. Y. Goldgur, F. Dyda, A. B. Hickman, T. M. Jenkins, R. Craigie, and D. R. Davies, Three new structures of the core domain of HIV-1 integrase: An active site that binds magnesium (1998), Proc. Natl. Acad. Sci. USA Vol.95, 9150 - 9154.

58. S. Maignan, J.P. Guilloteau, Q. Zhou-Liu, C. Clement-Mella, and V. Mikol, Crystal structures of the catalytic domain of HIV-1 integrase free and complexed with its metal cofactor: high level of similarity of the active site with other viral integrases (1998), J. Mol. Biol. 282: 359 - 368.

59. J.-Y. Wang, H. Ling, W. Yang, and R. Craigie, Structure of a two-domain fragment of HIV-1 integrase: implications for domain organization in the intact protein (2001), EMBO J., Vol. 20, 7333-7343.

60. A.B. Hickman, F. Dyda and R. Craigie, Heterogeneity in recombinant HIV-1 integrase corrected by site-directed mutagenesis: the identification and elimination of a protease cleavage site (1997), Protein Engineering 10, 601- 606.

61. V. Ellison, J. Gerton, K. A. Vincent, and P. O. Brown, An essential interaction between distinct domains of HIV-1 integrase mediates assembly of the active multimer (1995), J. Biol. Chem. Vol. 270, 3320-3326.

62. E. Deprez, P. Tauc, H. Leh, J. F. Mouscadet, C. Auclair, and J. C. Brochon, Oligomeric states of the HIV-1 integrase as measured by time-resolved fluorescence anisotropy (2000), Biochemistry Vol.39, 9275-9284.

63. H. Leh, P. Brodin, J. Bischerour, E. Deprez, P. Tauc, J. C. Brochon, E. LeCam, D. Coulaud, C. Auclair, J. L. Mouscadet, Determinants of Mg^{2+}-dependent activities of recombinant HIV-1 integrase (2000), Biochemistry Vol.39, 9285-9294.

64. E. Asante-Appiah and A. M. Skalka, A metal-induced comformational change and activation of HIV-1 integrase (1997), J. Biol. Chem. Vol.272, 16196 - 16205.

65. A. B. Hickman, I. Palmer, A. Engelman, R. Craigie, and P. Wingfield, Biophysical and enzymatic properties of the catalytic domain of HIV-1 integrase (1994), J. Biol. Chem. Vol. 269, 29279-29287.

66. R. L. LaFemina, P. L. Callahan, and M. G. Cordingley, Substrate specificity of recombinant human immunodeficiency virus integrase protein (1991), J. Virol. Vol. 65, 5624-5630.

67. A. L. Morgan, M. Katzman, Subterminal viral DNA nucleotides as specific recognition signals for HIV-1 and visna virus integrases under magnesium-dependent conditions (2000), J. Gen. Virol. Vol.81, 839-849.

68.A. Engelman and R. Graigie, Efficient magnesium-dependent human immunodeficiency virus type 1 integrase activity (1995), J.Virol. Vol. 69, 5908 - 5911.

69. S. Carteau, S.C. Batson, L.Poljak, J.-F. Mouscadet, H. de Rocquigny, J.-L. Darlix, B.P. Roques, E. Kas, and C. Auclair, Human immunodeficiency virus type 1 nucleocapsid protein specifically stimulates Mg^{2+}-dependent DNA integration in vitro (1997), J. Virol. Vol. 71, 6225 - 6229.

70.S.P. Lee and M.K. Han, Zinc stimulates Mg^{2+}- dependent 3'-processing activity of Human immunodeficiency virus type 1 integrase *in vitro* (1996), Biochemistry 35, 3837 - 3844.

71.C.A. Janeway, Jr., P. Travers, S. Hunt, M. Walport. Immunobiology. The immune system in health and disease. 3rd ed. New York, London: Garland, 1997.

72.T.C. Pierson, Y. Zhou, T.L. Kieffer, C.T. Ruff, C. Buck, and R.F. Siliciano, Molecular characterization of preintegration latency in HIV-1 infection (2002), J. Virol., Vol. 76, 8518 - 8531.

73.C.A. Royer, Approaches to teaching fluorescence spectroscopy (1995), Biophysical journal 68, 1191 - 1195.

74.J. R. Lakowicz, Principles of fluorescence spectroscopy (1983), Plenum Press, New York.

75.V. LeTilly and C. A. Royer, Fluorescence anisotropy assays implicate protein-protein interactions in regulating *trp* repressor DNA binding (1993), Biochemistry 32, 7753-7758.

76.T. Heyduk, Y. Ma, H. Tang, and R. H. Ebright, Fluorescence anisotropy: Rapid quantitative assay for protein-DNA and protein-protein interaction (1996), Methods in Enzymology Vol.274, 492-503.

77.M. E. Hawkins, W. Pfleiderer, F. M. Balis, D. Porter, and J. R. Knutson, Fluorescence properties of pteridine nucleoside analogs as monomers and incorporated into oligonucleotides (1997), Anal. Biochem. Vol. 244,86-95.

78. M. E. Hawkins, Fluorescent pteridine nucleoside analogs (2001), Cell Biochemistry and Biophysics Vol. 34, 257- 281.

79. M. E. Hawkins, W. Pfleiderer, A. Mazumder, Y. G. Pommier, and F. M. Balis, Incorporation of a fluorescent guanosine analog into oligonucleotides and its application to a real time assay for the HIV-1integrase 3'-processing reaction (1995), Nucleic Acids Res. Vol. 23, 2872-2880.

80. S.L. Driscoll, M.E. Hawkins, F.M. Balis, W. Pfleiderer, and W.R. Laws, Fluorescence properties of a new guanosine analog incorporated into small oligonucleotides (1997), Bioph. J. Vol. 73, 3277 - 3286.

81. K. Wojtuszewski, M.E. Hawkins, J.L. Cole, and I. Mukerji, HU binding to DNA: evidence for multiple complex formation and DNA bending (2001), Biochemistry Vol. 40, 2588 - 2598.

82. A.I. Roca and S.F. Singleton, Direct evaluation of a mechanism fro activation of the RecA nucleoprotein filament (2003), J. Am. Chem. Soc. 125, 15366 - 15375.

83. J.C. Myers, S.A. Moore, and Y. Shamoo, Structure-based incorporation of 6-methyl-8-(2-deoxy-β-ribofuranosyl)isoxanthopteridine into the human telomeric repeat DNA as a probe for UP1 binding and destabilization of G-tetrad structures (2003), J. Biol. Chem. Vol. 278, 42300 - 42306.

84. F. Eckstein, Oligonucleotides and analogues: A practical approach (1991), Oxford University Press, NY.

85. E. V. Barsov, W. E. Huber, J. Marcotrigiano, P. K. Clark, A. D. Clark, E. Arnold, and S. H. Hughes, Inhibition of Human Immunofeficiency Virus type 1 integrase by the Fab fragment of a specific monoclonal antibody suggests that different multimerization states are required for different enzymatic functions (1996), J. Virol. Vol. 70, 4484-4494.

86. T. Heyduk and J.C. Lee, Application of fluorescence energy transfer and polarization to monitor *Escherichia coli* camp receptor

protein and *Lac* promoter interaction (1990), Proc. Natl. Acad. Sci. USA Vol.87, 1744 - 1748.

87. E.A. Pyles and J. Ching Lee, Mode of selectivity in cyclic AMP receptor protein-dependent promoters in *Escherichia coli* (1996), Biochemistry Vol.35, 1162 - 1172.

88. A.D. Attie and R.T. Raines, Analysis of receptor-ligand interactions (1995), J. Chem. Educ. Vol 72, 119 - 124.

89. H.J. Motulsky and L.A. Ransnas, Fitting curves to data using nonlinear regression: a practical and nonmathematical review (1987), FASEB J. Vol. 1, 365 - 374.

90. S.L. Reid, D. Parry, H.-H. Liu, and B.A. Connolly, Binding and recognition of GATATC target sequences by the *Eco*RV restriction endonuclease: a study using fluorescent oligonucleotides and fluorescence polarization (2001), Biochemistry Vol.40, 2484 - 2494.

91. T. Yoshinaga and T. Fujiwara, Different roles of bases within the integration signal sequence of human immunodeficiency virus type 1 in vitro (1995), J. Virol. Vol. 69, 3233 - 3236.

92. A. Mazumder and Y. Pommier, Processing of deoxyuridine mismatches and abasic sites by human immunodeficiency virus type-1 integrase (1995), Nucleic Acids Res. Vol. 23, 2865 - 2871.

93. F.M.I. Van Den Ent, C. Vink, and R.H.A. Plasterk, DNA substrate requirements for different activities of the human immunodeficiency virus type 1 integrase protein (1994), J. Virol. Vol. 68, 7825 - 7832.

94. B.P. Scottoline, S. Chow, V. Ellison, and P.O. Brown, Disruption of the terminal base pairs of retroviral DNA during integration (1997), Genes & development 11, 371 - 382.

95. E. Brin and J. Leis, Changes in the mechanism of DNA integration *in vitro* induced by base substitutions in the HIV-1 U5 and U3

terminal sequences (2002), J. Biol. Chem. Vol. 277, 10938 - 10948.

96. T. Wang, M. Balakrishnan, and C.B. Jonsson, Major and minor groove contacts in retroviral integrase-LTR interactions (1999), Biochemistry 38, 3624 - 3632.

97. P.A. Sherman, M.L. Dickson, and J.A. Fyfe, Human immunodeficiency virus type 1 integration protein: DNA sequence requirements for cleaving and joining reactions (1992), J. Virol. Vol. 66, 3593 - 3601.

98. E. Brin and J. Leis, HIV-1 integrase interaction with U3 and U5 terminal sequences *in vitro* defined using substrates with random sequences (2002), J. Biol. Chem. Vol. 277, 18357 - 18364.

99. P. Brodin, M. Pinskaya, M. Buckle, U. Parsch, E. Romanova, J. Engels, M. Gottikh, and J.-F. Mouscadet, Disruption of HIV-1 integrase-DNA complexes by short 6-oxocytosine-containing oligonucleotides (2002), Biochemistry 41, 1529 - 1538.

100. A. Caumont, G. Jamieson, V.R. de Soultrait, V. Parissi, M. Fournier, O.D. Zakharova, R. Bayandin, S. Litvak, L. Tarrago-Litvak, G.A. Nevinsky, High affinity interactions of HIV-1 integrase with specific and non-specific single-stranded short oligonucleotides (1999), FEBS Let. Vol.455, 154-158.

101. S.P. Lee, M.L. Censullo, H.G. Kim, and M.K. Han, Substrate-length-dependent activities of Human immunodeficiency virus type 1 integrase *in vitro*: differential DNA binding affinities associated with different lengths of substrates (1995), Biochemistry 34, 10215 - 10223.

102. C. Branden and J. Tooze. Introduction to protein structure. 2nd ed. New York: Garland, 1999.

103. M.Hawkins, K.Wojtuszewski, J.R.Knutson, F.M.Balis, A comparison of time resolved anisotropies of 3-MI and 6-MI in single and double stranded oligonucleotides (2004), Biophys. J., 606a.

104. M. Katzman and M. Sudol, Mapping domains of retroviral integrase responsible for viral DNA specificity and target site selection by analysis of chimeras between human immunodeficiency virus type 1 and visna virus integrases (1995), J. Virol. Vol. 69, 5687- 5696.

105. T. Yoshinaga, Y. Kimura-Ohtani, and T. Fujiwara, Detecion and characterization of a functional complex of human immunodeficiency virus type 1 integrase and its DNA substrate by UV cross-linking (1994), J. Virol. Vol. 68, 5690 - 5697.

106. K. Gao, S.L. Butler and F. Bushman, Human immunodeficiency virus type 1 integrase: arrangement of protein domains in active cDNA complexes (2001), EMBO J. 20, 3565 - 3576.